1-1-1985

Neutron scattering investigations of amorphous, miscible polymer blends/

Cameron T. Murray
University of Massachusetts Amherst

NEUTRON SCATTERING INVESTIGATIONS
OF
AMORPHOUS, MISCIBLE POLYMER BLENDS

A Dissertation Presented

By

Cameron Taylor Murray

Submitted to the Graduate School of the
University of Massachusetts in partial fulfillment
of the requirements for the degree of

DOCTOR OF PHILOSOPHY

September 1985

Department of Polymer Science and Engineering

NEUTRON SCATTERING INVESTIGATIONS
OF
AMORPHOUS, MISCIBLE POLYMER BLENDS

A Dissertation Presented

By

Cameron Taylor Murray

Approved as to style and content by:

Richard S. Stein
Chairperson of Committee

Julio M. Ottino, Member

Murugappan Muthukumar, Member

Edwin L. Thomas, Member
Department Head
Polymer Science and Engineering

Dedicated with love to Renee

AKNOWLEDGEMENT

I would like to acknowledge my neutron scattering co-workers John W. Gilmer, Mark Berard and Vivek Soni for their companionship during the many trips to Oak Ridge National Laboratory. Also, the neutron scattering research could not have been accomplished without the support of the National Center for Small-Angle Scattering Research, and in particular George Wignall.

I would also like to acknowledge the help of all my fellow graduate students, in particular Paula Hahn for her friendship and editorial advice.

Final thanks go to my committee for their help and direction, especially my thesis advisor Professor Richard S. Stein who has been a source of insight and guidance for this project.

ABSTRACT

Neutron Scattering Investigations of

Miscible, Amorphous Polymer Blends

(September 1985)

Cameron Taylor Murray

B.A., Chemistry, Beloit College

M.S., Ph.D., University of Massachusetts

Directed by: Professor Richard S. Stein

The amorphous miscible blends of poly(styrene) / poly(o-chlorostyrene), poly(styrene) / poly(α-methylstyrene), and poly(styrene) / poly(vinylmethyl-ether) were studied using Differential Scanning Calorimetry, Thermal Gravimetric Analysis, and Small-Angle Neutron Scattering techniques. The objective of this investigation was to accurately measure the interaction between the components of the blends as a function of composition and temperature. The three different blend systems were selected to evaluate the effect of structure and specific interactions upon the behavior of the measured interaction function.

The recently developed concentrated blend scattering theory was combined with Koningsveld's generalized interaction function to provide an a priori treatment of a composition, temperature and molar mass-dependent interaction function. An empirical interaction function

was used to fit the neutron scattering data and the results of this fit were used to calculate the interaction function.

The neutron scattering study found that for blends without specific interactions the interaction function is small and positive and miscibility is possible if sufficiently low molar mass components are blended. Such systems show dominance of the thermodynamics of mixing by the entropy of mixing. The neutron scattering study also found that a blend system with specific interactions has a negative interaction function and the temperature dependence of the interaction function was found to be a result of the enthalpic interactions between components. The thermodynamics of such systems are mostly influenced by the enthalpy of mixing and as a result they can exhibit high molar mass compatibility of components.

Flory's equation-of-state molecular theory of mixing was quantitatively compared to the measured poly(styrene) / poly(o-chlorostyrene) interaction function and good agreement was found. The equation-of-state theory was able to predict a temperature-dependent interaction function which accounts for molar mass sensitivity of the phase diagram for this blend system. This theory was also used to qualitatively account for the temperature and composition dependence of the poly(styrene) / poly(vinyl-methylether) interaction function.

TABLE OF CONTENTS

LIST OF TABLES

LIST OF FIGURES

C H A P T E R I

INTRODUCTION

The phase behavior and thermodynamics of polymer-polymer mixtures have become important areas of scientific research because polymer blending provides a method for producing materials with new properties without synthesizing new polymers. Miscible blends usually have properties intermediate between the pure component properties. Immiscible blends have unique properties due to the two phase morphology of the mixture. Either state of the blend can yield materials suitable for applications in which homopolymers would be unsatisfactory. Reviews of polymer mixtures and their phase behavior have been compiled elsewhere [1,2] and thus, will not be included here.

Miscibility between polymer components has been shown to occur only rarely [1]. The lack of miscibility arises because there is so little entropy gained upon mixing high molecular weight components. Therefore, the free energy of mixing is largely determined by a delicate balance of enthalpy and liquid state effects, and this delicate balance is reflected in the blend phase behavior.

Recently, molecular theories of mixing have been developed which have improved the understanding of the details of the delicate thermodynamics in polymer mixtures. Presently these theories are being examined with regard to their ability to describe experimental data with reasonable molecular parameters. The goal of understanding the thermodynamics of two component blends is to be able to predict phase behavior, evaluate polymer pairs for the likelihood of miscibility, and to provide the foundation for understanding more complex multicomponent systems such as copolymers.

Background

Three blends, all containing poly(styrene), are examined in this dissertation. The other components of the binary blends are poly(α-methylstyrene), poly(o-chlorostyrene) and poly(vinylmethylether). The chemical structures of these components are shown in Figure 1.1. All three blend systems have been previously studied and the results of these studies are reviewed here.

Poly(styrene)/Poly(o-chlorostyrene) (PS/POCS). The blend of PS/POCS has been shown to have a phase diagram that is very sensitive to the molar mass of the components. Ryan [3] postulated that the high molecular weight blends have an hourglass phase diagram, one where

Poly (styrene)

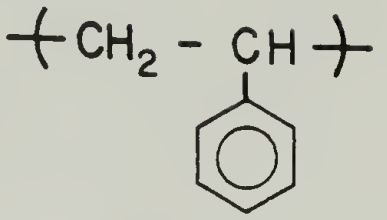

Poly (o - chlorostyrene)

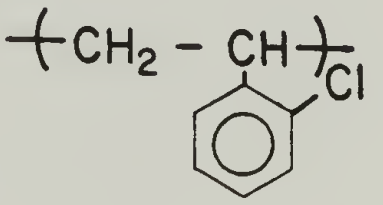

Poly (α - methyl styrene)

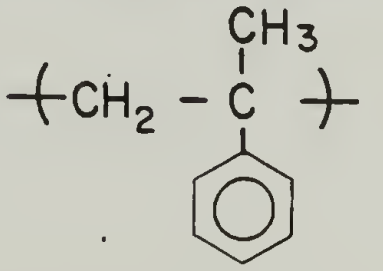

Poly (vinyl methyl ether)

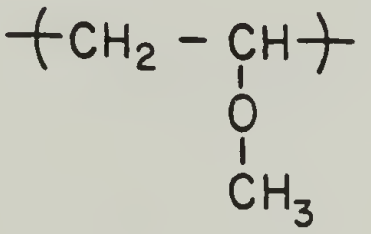

Figure 1.1 Chemical Structures of the Blend Components

the upper and lower critical solution temperatures (UCST and LCST) have merged. Also, upon slightly lowering the molar mass of the POCS component the UCST and LCST must separate sufficiently to have a miscible blend with no detectable LCST.

Zacharius [4] was the first to measure the interaction function for concentrated mixtures of the blend, in this case by vapor sorption techniques. Values of the interaction parameter, χ, obtained are subject to large errors, but definitely show that χ is positive. Also, using Flory's equation-of-state theory, Zacharius [4,5] concluded that the PS/POCS blend was very near its critical double point (CDP). The CDP is defined as the point when the UCST and LCST curves merge; near a CDP the equation-of-state theory accounts for the molar mass-dependence of the phase diagram.

Small-angle neutron scattering (SANS) measurements from dilute solutions of deuterated poly(styrene) (PSD) with POCS showed that POCS was a good solvent for the PSD [6]. The radius-of-gyration (Rg) of PSD was expanded by 30% from the theta condition value, and χ was found to be negative [6]. Gilmer [7] was the first to measure the phase diagram for a PS/POCS blend and LCST behavior was detected. Gilmer [7] used SANS to measure Rg and interaction parameter for concentrated mixtures. The Rg measured from three component experiments (PSD/PSH/POCS)

showed no expansion of the PSD coil, in contrast to the dilute solution results. From a binary blend (PSD/POCS) the interaction parameter was found to be positive and slightly concentration dependent.

Poly(styrene)/Poly(vinylmethylether) (PS/PVME). The PS/PVME blend can be made miscible or immiscible depending upon the casting solvent used [8], and LCST behavior is observed for the miscible blend [9]. Infrared spectroscopy has been used to determine the chemical nature of the PS/PVME interactions. Hsu [10] and Garcia [11] found that two absorption bands were sensitive to the state of miscibility of the blends: the C-H out-of-plane bending in poly(styrene) and the PVME C-O-C asymmetric rock. Both studies concluded that the lone pair electrons of the ether group interact with the aromatic ring of poly(styrene). Nuclear magnetic resonance (NMR) studies show that this blend is not miscible on the segmental level [12].

The interaction parameter has been measured in concentrated blends by vapor sorption [12] and by SANS [13] experiments. All studies confirm that χ is negative and approaches zero with increasing PVME content of the blend. Also, χ is found to have a negative inverse temperature dependence [13].

Poly(styrene)/Poly(α-methylstyrene) (PS/PαMS). The blend of PS/PαMS has been examined much less extensively than PS/PVME or PS/POCS. Most of the previous studies of this blend have evaluated miscibility by determination of the number and breadth of the glass transition(s) (Tg). Baer [14] measured Tg by dynamic mechanical methods and found a single transition, indicating miscibility. In a more detailed study, Wunderlich et al. [15] examined blends of low, medium and high molecular weight PS and PαMS by DSC. Wunderlich found that miscibility occurred for blends where both components were of molecular weight less that 50,000. This study also found that phase separation, determined as a broadened Tg or two Tg's, was detected before the samples became cloudy. Wunderlich's results agree with Krause's [16] prediction that miscibility will occur for low molecular weight blends of this system.

Rahlwes and Biskup [17] performed small-angle light scattering (SALS) on dilute solutions of a two component mixture of PS with PαMS. For a 70,000 M_w PαMS / 300,000 M_w PS, blend miscibility was found only in very dilute solutions (<.5%). A preliminary SANS study of dilute solutions of PS in deuterated PαMS found that the radius-of-gyration and the molecular weight of the D-PαMS was

equivalent in the blend and in the bulk [18]. Ballard and Rayner [18] concluded that it was possible to make truly compatible blends of PS(54,000 M_w) and D-PαMS(32,000 M_w).

In summary, the blend of PS/PαMS exhibits phase behavior similar to that of PS/POCS; low molecular weight materials are miscible, yet moderate increases in molecular weight result in immiscibility over all compositions.

Scope of this dissertation. The work presented in this dissertation measures the interactions between components in the blends of PS/POCS, PS/PαMS, and PS/PVME. The concentrated blend scattering theory developed by Stein et al. [19] is further refined to a priori allow for the interaction between components to have a composition dependence. The interactions between components can then be characterized by a semi-empirical generalized interaction function g. Using this latest refinement of scattering theory, small-angle neutron scattering experiments are performed to measure the composition and temperature dependence of g.

This investigation of PS/POCS blends builds upon the work of Gilmer [7]. The composition and temperature-dependence of g are compared to Zacharius' [5] prediction for a system near its critical double point. Also, the

equation-of-state theory prediction for the composition dependence of the interaction function is compared with experimental results.

The study on the PS/PVME blend is a continuation of the one initiated by Yang [13]. Yang's SANS data is compared to the Flory equation-of-state theory for this system using recently published characteristic parameters for PVME. These results will be compared with Yang's [13] evaluation of χ by the Sanchez lattice fluid theory.

The SANS technique for measuring the interaction function is also performed on the blend of PS/PαMS. This is the first time that the interaction function has been measured for this blend. The interaction parameter is evaluated for its composition and molar mass-dependence. Also, a preliminary investigation of phase separation by a nucleation and growth process is reported for this system.

The goal of this investigation is to gain insight into the relationship between the structures of the blend components and the interaction function and their phase behaviors. Several questions are raised based upon previous results from these blend systems. The blends of PS/POCS and PS/PαMS qualitatively have similar phase behavior; is this a function of chemical structure? Similarly, PS/PVME blends show an interaction function behavior very different from that of PS/POCS; how is this related to the thermodynamics of mixing between two

components? The equation-of-state theory will be used wherever possible to provide a molecular interpretation of the behavior of the interaction function.

Thermodynamics of Polymer Miscibility

Phase Behavior. The thermodynamic criteria for a spontaneous occurrence, such as mixing, is that the free energy change in going from the initial to the final state be negative. This criteria can be expressed

$$\Delta G_{mix} = \Delta H_{mix} - T\Delta S_{mix} < 0 \qquad (1.1)$$

where ΔH_{mix} and ΔS_{mix} are the enthalpy and entropy of mixing at the experimental temperature T. Detailed consideration of ΔG_{mix} as a function of composition shows that the criteria given in eq 1.1 is a necessary, but not sufficient condition for miscibility. Mixtures often are unstable while $\Delta G_{mix}<0$ (though not relative to pure components) and ΔG_{mix} can be lowered by separating into two phases, each phase composed of a mixture of the blend components. Any process that lowers the free energy will be favored thermodynamically and will occur at a rate which is dependent upon kinetic considerations.

Figure 1.2 illustrates this situation by plotting the free energy of mixing as a function of composition at various temperatures. The relationship between the free

energy curves and the phase diagram is shown in Figure 1.3. Examining Figure 1.2, the chemical potential of component i is seen as the $\phi_i=0$ intercept of the line tangent to the ΔG_{mix} curve at the composition of the blend ϕ_2. The chemical potential is also defined as the partial molar free energy change upon mixing

$$\Delta\mu_i = \left(\frac{\partial \Delta G_{mix}}{\partial n_i} \right)_{P,T} \qquad (1.2)$$

where the derivative is taken with respect to n_i, the moles of component i.

In Figure 1.2A the homogeneous mixture of composition ϕ_2 has a free energy equal to the depth $\phi_2 P$. Upon phase separation into phases with arbitrary compositions ϕ_2' and ϕ_2'' the free energy of the system would become $\phi_2 Q$. A free energy increase from $\phi_2 P$ to $\phi_2 Q$ is not thermodynamically favored, and the homogeneous phase is stable. Figure 1.2A corresponds to temperature T_1 in Figure 1.3. At this temperature the system shows miscibility over all compositions of the blend. The curvature of the free energy function will determine the stability of a phase, and for a phase to be stable or metastable

$$\left(\frac{\partial^2 \Delta G_{mix}}{\partial \phi_2^{\,2}} \right)_{P,T} > 0 \qquad (1.3)$$

Figure 1.2B illustrates a free energy curve where phase separation will be exhibited and this figure corresponds to temperature T_2 in Figure 1.3. Using the same reasoning as before, Figure 1.2B shows that the homogeneous phase has a free energy equal to $\phi_2 P$, which is larger than the free energy $\phi_2 Q$ for the two phase system. Therefore, the free energy is reduced upon phase separation while for both cases $\Delta G_{mix} < 0$. A mixture of compostion ϕ_2 is considered absolutely unstable if at temperature T,

$$\left(\frac{\partial^2 \Delta G_{mix}}{\partial \phi_2^{\,2}} \right)_{P,T} < 0 \qquad (1.4)$$

because any infinitesimal change in composition (through composition fluctuations) will result in lowering the free energy and phase separation. Such phase separation behavior is called spinodal decomposition. The boundary between regions of stability/metastability and instability are called the spinodal points. The spinodal points in Figure 1.2B are the inflection points in the free energy curve, defined as the stability limit

$$\left(\frac{\partial^2 \Delta G_{mix}}{\partial \phi_2^{\,2}} \right)_{P,T} = 0 \qquad (1.5)$$

The locus of spinodal points is plotted as a function of temperature as the dashed curves on the phase diagram in Figure 1.3.

For a mixture with an initial composition between the inflection points and the minima in the free energy diagram, ΔG_{mix} will be described by eq 1.3 yet phase separation will still yield a reduction in ΔG_{mix}. In order to phase separate, the system must proceed through a state of higher free energy. Phase separation in these metastable regions can proceed by a nucleation and growth process. At the metastable boundary, called the binodal, the chemical potential of each component must be equal in both phases

$$\Delta\mu_1' = \Delta\mu_1'' \quad \text{and} \quad \Delta\mu_2' = \Delta\mu_2'' \tag{1.6}$$

The binodal curve is plotted in Figure 1.3 as the solid line curves.

If upon changing the temperature, the unstable region vanishes, then this takes place at a point where the two inflection points defined by eq 1.5 coincide. At the critical point eq 1.5 and

$$\left(\frac{\partial^3 \Delta G_{mix}}{\partial \phi_2^{\,3}} \right)_{P,T} = 0 \tag{1.7}$$

must hold. Figure 1.2C illustrates the free energy diagram at the critical temperature and Figure 1.3 shows

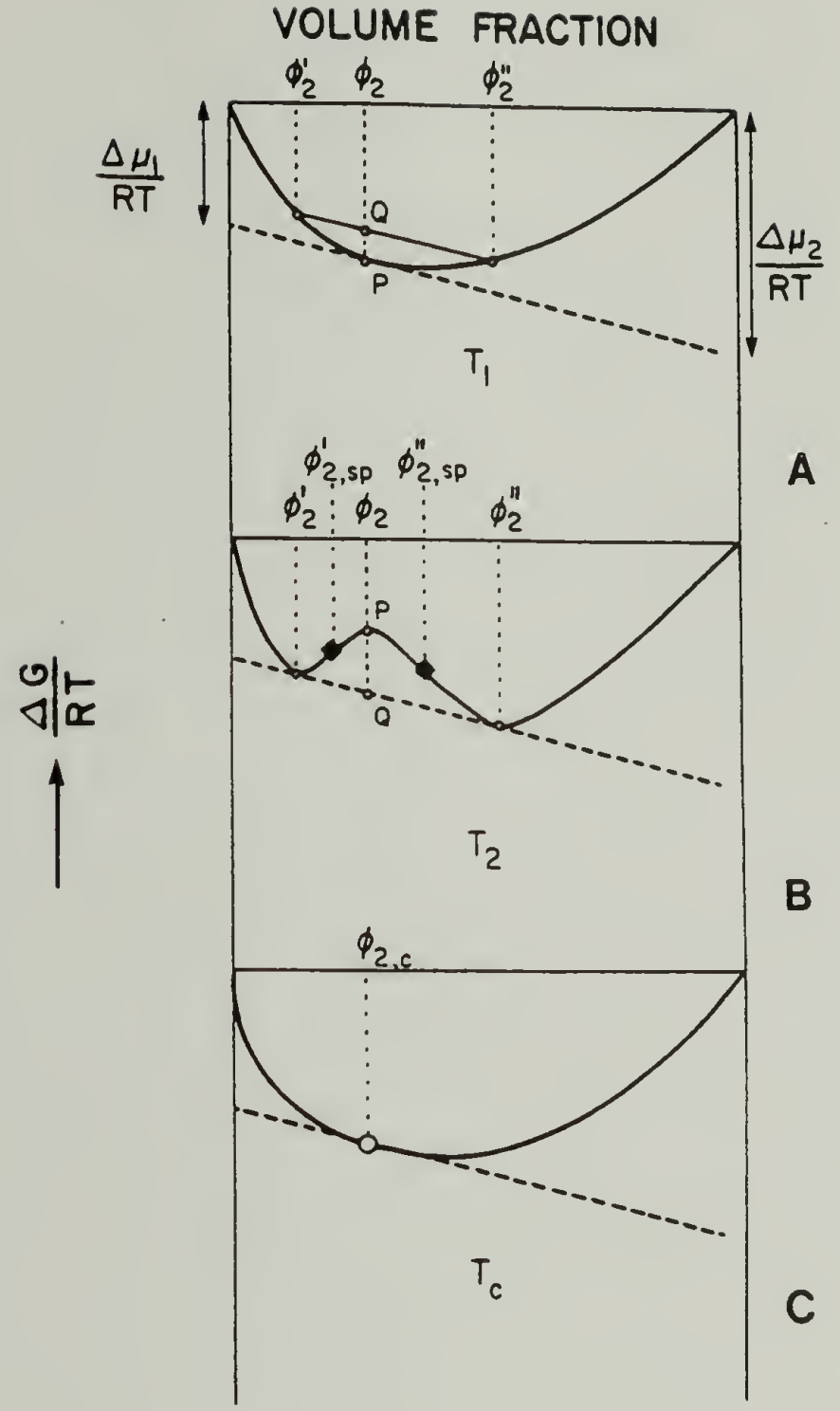

Figure 1.2 Free Energy of Mixing as a Function of Concentration in a Binary Blend

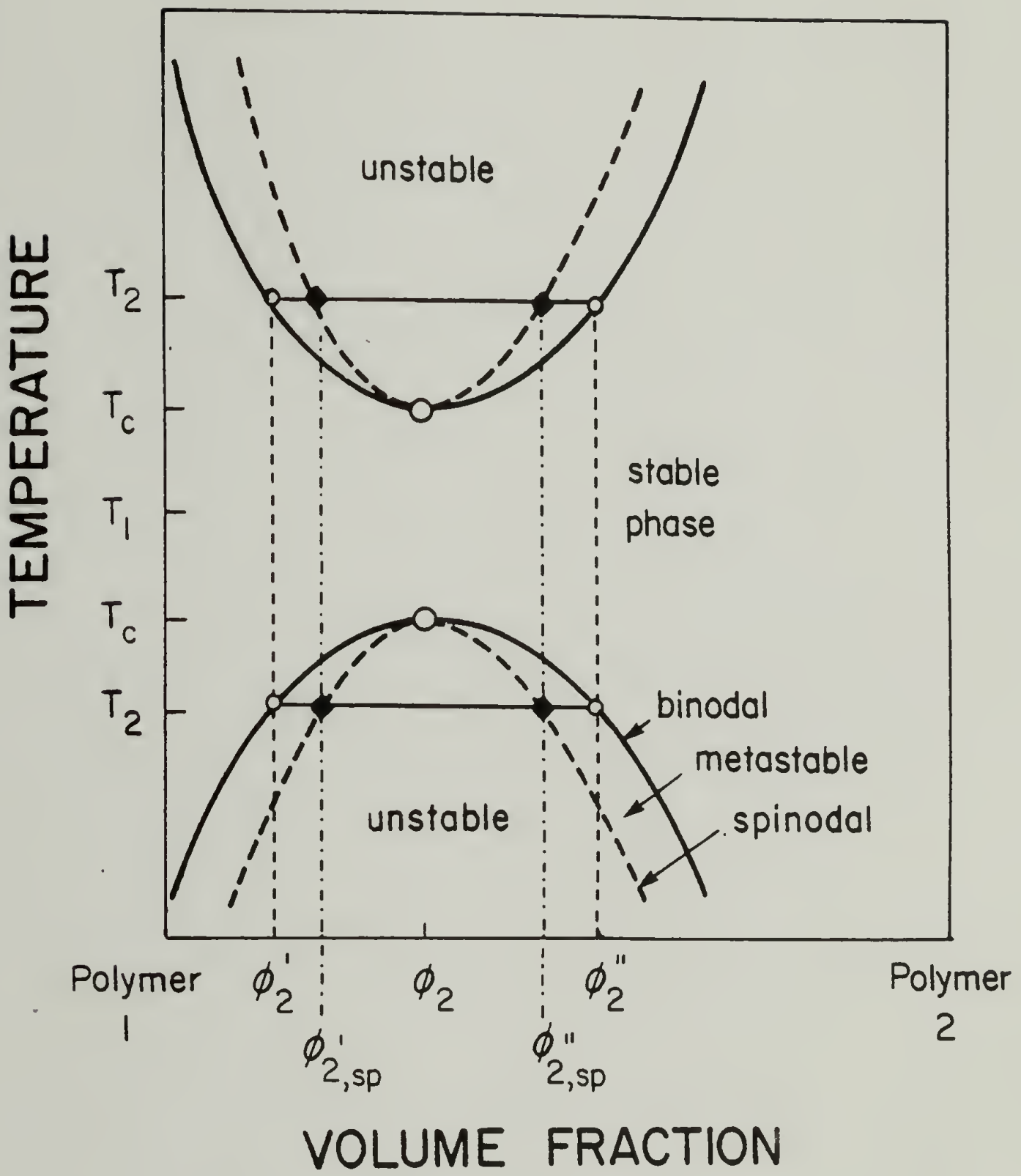

Figure 1.3 Phase Diagram for an Idealized Binary Blend

that the binodal and spinodal merge at the critical temperature, T_c. The critical temperature that occurs upon cooling the mixture is called the upper critical solution temperature (UCST), and such a phase diagram is said to show UCST behavior. The lower critical solution temperature (LCST) occurs upon heating the mixture and the corresponding phase diagram has LCST behavior.

Flory-Huggins Lattice Model. It was observed in the mid-1930's that the partial molar entropy of solutions of long chain compounds and simple solvents was greater than predicted by Raoult's law, even when the heat of mixing was zero [20,21]. Meyer [22] introduced an idealized model of such polymer-solvent solutions as a quasi-solid lattice in order to explain the excess enthalpy observed for these solutions. Statistical mechanical treatments of the lattice model were developed by Flory [23,24] and Huggins [25,26] to quantify the additional entropy arising from disorientation of a solid polymer chain upon the lattice. Following an approach developed by Fowler and Rushbrooke [27] the lattice is distributed throughout the mixture components such that

$$N = y_1 n_1 + y_2 n_2 \tag{1.8}$$

where N is the total number moles of lattice sites, and n_1 and n_2 are the number of moles of polymeric components 1

and 2, respectively. Each polymer molecule occupies y_1 or y_2 lattice sites, and y_i is given as

$$y_i = Z_i(v_i/v_0) \tag{1.9}$$

where Z_i and v_i are the degree of polymerization and molecular volume per segment of component i. v_0 is the volume of one lattice site. Often, v_0 is chosen to be equal to the molecular volume of a given component, thereby designating that component as the 'solvent'.

Each chain is required to occupy a continuous sequence of lattice sites and the volume of the lattice does not change with mixing. The assumptions made by Flory to calculate the number of configurations available to each chain have been refined in the theories of Huggins [26] and others [28,29], but analysis of the results indicates that the effect of these refinements are inconsequential [30,31]. Following Flory's derivation Scott [32], Tompa [33] and Guggenheim [34] were the first to obtain the entropy of mixing for two polymers with no solvent as

$$\Delta S_{comb} = -R(n_1 \ln\phi_1 + n_2 \ln\phi_2) \tag{1.10}$$

where ϕ_1, ϕ_2 are the volume fractions of the respective components and ϕ_i is defined as

$$\phi_i = y_i n_i / (y_1 n_1 + y_2 n_2) \tag{1.11}$$

The adjective and subscript 'comb' in eq 1.10 stand for the combinatorial entropy and are being included in expectation of the need to acknowledge other contributions to the entropy, as will be discussed in a later section of this chapter.

In order to calculate the change in free energy of mixing a polymer with a solvent, the heat of mixing must be evaluated. Flory [24] and Huggins [26] both assumed the heat of mixing could be represented by a relationship suggested by Scatchard [35], van Laar [36], and Hildebrand [37] for simple molecules. The total heat of mixing becomes

$$\Delta H_{mix}/RT = \chi\phi_1\phi_2(y_1 n_1 + y_2 n_2) \qquad (1.12)$$

where χ is the polymer-solvent interaction function defined as

$$\chi = \frac{z}{2}(\varepsilon_{12} + \varepsilon_{22} - \varepsilon_{12}) = \frac{z}{2}(\varepsilon_{11}^{1/2} - \varepsilon_{22}^{1/2}) \qquad (1.13)$$

Here ε_{11}, ε_{22} are the pure component contact energies per segment and ε_{12} is the contact energy between dissimilar segments. The geometric mean contact energy of the pure components is used in the second equality of eq 1.13 for ε_{12}. For weakly interacting components the geometric constraints of the chain reduce dipole-dipole interactions sufficiently to make the geometric mean assumption in eq

1.13 valid. The interaction parameter will be characteristic of each polymer-polymer pair and should be concentration, molar mass and temperature-independent.

The free energy of mixing is defined by eq 1.1 and using the lattice results for the entropy (eq 1.10) and the enthalpy (eq 1.12) of mixing the total free energy of mixing becomes

$$\frac{\Delta G_{mix}}{RT} = n_1 \ln\phi_1 + n_2 \ln\phi_2 + \chi\phi_1\phi_2(y_1 n_1 + y_2 n_2) \qquad (1.14)$$

or the free energy of mixing per mole of lattice sites, $\Delta G_{mix}/NRT$, is obtained by dividing through by the total number of moles of lattice sites, N (eq 1.8):

$$\frac{\Delta G_{mix}}{NRT} = \frac{\phi_1}{y_1} \ln\phi_1 + \frac{\phi_2}{y_2} \ln\phi_2 + \chi\phi_1\phi_2 \qquad (1.15)$$

The volume fractions have been defined previously in eq 1.11. The chemical potential is defined by eq 1.2, and is obtained from eq 1.14 as,

$$\Delta\mu_1/RT = \ln\phi_1 + \phi_2(1-y_1/y_2) + y_1\chi\phi_2^2$$
$$\Delta\mu_2/RT = \ln\phi_2 + \phi_1(1-y_2/y_1) + y_2\chi\phi_1^2 \qquad (1.16)$$

Examining the free energy expression in eq 1.15 indicates why polymer blends are so much less resistant to demixing than other solutions. The combinatorial entropy terms are inversely proportional to component molecular weight, resulting in an entropy for polymer blends that is

essentially zero. The entropy is no longer a driving force for mixing and energy effects will dominate the free energy function. A small positive heat of mixing will suffice to make $\Delta G_{mix} > 0$ and the blend thermodynamically incompatible. This is a likely case because most polymer blends mix endothermally (i.e., $\Delta H_{mix} > 0$) [38].

Scott [32] has applied the stability limit (eq 1.5) and the critical condition (eq 1.7) to obtain the critical composition and critical interaction parameter as

$$(\phi_i)_c = \frac{y_i^{1/2}}{y_1^{1/2} + y_2^{1/2}} \tag{1.17}$$

$$\chi_c = \frac{1}{2}\left(y_1^{-1/2} + y_2^{-1/2} \right)^2$$

Phase separation will occur in a miscible system if the interaction parameter exceeds χ_c. The only temperature dependent term in eq 1.15 is the heat of mixing term defined by the interaction parameter. Since χ is inversely proportional to temperature (eq 1.12), χ will exceed χ_c upon cooling a miscible blend. Therefore, the Flory-Huggins theory can only account for UCST phase behavior.

The major failing of the Flory-Huggins lattice treatment is that this model doesn't take into account the liquid structure or properties peculiar to the individual components. These so called 'equation-of-state' effects

are known to greatly affect the equilibrium properties of the liquid [39]. The quasi-solid lattice model also assumes no change in volume upon mixing, an effect that is observed in many mixtures.

Generalization of the Flory-Huggins Theory. Several theories have been developed to explain phase behavior on a more molecular level than is possible by the lattice model. These include Flory's equation-of-state [39], Sanchez and Lacombe's lattice fluid theory [40], and Huggins' new lattice model [41]. The combinatorial entropy terms derived in the lattice treatment also can be separated out of these molecular models of mixing. Therefore, Koningsveld [38,42] has suggested that the Flory-Huggins equation (eq 1.15) be generalized to

$$\frac{\Delta G_{mix}}{NRT} = \sum \frac{\phi_{1,i}}{y_{1,i}} \ln\phi_{1,i} + \sum \frac{\phi_{2,j}}{y_{2,j}} \ln\phi_{2,j} + \Gamma \quad (1.18)$$

where $\phi_{1,i}$, $\phi_{2,i}$ are the volume fractions of species i in polymer 1 and species j in polymer 2, and $y_{1,i}$, $y_{2,j}$ are the number of lattice sites occupied by species i and j in polymers 1 and 2. Equation 1.18 accounts for the polydispersity of each polymer component. A two component mixture of polydisperse species is called a quasi-binary mixture. Separation of the combinatorial entropy terms

from a model-dependent enthalpy correction term, Γ, will allow for evaluation of the non-combinatorial contributions to the free energy.

Guggenheim [43] and Maron [44] have also suggested that an empirical interaction function which depends upon temperature, pressure and composition should be included with the total free energy. The enthalpy correction term is defined in terms of the overall interaction function g as

$$\Gamma(p,T,\phi) = g(p,T,\phi)\phi_1\phi_2 \qquad (1.19)$$

where the ϕ's in eq 1.19 are the volume fractions of the polymers, i.e., $\phi_1 = 1-\phi_2$.

The chemical potentials for the generalized Flory-Huggins theory are obtained as

$$\Delta\mu_1/RT = \ln\phi_1 + (1-y_{n,1}/y_{n,2})\phi_2 + y_{n,1}(g-\phi_1(\partial g/\partial\phi_2))\phi_2^2 \qquad (1.20)$$

$$\Delta\mu_2/RT = \ln\phi_2 + (1-y_{n,2}/y_{n,1})\phi_1 + y_{n,2}(g-\phi_2(\partial g/\partial\phi_1))\phi_1^2$$

Comparing this result to eq 1.16 the relationship between χ and g can be seen to be

$$\chi = g - \phi_1(\partial g/\partial\phi_2) \qquad (1.21)$$

If the interaction function g is independent of composition then, and only then, does g equal the Flory interaction parameter χ.

The binodal curve is a complex function to calculate, and Flory [24,45], Maron [44] and Koningsveld [46] have developed techniques to determine the binodal. The spinodal can be obtained directly from eq 1.20 and the stability criteria (eq 1.6). For the quasi-binary system the spinodal becomes [46,38]

$$\frac{\partial^2(\Delta G_{mix}/NRT)}{\partial\phi_2^2} = \frac{1}{\phi_1 y_{w,1}} + \frac{1}{\phi_2 y_{w,2}} + \partial^2\Gamma/\partial\phi_2^2 = 0 \qquad (1.22)$$

where $y_{w,1}$ and $y_{w,2}$ are the weight average number of lattice sites occupied by components 1 and 2. The second derivative of the enthalpy correction term is

$$\frac{\partial^2\Gamma}{\partial\phi_2^2} = -2g - 2(\phi_1 - \phi_2)\frac{\partial g}{\partial\phi_2} + \phi_1\phi_2\frac{\partial^2 g}{\partial\phi_2^2} \qquad (1.23)$$

The spinodal curve is primarily determined by the weight average number of lattice sites of each component, but it should be remembered that the interaction function may be affected by the distribution of molecular weight of each component.

The critical state is characterized by the derivatives of the free energy given in eqs 1.5 and 1.7. The quasi-binary version of these conditions yields [46]

$$\frac{y_{z,1}}{y_{w,1}\phi_1} - \frac{y_{z,2}}{y_{w,2}\phi_2} = -\partial^3\Gamma/\partial\phi_2^3 \qquad (1.24)$$

where $y_{z,1}$ and $y_{z,2}$ are the z-average number of lattice

sites occupied by the components of the blend. The third derivative of the enthalpy correction term is given as

$$\frac{\partial^3 \Gamma}{\partial \phi_2^3} = 6g(\partial g/\partial \phi_2) - 3(\phi_1 - \phi_2)(\partial^2 g/\partial \phi_2^2) - \phi_1\phi_2(\partial^3 g/\partial \phi_2^3) \quad (1.25)$$

For a strictly binary system the critical point is located at the maximum or minimum of the spinodal, as illustrated in Figure 1.3. The quasi-binary critical state equation (eq 1.24) indicates that the critical point will be shifted away from the spinodal maximum and minimum. The direction and magnitude of this shift will be determined by the molecular weight distribution of both components.

The generalized Flory-Huggins equation in the form of eq 1.18 will be used for examining the thermodynamics of polymer blends in this investigation. The model-dependent interaction functions under consideration in this study are limited to Flory's equation-of-state and Koningsveld's empirical interaction function.

Equation-of-State Theory. Flory's equation-of-state theory [39] considers the role of free volume in polymer solution thermodynamics. During the mixing process, the free volume of each component is modified. An intermediate value for the free volume is attained which is characteristic of the mixture. For polymer-solvent

systems the difference in free volume is quite significant, but polymer-polymer mixtures generally have small differences in free volume.

As a result of this change in free volume there is a change in the total volume of mixing. The enthalpy and entropy of mixing are volume dependent [31], and generally a change in volume results in a net positive contribution to the free energy of mixing [47]. This volume contribution to the free energy reduces the likelihood of miscibility and becomes more significant with increasing temperature.

The Flory [39] derivation follows Prigogine's [48] formalism which separates the total degrees of freedom of a liquid into internal and external components. The external degrees of freedom depend upon intermolecular interactions only, and are equivalent to the translational degrees of freedom. The internal degrees of freedom depend upon chemical bonding forces. For N molecules with r segments per chain there are $3cN$ ($c<1$) total external degrees of freedom which contribute to the configurational partition function. Covalent linkages in a chain molecule reduce the external degrees of freedom relative to a small molecule pure component because some intermolecular contacts are replaced by intramolecular ones. The empirical nature of c allows for the uncertainty involved in estimating the volume dependent degrees of freedom.

Based upon these assumptions, the partition function for the system of N r-mers is:

$$Z(T,V) = Z_{int}(T) \star Z_{ext} \qquad (1.26)$$

The partition function associated with the internal degrees of freedom, Z_{int} , is assumed to be independent of density and unaffected by the local structure of the liquid. Therefore, Z_{int} does not contribute to the equation-of-state. The partition function associated with the external degrees of freedom depends upon the liquid structure and is equal to

$$Z = (2\pi mkT/h^2)^{3Ncr/2} \star Q \qquad (1.27)$$

where the configurational integral is expressed as

$$Q = Q_{comb}\left(\frac{4\pi\gamma}{3} (\tilde{v}^{1/3} - v^{\star 1/3})^{3Ncr}\right)\exp(-E_o/kT) \qquad (1.28)$$

The mass of a segment is denoted by m; k is Boltzman's constant; h is Plank's constant; v is the volume per segment; $v^{\star}$ is the hard core volume of the segment; E_o is the mean molecular energy; and γ is a geometric factor equal to 1.3 [49].

Q_{comb} is the combinatorial factor that counts the number of ways of interspersing the rN elements amongst themselves, which has a value of unity for a one component system. Flory [39] assumed that the intersegmental energy originates from interactions between surfaces of adjoining

segments and E_o is of the van der Waals form, inversely proportional to volume. The right hand side of eq 1.28 is a kinetic contribution added by McMaster [49] when he adapted the equation-of-state to polymer-polymer mixtures. This factor results in an entropic contribution to the free energy [4].

The resulting equation-of-state is then

$$\tilde{p}\tilde{v}/T = \tilde{v}^{1/3} / (\tilde{v}^{1/3} - 1) - 1/\tilde{v}\tilde{T} \qquad (1.29)$$

where the tilde quantities represent reduced variables of temperature, pressure and volume; $\tilde{T}=T/T^*$; $\tilde{p}=p/p^*$; and $\tilde{v}=v/v^*$. It is more convenient to replace the reduced volume with the specific volume v_{sp} (= 1/density) so that

$$\tilde{v} = v_{sp}/v_{sp}^* \qquad (1.30)$$

The hard core specific volume per segment v_{sp}^*, the characteristic pressure p^*, and the characteristic temperature T^* can be calculated from measurements of the thermal expansion coefficient α, the thermal pressure gradient γ, and the specific volume of the segment v_{sp}.

These relationships are obtained from the equation-of-state as

$$v^{*}_{sp} = v_{sp}\left(\frac{1 + \alpha T}{1 + 4T\alpha/3} \right)^{3} \qquad (1.31)$$

$$p^{*} = \tilde{v}^{2}\tilde{T}v = \tilde{v}^{2}T\alpha/\beta \qquad (1.32)$$

$$T^{*} = \tilde{T}\tilde{v}^{4/3} / (\tilde{v}^{1/3} - 1) \qquad (1.33)$$

Where β is the thermal expansion coefficient.

Adaptation of the equation-of-state theory to mixtures requires the adoption of a set of combining rules:

1. The hard core volumes of the r-mers are chosen to be equal, and the total volume dependent degrees of freedom is 3rNc.

2. The close-packed volume of the mixture is set equal to the sum of the pure component hard core volumes.

3. The total number of pair interactions in the mixture is equal to the sum of the pure component pair interactions.

The total number of chains in the polymer-polymer mixture, N, is equal to $N_1 + N_2$. The combining rules establish c,

r and s for the mixture as

$$c = \psi_1 c_1 + \psi_2 c_2 + \psi_1 \psi_2 c_{12}$$
$$r = \psi_1 r_1 + \psi_2 r_2 \qquad (1.34)$$
$$s = \psi_1 s_1 + \psi_2 s_2$$

where ψ_1 and ψ_2 denote the segment fractions of the respective components, s is the mixture surface parameter, and r is the number of lattice sites occupied by a chain in the mixture. The subscripted values of r, s, and c indicate the pure component values for these parameters. The quadratic correction term c_{12}, introduced by Lin [50], characterizes the deviation from linear additivity of the external degrees of freedom. Generally, specific interactions imply a volume decrease upon mixing. Such a decrease in volume reduces the number of external degrees of freedom and c_{12} characterizes the magnitude of this non-additivity of volumes.

The equation-of-state obtained for the two component mixture is identical to eq 1.29 if the following definitions are retained

$$p^* = \psi_1 p_1^* + \psi_2 p_2^* - \psi_1 \Theta_2 X_{12}$$
$$T^* = p^*/(\psi_1 p_1^*/T_1^* + \psi_2 p_2^*/T_2^*) \qquad (1.35)$$

where Θ_2 is the surface fraction of component 2 and X_{12} is

the exchange energy interaction parameter. Θ_2 is defined in terms of the surface parameter as

$$\Theta_2 = s_2 r_2 N_2 \; / \; srN \tag{1.36}$$

Eichenger and Flory [51] subsequently have included an entropic correction parameter to the theory in order to improve agreement with experiments. Q_{12} accounts for the entropy of interaction between unlike segments. This approach is consistent with Guggenheim's [52] proposal that intermolecular interactions are not entirely energetic in origin.

The free energy of mixing is obtained from the standard relation

$$\Delta G_{mix} = -kT \ln\left(Z \; / \; \prod_{i=1}^{N} Z_{ext} \right) \tag{1.37}$$

where Z (eq 1.26) and Z_{ext} (eq 1.27) have been defined previously. Upon evaluation of ΔG_{mix} for the quasi-binary blend of interest here, the Q_{comb} term of eq 1.28 becomes identical to the Flory combinatorial entropy given in eq 1.10. Therefore, the free energy can be expressed in the generalized Flory-Huggins form of eq 1.18, where in the

low pressure limit the interaction function g becomes [53,54]

$$
\begin{aligned}
g = {} & 3\ln(m_1/m_2)^{1/2}(c_1 - c_2 + \psi_1 c_{12}) \\
& + 3c_{12}\ln\left\{\left((2\pi m_2 kT)^{1/2}/h\right)(\gamma v^*)^{1/3}(\tilde{v}^{1/3} - 1)\right\} \\
& + (3c_1/\psi_2^2)\ln\left((\tilde{v}_1^{1/3} - 1)/(\tilde{v}^{1/3} - 1)\right) \qquad (1.38) \\
& + (v^*/kT\psi_2^2)\left(p_1^*(1/\tilde{v}_1 - 1/\tilde{v}) + \Theta_2^2(X_{12}/\tilde{v} - T\tilde{v}Q_{12})\right)
\end{aligned}
$$

The simplifications made in obtaining eq 1.38 arise from the following assumptions concerning high molecular weight components [49,53]: 1) the pure component properties are independent of the chain length, 2) the end group contribution to the free energy is negligible, and 3) for a quasi-binary mixture, the contributions made by the two components to the free energy are totally reflected in the system parameters, c_{12}, X_{12}, and Q_{12}.

McMaster [49] has calculated binodal and spinodal phase diagrams in order to evaluate the effect of liquid properties upon the miscibility of polymer blends. McMaster's results have previously been summarized, and are as follows [4]:

1. Negative or very small positive values for X_{12} are required for equilibrium miscibility to occur. Negative values of X_{12} result in a phase diagram exhibiting LCST behavior only. Very large positive

values result in an hourglass type phase diagram where miscibility is only possible in dilute solutions. As X_{12} increases from negative to positive values both UCST and LCST behavior may be exhibited. The temperature range of miscibility between the UCST and the LCST will decrease with increasing X_{12}.

2. Low molar mass of either or both components favors miscibility.

3. If the equation-of-state parameters of v^*, T^*, and p^* are similar, the more likely is blend miscibility. Since the theory is most sensitive to the critical temperature, this indicates that similar thermal expansion coefficients help miscibility.

4. If $T_1^* > T_2^*$ then miscibility will occur if $p_1^* > p_2^*$. In terms of measurable pure component properties, if $\alpha_1 < \alpha_2$ miscibility will occur when $\gamma_1 > \gamma_2$.

5. A positive value of Q_{12} favors miscibility. Q_{12} and X_{12} affect the free energy in similar manners, but with opposite sign.

In Figure 1.4 an idealized temperature dependent interaction function, g(T) is plotted. Curves 1 and 2 of Figure 1.4 show the contributions to g(T) from enthalpic and equation-of-state sources, respectively. Curve 3 is the sum of these effects and represents g(T) for the blend. For an initially homogeneous blend $g(T)<g_c$, where g_c is the value of the interaction function at the stability limit.

Upon cooling, the enthalpic contributions due to contact energy dissimilarities increase g(T) for systems with no specific interactions. At the temperature where $g(T)=g_c$ phase separation occurs, accounting for UCST phase behavior. The simple Flory-Huggins lattice model only considers this enthalpic contribution to the interaction function and can only predict UCST behavior.

The equation-of-state effects considered in this section, shown by Curve 2, show that upon heating from the miscible state g(T) again exceeds g_c and LCST phase behavior is predicted. Flory's equation-of-state theory considers both effects upon g(T), and for appropriate polymer pairs will predict UCST and LCST phase behavior.

Systems with specific enthalpic interactions will have an enthalpy contribution to g(T) that is the negative image of Curve 1. Such systems will only show LCST behavior because g(T) will always decrease with decreasing temperature.

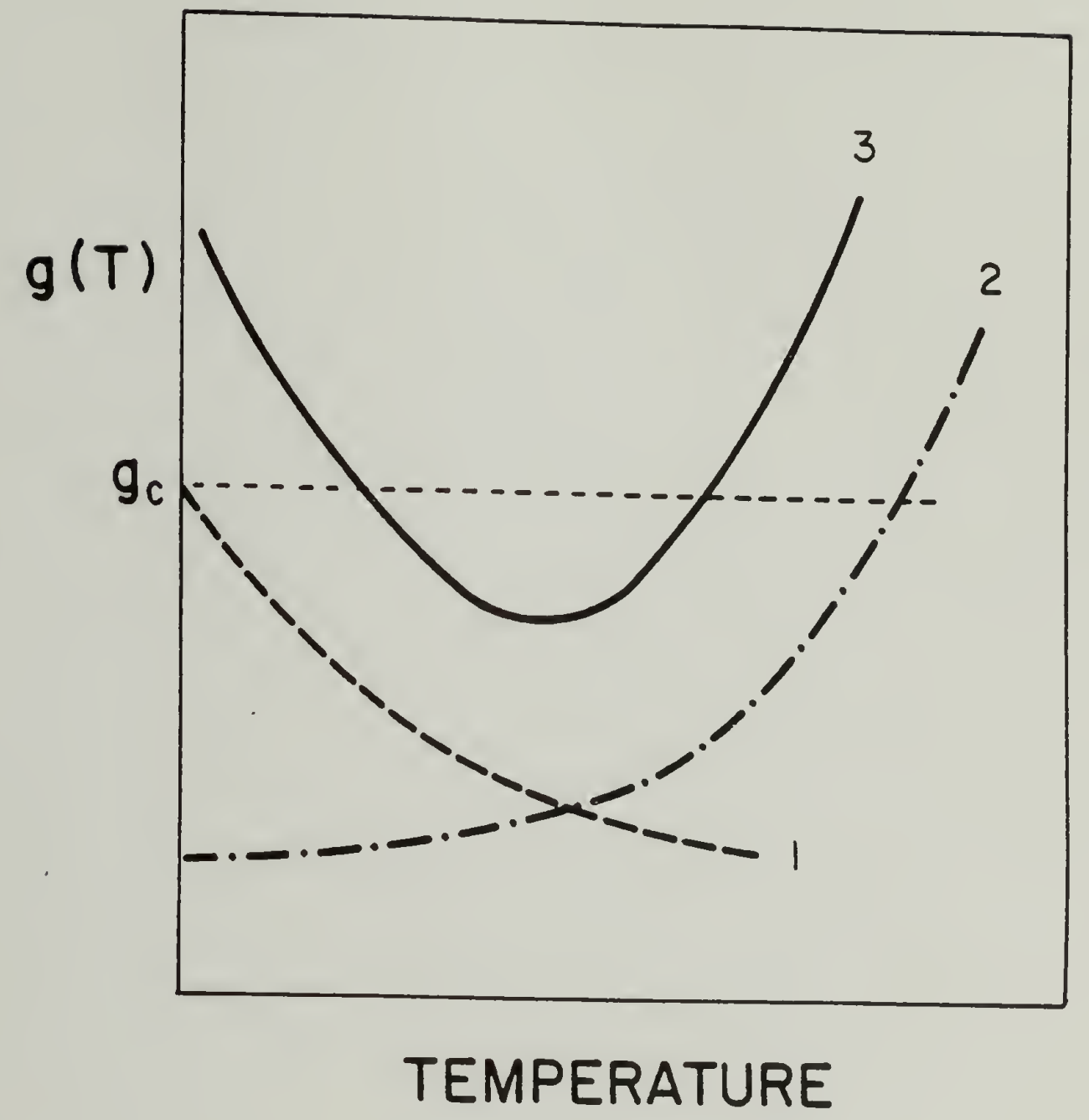

Figure 1.4 Idealized Temperature Dependence of the Interaction Function

Empirical Interaction Function. Equation-of-state theories have attempted to model the coarse behavior of a given system over a wide range of conditions which lead to LCST or UCST phase behavior. In general, molecular models of mixing aim to be able to predict blend behavior from pure component properties. These models of mixing are always an approximation to real liquids and, as a consequence, their ability to predict phase behavior is often only approximate. Koningsveld [38] has approached the study of phase behavior by investigating sensitive variables such as spinodal loci and critical points over limited regions near the phase boundary. The goal of these studies is to quantify the effect of molar mass, composition and temperature upon these variables. With this understanding, Koningsveld is able to predict phase behavior for the same system under new conditions.

The simplest empirical interaction function was suggested by Tompa [55] and subsequently by Koningsveld [56] to be a polynomial function in composition

$$g = g_0 + g_1\phi_1 + g_2\phi_2^2 \qquad (1.39)$$

Assuming that the composition and temperature dependence of the interaction function can be separated, then g_0 becomes the only temperature-dependent coefficient

$$g_0(T) = g_{0,1} + g_{0,2}/T + g_{0,3}T + g_{0,4}\ln T \qquad (1.40)$$

Often the coefficients $g_{0,3}$ and $g_{0,4}$ are small and $g_0(T)$ is left with the usual 1/T dependence [38]. A negative value of $g_{0,2}$ or dominance by the linear or log terms in eq 1.40 can provide for LCST phase behavior. The empirical interaction function of eq 1.39 can also describe irregularly shaped phase diagrams. Double peaked spinodal curves and multiple critical point mixtures have been found in polymer-solvent [38] and polymer-polymer [38,57] blends. The interaction function has to have at least a quadratic composition dependence to describe such phase diagrams [57].

The most significant advantage of semi-empirical interaction functions such as eq 1.39 is the ability to fit experimental data. The severest criticism of such interaction functions is that no new insights into blend thermodynamics is obtained by merely describing the data. Koningsveld's [38] contention is that molecular theories cannot sufficiently predict phase boundaries.

Scattering Techniques and Theory

The scattering of radiation by an isotropic condensed two phase system arises from fluctuations in density and concentration. These fluctuations result in a change in the contrast of a small volume element with its surroundings. Density fluctuations occur, even in pure

liquids, due to thermal motions of molecules. The radiation scattered due to density fluctuations is totally incoherent, the fluctuations are random in space and time. The incoherent scattering of a homogeneous mixture is obtained from the density fluctuations of the pure components.

Concentration fluctuations arise in a binary mixture and cause scattering of radiation as a consequence of the free energy density of the homogeneous phase. The greater the energy cost in changing the local concentration, $\partial^2 \Delta G_{mix} / \partial \phi_2^2 > 0$, the smaller the size of concentration fluctuations in the system. The scattering from concentration fluctuations is spatially correlated, giving rise to coherent scattering. The fluctuation theory of scattering relates the zero angle forward scattered intensity to the second derivative of the free energy as [58,59].

$$R(0)^{-1} = \frac{\partial^2 (\Delta G_{mix}/NRT)}{\partial \phi_2^2} \qquad (1.41)$$

R(0) is the Rayleigh factor at q=0, where $q=4\pi/\lambda \sin(\theta/2)$, θ is the angle between the incident and scattered waves, and λ is the wavelength of the incident radiation in vacuum. The Rayleigh factor is a convenient

measure of the intensity of scattered radiation that is independent of geometry,

$$R(q) = \frac{Is(q)p^2}{I_0 V_s} \qquad (1.42)$$

where Is is the intensity of scattered radiation, I_0 is the incident intensity, p is the sample-to-detector distance, and Vs is the volume of a scattering element.

Recalling the previous discussion of phase behavior, it is evident that as a miscible blend is brought to a phase boundary the scattering will increase ($\partial^2 \Delta G_{mix}/\partial \phi_2^2$ decreases) and, at the spinodal, the scattering becomes infinite ($\partial^2 \Delta G_{mix}/\partial \phi_2^2 = 0$). The magnitude of R(0) in the miscible phase will be a sensitive probe of the free energy function, as shown in eq 1.42. As a consequence of these considerations, scattering methods have become the most useful probe of the thermodynamics and phase behavior of concentrated miscible blends.

Using the result derived previously from the generalized Flory-Huggins theory for $\partial^2(\Delta G_{mix}/NRT)/\partial \phi_2^2$, then for the case of a quasi-binary mixture of polymer components eq 1.42 becomes

$$\frac{K}{R(0)} = \frac{1}{y_{w,1}\phi_1} + \frac{1}{y_{w,2}\phi_2} + \partial^2 \Gamma/\partial \phi_2^2 \qquad (1.43)$$

where K is a constant dependent upon the type of radiation used in the experiment and $\partial^2 \Gamma/\partial \phi_2^2$ is defined in eq 1.23.

The volume fraction ϕ_i's represent whole mixture volume fractions. Equation 1.43 shows that the interaction function g can be determined for such a system from either light, X-ray, or neutron scattering experiments. However, this conclusion is only partially correct. Additionally, the wavelength of the radiation must roughly correspond to the size of the concentration fluctuations occurring in the system for scattering to be detected.

Small-angle neutron scattering (SANS) techniques have recently come to the forefront of research on the morphology and thermodynamics of polymeric systems [60-62]. This rise to prominence is a consequence of the nuclear nature of neutron scattering where elemental isotopes have large differences in scattering power. As an example, deuterium has a positive scattering length (a measure of scattering power) while hydrogen has a negative scattering length. Therefore, it is possible to artificially enhance the neutron scattering contrast between polymer components or morphological subsections by labelling with deuterium.

This isotropic labelling is not difficult and the ability to partially or selectively label chains in the polymer system provides for unique investigations of bulk properties of polymers. Neutrons are also absorbed only slightly, allowing for greater depth probing than possible by X-rays [63]. Neutron scattering is also unaffected by

Table 1.1

Scattering Equation Constants

light scattering*

$$K_L = \frac{2\pi\, n^2}{N_a \lambda_0^4} 2 \left[\frac{\partial n}{\partial c_1} \right]^2_{T,P}$$

X-ray scattering

$$K_X = \frac{N_a i \left(\rho_1^e - \rho_2^e \right)^2}{\rho_2}$$

neutron scattering

$$K_N = \frac{N_a}{m_2} \left(a_1 (v_2 / v_1) - a_2 \right)^2$$

definitions:

- n - refractive index of solution
- λ_0 - wavelength of radiation in vacuum
- N_a - Avagadro's number
- c_1 - concentration of solute
- i_e - Thompson scattering coefficient $= 7.94 \times 10^{-26}$
- p_i^e - electron density of component i
- a_i - neutron scattering length of component i
- v_i - molecular volume of component i
- ρ_i - sample density

* $(\partial n / \partial c_1)_{T,P}$ is determined experimentally for the system.

the scattering of dust, a limitation well known in light scattering experiments of concentrated systems [64]. Finally, thermal neutrons (wavelength of 5 to 15 A) can be used to probe structures in a size range of 5 to 500 A, a range appropriate for most polymer investigations [62].

The proportionality constant in eq 1.43 has been determined for light scattering [65-67], x-ray scattering [68], and neutron scattering experiments [7,19,69]. These proportionality constants are given in Table 1.1. This dissertation will concentrate on SANS techniques, thus, for this study eq 1.43 becomes,

$$\frac{(a_1(v_2/v_1)-a_2)^2}{R(0)v_2} = \frac{1}{Z_{w,1}(v_1/v_2)\phi_1} + \frac{1}{Z_{w,2}\phi_2} + \partial^2\Gamma/\partial\phi_2^2 \qquad (1.44)$$

the identity in eq 1.9 and the lattice volume, v_0, has been set equal to v_2. Then in eq 1.44 a_i, Z_i, and v_i represent the neutron scattering length per repeat unit, the weight average degree of polymerization, and the molecular volume of component i, respectively.

C H A P T E R I I

EXPERIMENTAL TECHNIQUE AND RESULTS

Experimental Technique

Samples. The molar mass distributions for all polymer samples used in this investigation have been characterized and are listed in Table 2.1. Throughout this dissertation samples will be referred to by the blend composition and the component molecular weights. Therefore, the 50 - 50 blend of 233,000 Mw hydrogenous poly(styrene) and 30,000 Mw poly(α-methylstyrene) is expressed as PS(233)/PαMS(30) 50/50 . This nomenclature is evident in the samples listed in Table 2.1.

The deuterated poly(styrenes) (PSD) of narrow molar mass distribution were obtained from Polymer Laboratories Ltd. of Amherst, Massachusetts. The narrow molar mass distribution poly(α-methylstyrenes) were obtained from Polymer Laboratories and Scientific Polymer Products of Ontario, New York. These samples were used in the blends without further preparation.

The broad molar mass distribution poly(vinyl-methylether) component used by Yang [13] in the SANS measurements was also obtained from Scientific Polymer Products. The PVME was maintained at 70^{o}C for 2 days

Table 2.1

Molar Mass Characterization of Pure Components

PS/POCS Blends	Mw	Mn	Mw/Mn	Mz/Mw
PSD(30.5){1}	30,500	29,000	1.05	
POCS(65.4) {2}	65,400	56,800	1.15	
PS/PαMS Blends				
PSD(4.4) {1}	4,400	4,230	1.04	
PSD (10.7){3}	10,000	9,900	1.07	
PSH(63){1}	63,000	60,580	1.04	
PSH(80){1}	82,000	75,300	1.09	
PSD (233){4}	255,000	230,000	1.11	1.06
PSH(233){1}	233,000	219,800	1.06	
PαMS (30)	23,000	20,400	1.15	
PαMS (50)	52,100	50,100	1.04	
PαMS (75)	76,500	69,600	1.09	
PαMS (150)	156,000	144,000	1.08	
PS/PVME Blends				
PSD (233){4}	255,000	230,000	1.11	1.06
PVME(99){4}	99,000	46,500	2.13	1.72

{1} Mn values calculated from the manufacturer's determination of Mw and the ratio Mw/Mn

{2} determined by Gilmer[7]

{3} deuterated molecular weight is 'Polystyrene equivalent' molar mass, actual molar mass is 7.75% larger

{4} molar mass characterization of Yang [13]

before blending to remove moisture from the sample. The poly(o-chlorostyrene) was obtained with a narrow molar mass distribution by a free radical polymerization and fractionation using gel permeation chromatography. The synthesis, fractionation and molecular weight characterization of the POCS component has been described in detail by Gilmer [7].

Freeze Drying. The PSD/POCS and PSD/PαMS blends were prepared by the freeze drying technique. Both blend components were dissolved in benzene, 1% w/v solution, and filtered through a 0.2 um Teflon Millipore filter. The solutions were then rapidly frozen by immersion in liquid nitrogen. After 20 minutes of immersion, the frozen samples were then placed on a vacuum line and the pressure was reduced to less than .1 torr. The frozen samples were allowed to warm to room temperature causing the benzene to sublime off into a cold trap maintained at liquid nitrogen temperatures. Sublimation was continued for 24 hours and was followed by drying in an oven under low vacuum at 80^{o}C for 2 to 4 days. The freeze drying technique yielded a fluffy powder in which the components are intimately mixed. Such a mixture may not be the equilibrium state for these components and, thus, the blended samples must be compression molded and annealed above the glass transition (Tg) to determine the equilibrium state for the blend.

Sample Preparation. The PS/PαMS blends were prepared in the form of thin films for cloud point, DSC and optical microscopy experiments and both PS/POCS and PS/PαMS blends were prepared as thick samples for the SANS studies.

Thin films of the PS/PαMS blends were prepared by initial compression molding of the freeze dried powder into disks of 6.5 mm diameter and .051 mm thickness using a brass shim mold. The compression molding was performed at 175^{o}C with cycling of pressure up to a maximum of 1000 psi. DSC samples were obtained by breaking these disks into pieces and placing 5-10 mg into a sample pan. Optical quality thin films were finally produced by gently pressing (<100 psi) the molded disks between glass cover slips at 175^{o}C.

The PS/POCS SANS samples were prepared by compacting the freeze dried powder in a 13 mm diameter KBr pellet press. Pressure was applied at room temperature and slowly increased to a maximum of .8 metric tons over a 20 minute period. The PS/POCS pellets were removed and placed in a 13 mm diameter hole of a 1 mm thick metal template. The template was coated with a Teflon spray release agent to aid in removal of the sample after melt pressing. The template was placed between layers of Mylar and the melt pressing was performed in a modified Carver C press. This press allows for samples to be under vacuum during pressing [7]. The vacuum was maintained at less

than 1 torr while the sample was heated to 5 degrees above the glass transition of the miscible blend. After temperature equilibration the sample was melt pressed for 25 minutes with a gradual increase in pressure up to 2 tons. The sample was cooled to 100°C and carefully removed from the template.

The PS/PαMS SANS samples were made in a manner similar to the PS/POCS samples. After KBr pelletization, the sample was ground into a fine powder with a mortar and pestle to permit pressing of void free samples. The powder was placed into the 13 mm diameter hole of the metal template but no Teflon release agent was used. The template was placed between sheets of aluminum foil and the modified Carver C press was used to mold the samples. The samples were heated to 10°C above the glass transition and after thermal equilibration the pressure was cycled on and off gradually increasing to an ultimate pressure of 2000 psi. The sample sandwich of template and aluminum foils was then transferred to a hot plate preheated to the Tg of the blend. A sharpened 12 mm cork boring tube was used to core out the sample, removing it from the template. This removal technique was developed in order to eliminate the cracking of the sample upon cooling.

Differential Scanning Calorimetry (DSC). Differential scanning calorimetry was used to measure the glass transitions of the pure component and blends of PS/PαMS.

The DSC sample preparation is mentioned in the sample preparation section of this chapter. A Perkin-Elmer DSC-2 equipped with a Thermal Data Analysis Station (TADS) was used to measure the thermograms.

The blend glass transitions were determined by scanning the range of 23^{o} to 197^{o}C at 20^{o}C/min. A glass transition temperature was identified as the temperature of half the change in heat capacity observed for the entire pseudo-second order transition. Thermograms of miscible blends exhibit a sharp glass transition while immiscible blends exhibit a broadened single transition or the two pure component glass transitions. After the initial thermogram was measured the samples were annealed at 227^{o}C for 1 hour and the thermogram was remeasured. The second thermogram represents the equilibrium state of the blend at the annealing temperature.

Phase Boundary Determination. In order to obtain an approximate phase diagram for the PS/PαMS blend system, optical microscopy and cloud point measurements were performed. Samples in the form of thin films pressed between glass cover slips were obtained as mentioned in the sample preparation section of this chapter.

Optical microscopic examination of the phase morphology as a function of temperature was performed on a Leitz microscope at 400x magnification. A Valley Forge PC6040 was used to control the temperature of a Koffler

microscope hot stage. The samples were heated at 2-3°C/min from 180°-250°C and the microscope image was recorded on video tape. Phase separation was observed as the appearance of a mottled domain structure throughout the sample.

Cloud point measurements were initiated to more quantitatively measure the onset of phase separation. In the cloud point experiment the intensity of scattered radiation at a fixed angle (50°θ) was measured as a function of the temperature of the blend. Using a Mettler FP-2 controller and FP-21 hot stage the samples were heated at 2°C/min from 180° to 250°C while the intensity was detected with an RCA 4840 photomultiplier tube. The cloud point was taken as the temperature at which the scattering greatly increased.

Thermal Gravimetric Analysis (TGA). The thermal degradation temperature of the components in the PS/PαMs blends were studied using a Perkin-Elmer Thermalanalysis Station (TGS-2). Freeze dried blend powders and thin film samples with a weight of 5 to 10 mg were heated in the TGS-2 from 50° to 500°C at a rate of 20°C/min under a nitrogen atmosphere. The percent of the sample remaining (weight percent) at a given temperature, and the derivative of this curve, were recorded by the TGS-2 as a function of temperature. The PαMS component of these blends degrades at a lower temperature than the PS

component and the PαMS degradation temperature was taken as the temperature of 2% weight loss. After this temperature subsequent weight loss was very rapid. The onset of the PS component thermal degradation occurred after most of the PαMS component had degraded, therefore the PS degradation temperature was determined from the peak in the weight loss-temperature derivative curve.

Small-Angle Neutron Scattering (SANS). The SANS measurements of the PS/POCS and PS/PαMS amorphous, miscible blends were performed at the Oak Ridge National Laboratory (ORNL) in cooperation with the National Center for Small-Angle Scattering Research (NCSASR).

The PS/POCS blends were studied using the 30 meter SANS camera at the High Flux Isotope Reactor [70]. The incident beam has a wavelength of 4.74 A, with a dispersion in wavelength of 6%. The beam was collimated by a 1.85 cm diameter source slit located 7.5 meters from the sample. The area detector (64 x 64 cm^2) with 1 cm^2 element size was positioned at 12.25 meters from the sample in the evacuated flight path. Samples were placed in cells with quartz windows. Scattering measurements were taken at 25°, 125° and 135°C using a brass heating block and a simple temperature controller that maintained the temperature ± 2°C.

The PS/PαMS SANS experiments were performed on the 10 meter camera at the Oak Ridge Reactor. The incident beam had a wavelength of 4.74 A, with a dispersion in wavelength of 5%. The beam was collimated with a 2.0 cm diameter source slit placed 4.5 meters from the sample. As before, the samples were placed in quartz window sample cells. Scattering studies above the glass transition of the blends were not possible due to the flow of the low molar mass blend components out of the sample cell.

The neutron scattering data was corrected for instrumental background and detector sensitivity as well as sample and quartz cell transmissions. The incoherent level of each blend was subtracted from the corrected scattering curves. The blend incoherent level was determined from the measured incoherent levels of the pure components by

$$R_{blend,inc} = \Phi_1 R_{1,inc} + \Phi_2 R_{2,inc} \qquad (2.1)$$

where Φ_i and $R_{i,inc}$ are the volume fraction and incoherent level of component i, respectively. In order to obtain absolute intensity values (Rayleigh ratios) for all scattering experiments, the scattering from calibration standards was measured. The 30-m camera was calibrated with an irradiated aluminium-4 standard with a zero-angle scattering intensity $R(0) = 129 \pm 10\ cm^{-1}$. The 10-m camera was calibrated using a PSD/PSH sample that had been

previously calibrated on the 30-m apparatus. The PSD/PSH sample has a radius-of-gyration (Rg) of 74 A and a zero-angle intensity of R(0) = 75.75 $\pm$5 cm^{-1}.

Experimental Results

DSC measurements. Figure 2.1 shows the DSC thermogram for the pure components PSD(4.4) and PαMS(25). The low molar mass deuterated poly(styrene) has a glass transition of 87^{o}C while a high molar mass PSD has been shown to have a Tg of 100-105^{o}C [13].

Figure 2.2 illustrates the DSC thermogram for a polymer blend that exhibits equilibrium miscibility. Before and after annealing at 227^{o}C the PS(233)/PαMS(30) 50/50 blend shows a single, sharp glass transition. It is well documented that miscible blends show such transitions at temperatures intermediate between the pure component glass transition temperatures [71]. The transition temperature for the blend in Figure 2.2 is taken from the midpoint of the change in heat capacity to be 129^{o}C.

In Figure 2.3 the DSC thermogram of an immiscible blend is illustrated. Prior to annealing this sample the DSC curve shows a very broad glass transition. After annealing at 227^{o}C for one hour the DSC thermogram indicates the sample has undergone complete phase

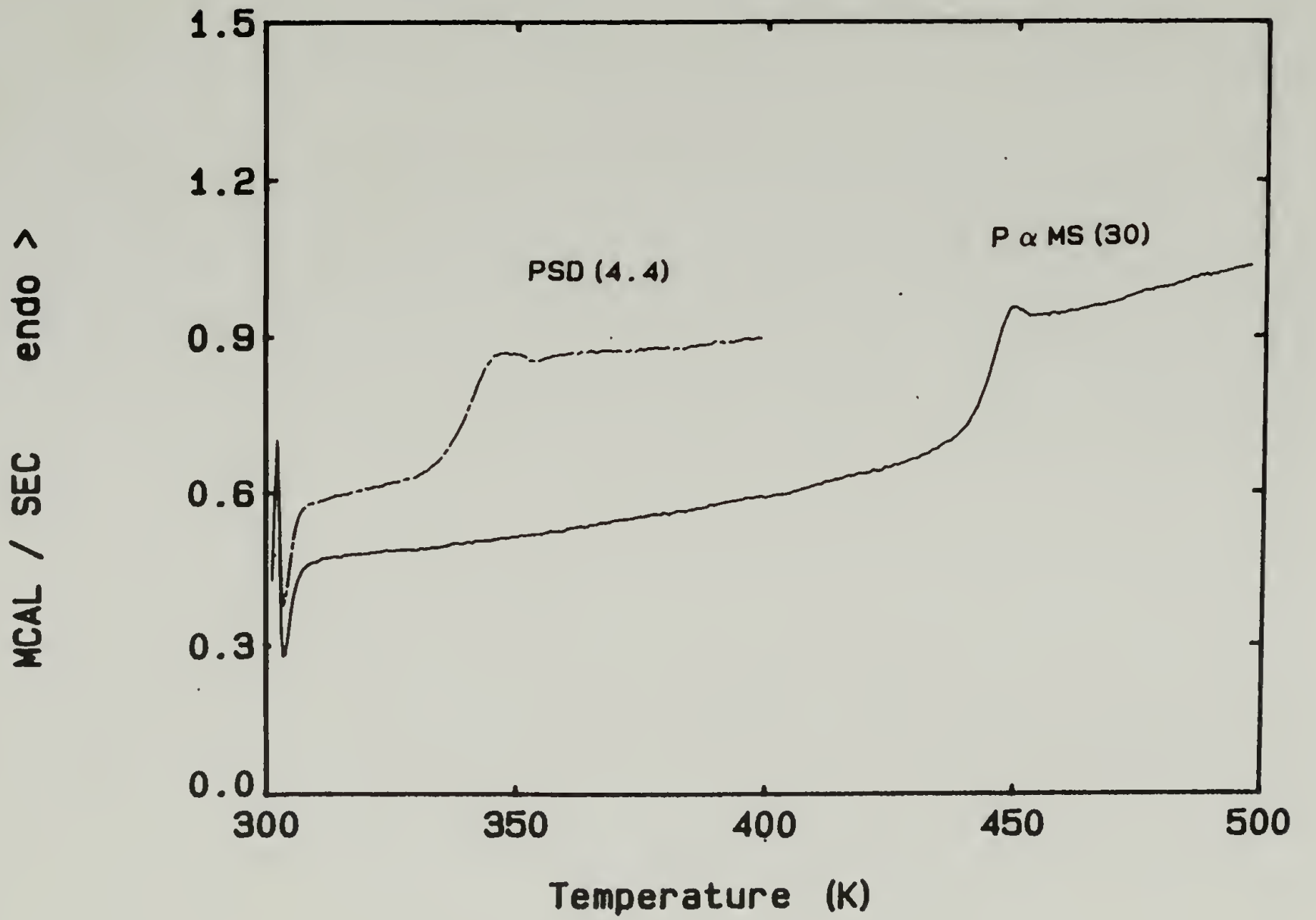

Figure 2.1 DSC Thermogram of PSD(4.4) and PMS(30)

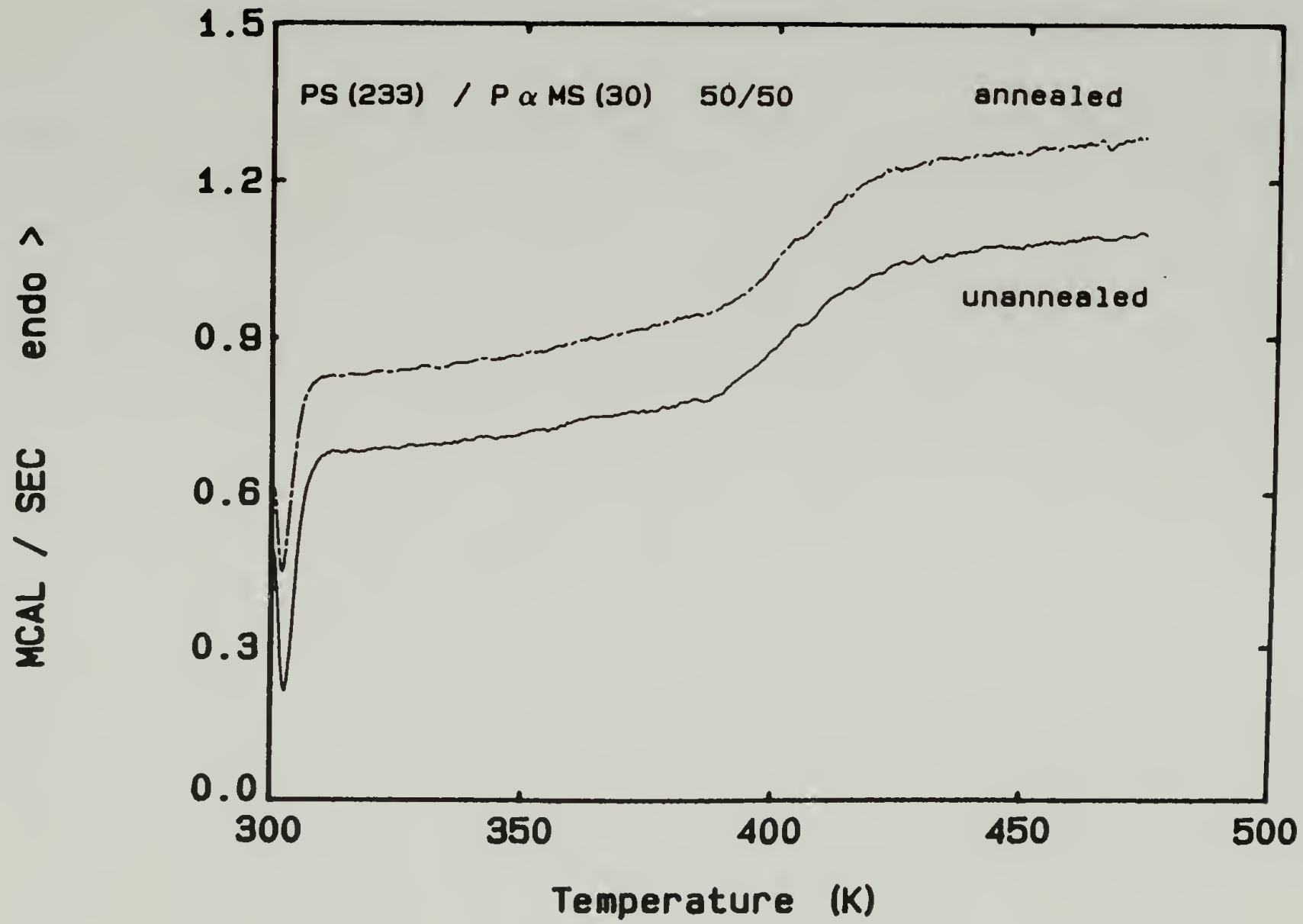

Figure 2.2 DSC Thermogram of PSD(233)/PαMS(30) 50/50

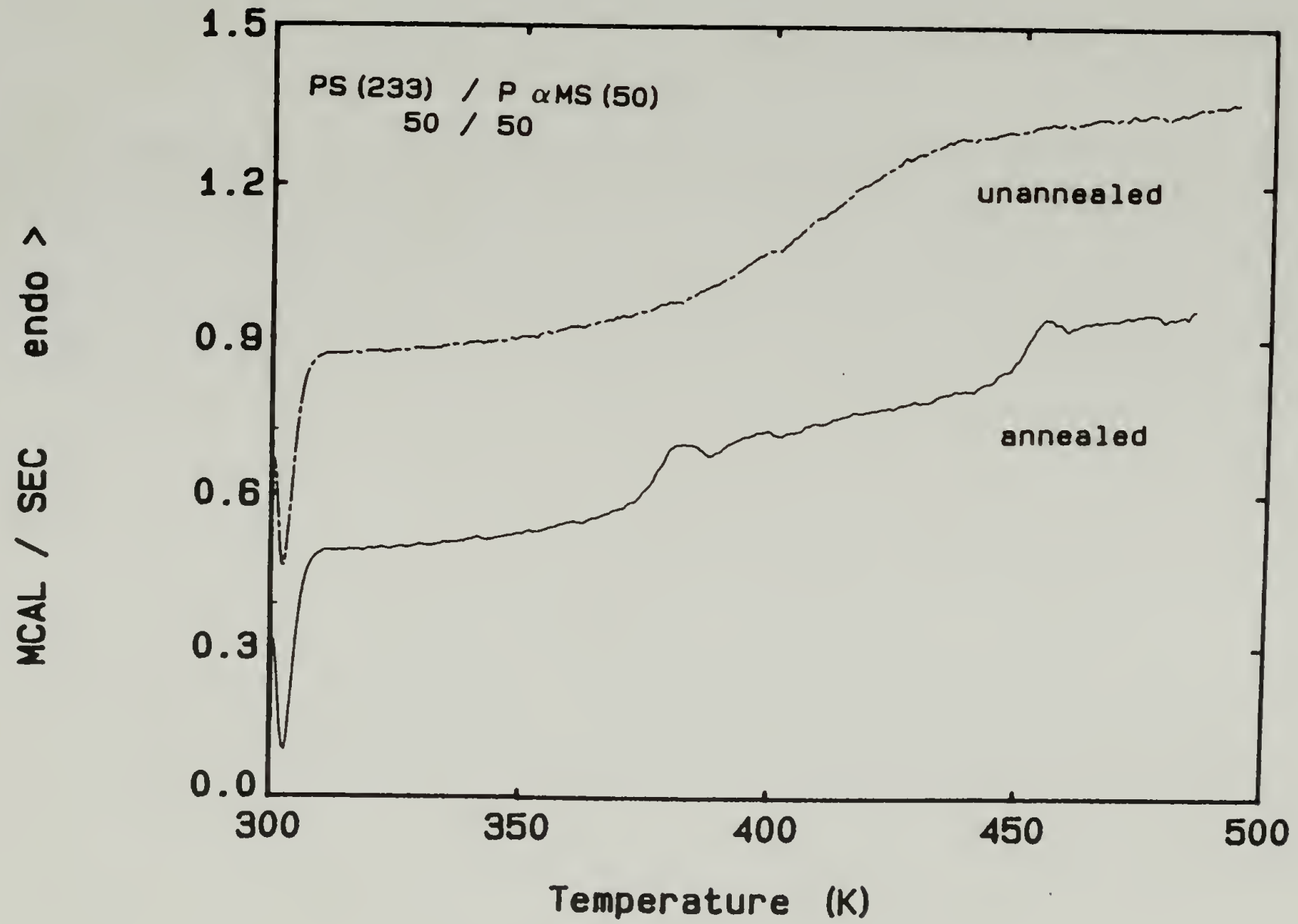

Figure 2.3 DSC Thermogram of PSD(233)/PαMS(50) 50/50

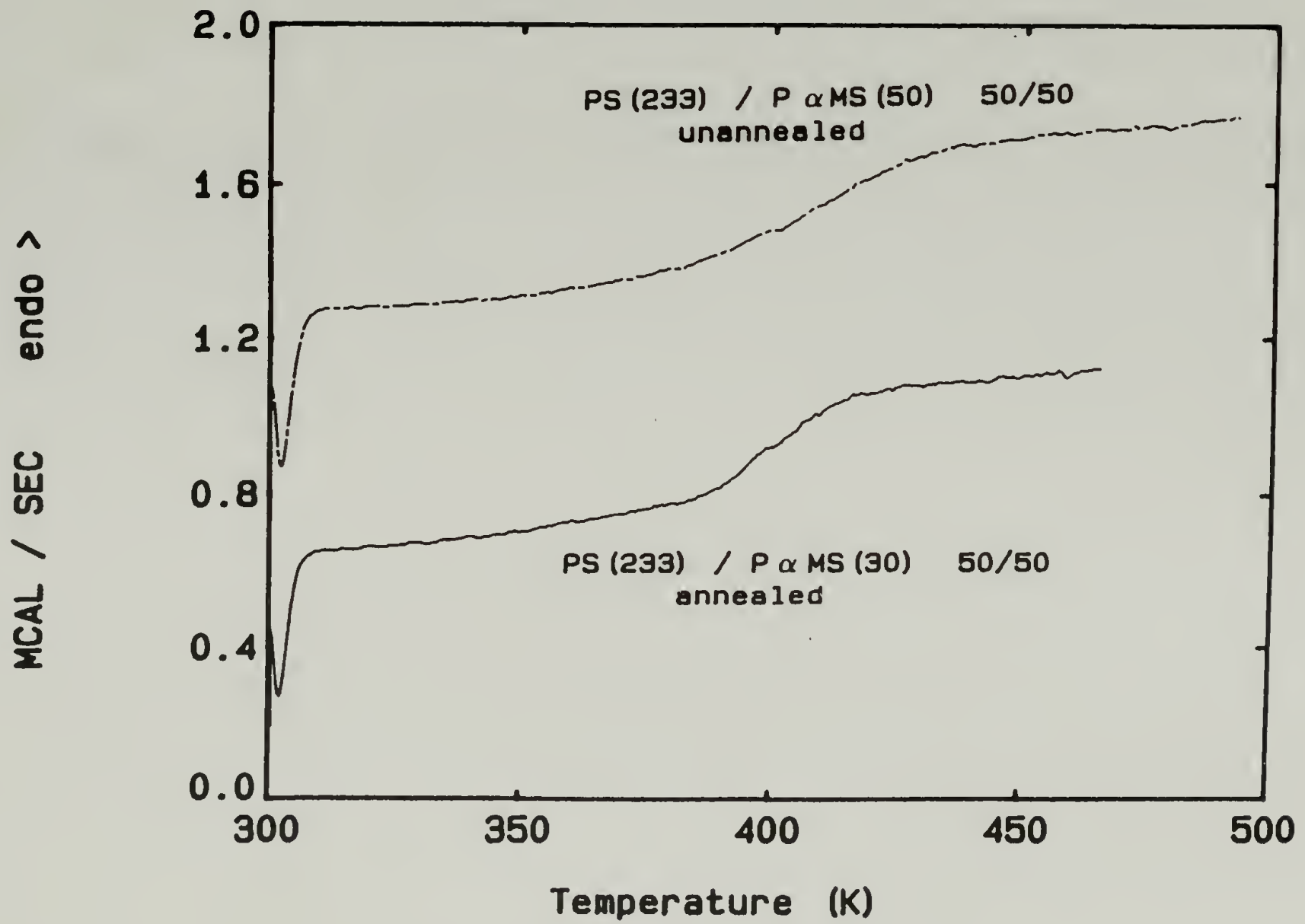

Figure 2.4 DSC Thermogram Comparing PSD(233)/PαMS(30) and PSD(233)/PαMS(50) 50/50 Blends

Table 2.2

DSC Determination of PS / PαMS Blend Miscibility

Blend system	Before annealing	After 227°C annealing
PS(233)/PαMS(150) hours)	broad Tg	2 Tgs (1.5
PS(233)/PαMS(75)	broad Tg	2 Tgs (.5 hour)
PS(233)/PαMS(50)	broad Tg	2 Tgs (.5 hour)
PS(233)/PαMS(30)	sharp Tg	single sharp Tg (1.0 hour)
PS(93)/PαMS(30)	sharp Tg	
PS(10.7)/PαMS(30)	sharp Tg	

separation. The thermogram of the annealed sample in Figure 2.3 has two separate glass transitions at the temperatures of the pure components' Tg.

To further illustrate the difference between miscible and immiscible blend thermograms, the DSC traces of the 50/50 blends of PS(233)/PαMS(30) and PS(233)/PαMS(50) are compared in Figure 2.4. The unannealed sample of the PS(233)/PαMS(50) blend has a significantly broader glass transition than even the annealed PS(233)/PαMS(30) sample. Table 2.2 summarizes the results from a DSC examination of the Tg measurements for PS/PαMS blends with various molecular weights. The results listed in Table 2.2 indicate that the blend 50/50 blend of PS(233)/PαMS(30) is miscible at 227^{o}C, while the higher molecular weight 50/50 blends are immiscible.

TGA measurements. The weight percent of polymer remaining as a function of temperature for various PS and PαMS pure components is plotted in Figure 2.5. Poly(α-methylstyrene) degrades at a lower temperature than poly(styrene) and from Figure 2.5 it can be seen that the PαMS degradation temperature is 280^{o}C while that of PS is 350^{o}C.

Figure 2.6 shows the TGA curves for various PS/PαMS blends. The onset of blend degradation corresponds to the PαMS degradation temperature. The PS degradation affects the blend TGA curves by causing the inflection points

observed in Figure 2.6. The PαMS degradation in the blend lowers the PS degradation temperature slightly, an effect that has been observed previously for this blend system [72].

Cloud point and optical microscopy studies. Only preliminary results were obtained from these measurements on the PS/PαMS blend system. Table 2.3 lists the PS/PαMS blends and the experimental conditions of the optical microscopy experiments. Table 2.3 also lists the temperature at which phase separation was observed. The appearance of a mottled domain structure throughout the sample was taken as indication of phase separation. For the PS/PαMS blends the phase separation was observed as a very subtle change in appearance of the blend morphology due to the small refractive index difference between PS (n_D = 1.588) and PαMS (n_D = 1.632). Also complicating the optical microscopy experiments is the slow kinetics of phase separation for these high Tg blends.

The cloud point investigations confirm the result obtained by optical microscopy: the small refractive index difference and slow kinetics limit the accuracy of the cloud point detection. In the cloud point experiment these considerations cause the intensity of scattered radiation to be quite small and increases in intensity occur over a broad temperature range. The results of the PS/PαMS cloud point study contrast sharply with PS/PVME

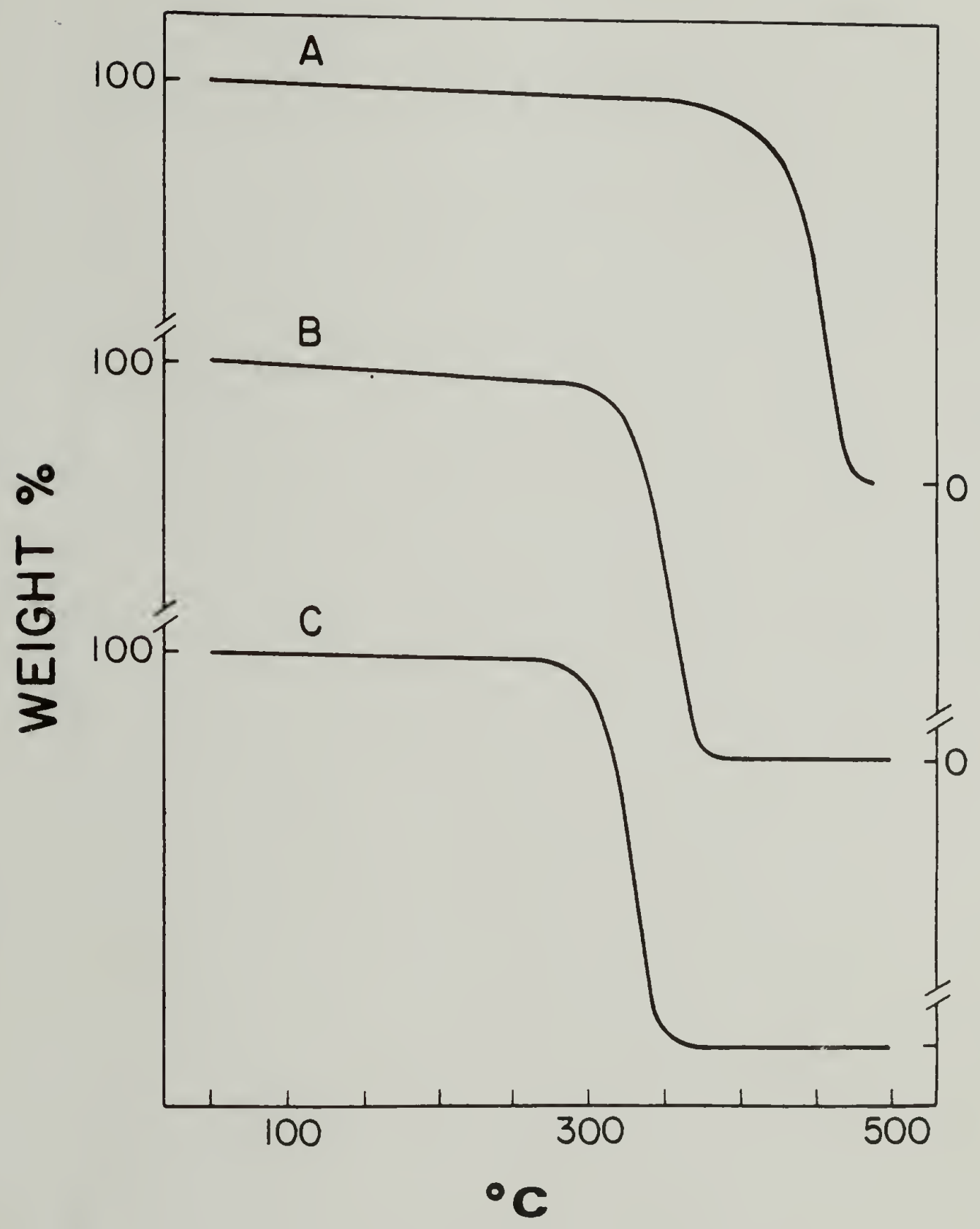

Figure 2.5 TGA Weight Percent of PS and PαMS pure components

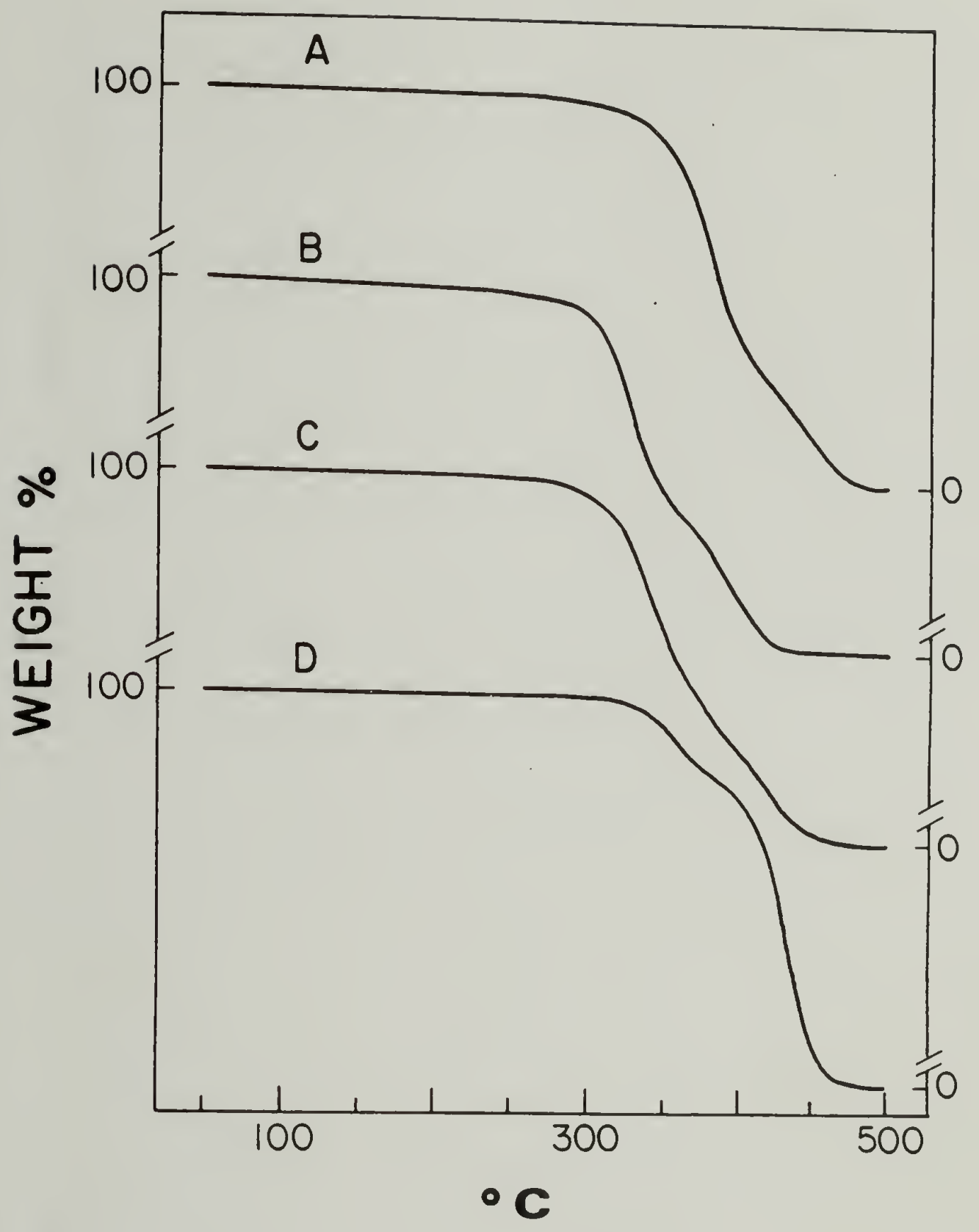

Figure 2.6 TGA Weight Percent of PS/PαMS Blends

Table 2.3

Optical Microscopy Results for Blends of

PS / PαMS

Sample	Phase Separation Temperature	Experimental Conditions
PS(80)/PαMS(75) 50/50	230 ^{o}C	3^{o}C/min
PS(80)/PαMS(150) 50/50	220 ^{o}C	5^{o}C/min
PS(63)/PαMS(150) 50/50	240 ^{o}C	1^{o}C/min
75/25	220 ^{o}C	1^{o}C/min
25/75	240 ^{o}C	1^{o}C/min

experiments. The larger refractive index difference between the components (where n_D = 1.467 for PVME) and the more rapid phase separation kinetics make the PS/PVME cloud point a much better measure of the phase diagram for this blend.

Small-angle neutron scattering measurements. The angular-dependent corrected SANS intensity, R(q), is extrapolated to obtain the zero-angle Rayleigh ratio, R(0), as required by eq 1.44. Extrapolation was performed by using either the Zimm or Debye analytical functions which describe the angular dependence of scattering from a Gaussian chain.

The Zimm extrapolation technique assumes that the scattering can be described by

$$R(q)^{-1} = R(0)^{-1} + b_1 q^2 + \ldots\ldots \qquad (2.2)$$

where q is the scattering vector equal to $4\pi/\lambda \sin(\theta/2)$ and b_1 is a constant, which for a concentrated two component blend, is given by [7]

$$b_1 = \frac{(Rg_A^o)^2}{(3\phi_A y_A)} + \frac{(Rg_B^o)^2}{(3\phi_B y_B)} \qquad (2.3)$$

In eq 2.3 ϕ_i, y_i, and Rg_i are the volume fraction, number of repeat units of the chain, and radius-of-gyration of component i, respectively. The Zimm extrapolation provided by eq 2.2 is valid if the data collected has a

value of $qR_g < 1$, otherwise higher order powers of q^2 must be included in the extrapolation [73]. Ullman has shown that the q^4 terms are sufficient to describe the scattering from high qR_g regions [73]. Due to void scattering in the low q region for the PS/POCS samples, the scattering was measured over a qR_g range of .8-2.0. The PS/POCS scattering data was fit to the equation

$$R(q)^{-1} = R(0)^{-1} + b_1 q^2 + b_2 q^4 \qquad (2.4)$$

where b_1 and b_2 are now simply considered as the coefficients of the fit of the scattering data. The least-squares weighted fitting was performed using the computer program POLYFT written by this author and contained in Appendix II.

Figure 2.7 shows a typical SANS curve from the blend of PSD(30.5)/POCS(65.4). The data is plotted in the Zimm form ($R(q)^{-1}$ vs. q^2) and the solid line is the best fit of the data to eq 2.4. The error in each data point of Figure 2.7 is less than the size of the mark for each data point, except at large values of q. A typical error associated with a high angle q value is drawn on Figure 2.7. The extrapolated values of R(0), the PSD(30.5)/POCS(65.4) blend compositions and the standard deviation of R(0) are all listed in Table 2.4 for the three experimental temperatures.

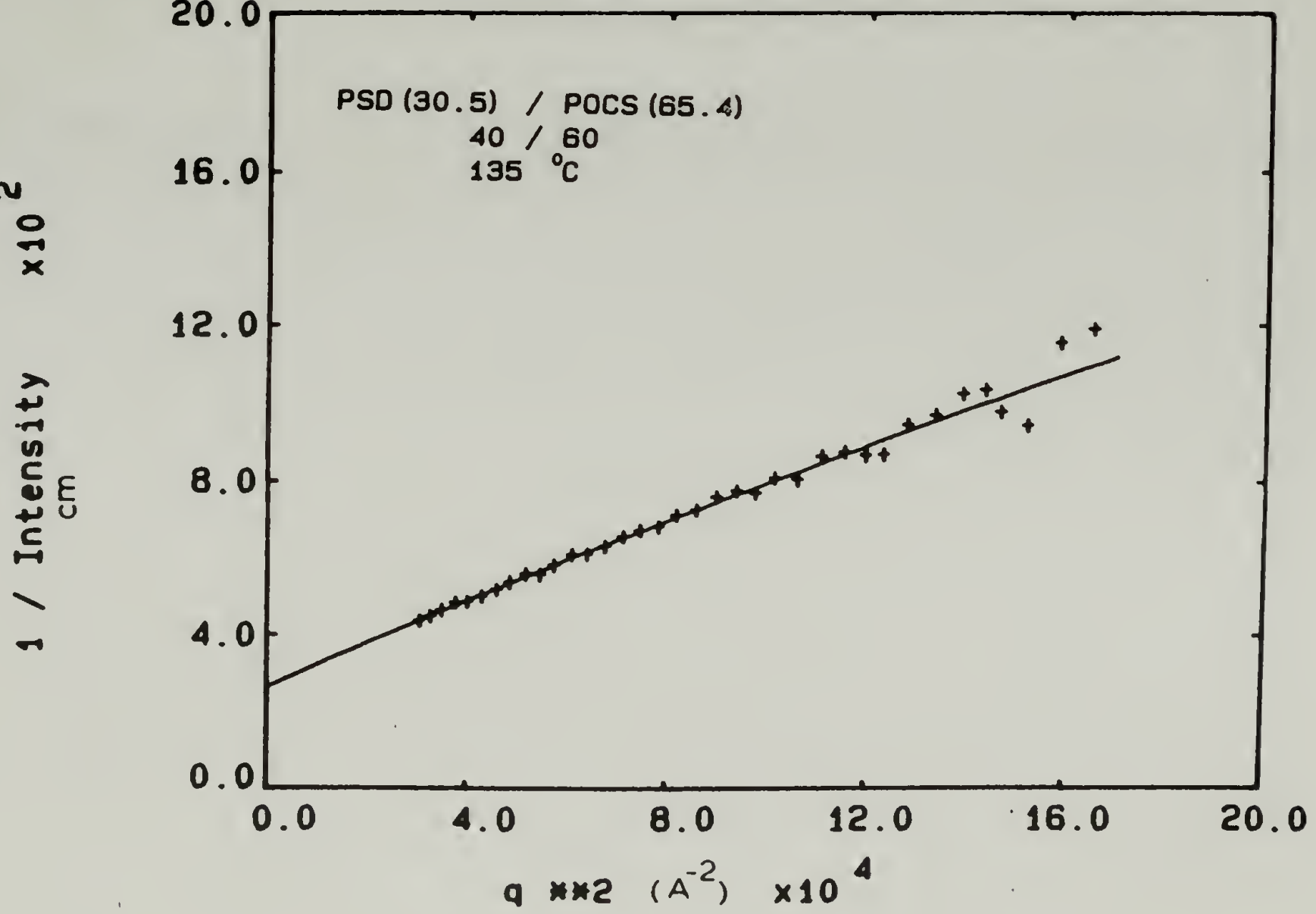

Figure 2.7 PSD(30.5)/POCS(65.4) 40/60 Neutron Scattering Data Plotted in the Zimm Form

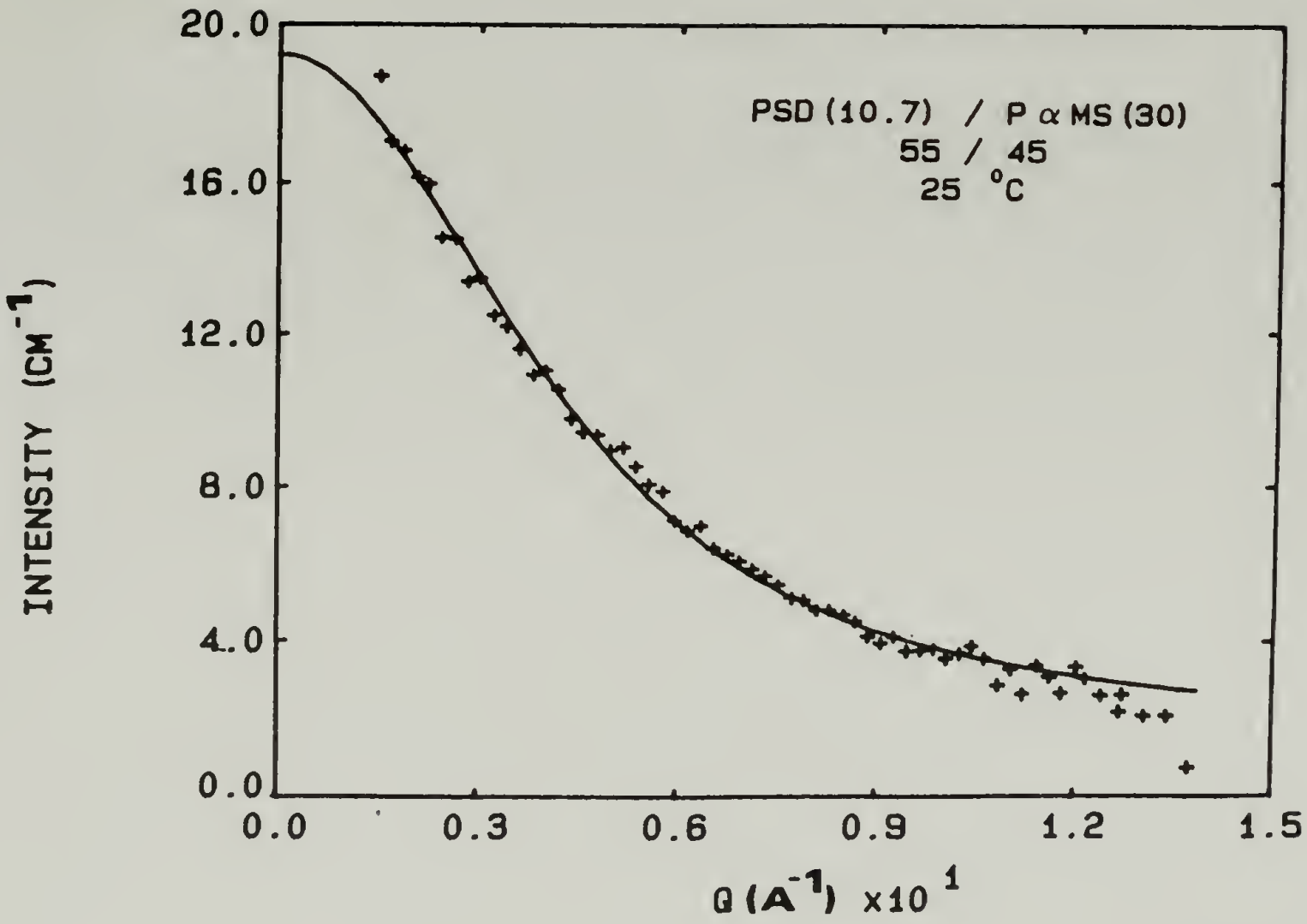

Figure 2.8 PSD(10.7)/PαMS(30) 55/45 Neutron Scattering Data

Table 2.4

Rayleigh Factor at q=0 for the Blend of

PSD(30.5) / POCS(65.4)

	Volume Fraction POCS	Rc(0) (cm^{-1})	Deviation (cm^{-1})
T=25°C	0.193	29.94	0.90
	0.322	48.78	0.20
	0.476	55.56	0.20
	0.629	38.76	0.20
	0.787	22.32	0.90
T=125°C	0.191	32.15	0.90
	0.320	54.35	0.20
	0.474	55.25	0.20
	0.627	38.61	0.20
	0.786	21.74	0.90
T=135°C	0.191	29.33	0.90
	0.319	50.51	0.20
	0.473	56.18	0.20
	0.626	37.45	0.20
	0.786	20.88	0.90

Table 2.5

Rayleigh Factor at q=0 for the Blend of

PS / PαMS

PS(10.7) / PαMS(30)

Volume Fraction PαMS	R(0) (cm^{-1})	Deviation (cm^{-1})
.083	10.17	.02
.456	19.65	.01
.615	14.26	.01
.677	12.55	.01
.687	12.27	.01
.784	8.96	.02
.860	5.99	.03

PS(10.7) / PαMS(25)

.517	16.00	.01

PS(10.7) / PαMS(75)

.517	19.80	.01

PS(10.7) / PαMS(139)

.514	19.80	.01

Table 2.6

Rayleigh Factor at q=0 for PSD(233) / PVME(99) Blends

as Determined by Yang[13]

Temperature °C	Volume Fraction PVME in Blend								
	.906	.890	.810	.762	.713	.615	.516	.415	.210
25	7.61			7.30	7.25	7.20			5.82
71	14.66				16.13		11.38		9.18
121						56.69	34.15	27.22	17.99
131			60.04	79.01	97.94		46.95	34.55	21.25
136	78.22		97.40	88.22	128.70	71.01	61.29		24.76
141	107.51	116.06		138.00	211.40	103.30	77.07	51.57	28.62
147	125.68	241.78		220.70		143.80	108.80	63.89	
152	254.73		482.16			269.10	205.10	91.21	41.21
157						592.30	328.20	145.50	47.56

R(0) obtained from Appendix III of reference 13.

The PSD(10.7)/PαMS(30) SANS data was extrapolated to the zero-angle scattered intensity using the Zimm form given in eq 2.3 as well as by fitting the R(q) data to a Debye scattering function. The Debye function describes the angular dependence of scattering from a Gaussian coil as

$$R(q) = \frac{2R(0)}{u^2}\left(e^{-u} - 1 + u \right) \qquad (2.5)$$

where u=qRg. Figure 2.8 shows a typical corrected neutron scattering curve from a PSD(10.7)/PαMS(30) blend plotted in the form of R(q) vs q. The solid line in Figure 2.8 is the best fit of the data to the Debye function given in eq 2.5. The least-squares weighted fitting was performed with the computer program DEBYE written by this author and contained in Appendix II. The zero-angle extrapolated Rayleigh ratios, the PSD(10.7)/PαMS(30) blend compositions, and the standard deviation in R(0) are contained in Table 2.5.

The Zimm extrapolation of the scattering curve shown in Figure 2.8 was performed and the value of the Rayleigh factor determined is lower that of the Debye fit value, but within experimental error of the determination of R(0). The Zimm method of extrapolation is a small-angle approximation of the Debye function, therefore it is

preferable to extrapolate to R(0) with the Debye fit when the data is obtained at intermediate values of the scattering vector.

The neutron scattering determination of R(0) for the PSD(233)/PVME(99) blends performed by Yang at the National Bureau of Standards [13] are listed in Table 2.6. Details of the experimental technique employed in the PSD/PVME studies have been described elsewhere [13,74].

C H A P T E R I I I

CALCULATED RESULTS AND DISCUSSION

Interaction Function

Method of Calculation. The second derivative of the enthalpy correction term, $\partial^2\Gamma/\partial\phi_2^2$, was determined for each blend composition from the SANS measured values of R(0) contained in Tables 2.4-2.6 using eq 1.44. The $\partial^2\Gamma/\partial\phi_2^2$ values were then related to the interaction function g by

$$\partial^2\Gamma/\partial\phi_2^2 = -2g-2(\phi_1-\phi_2)(\partial g/\partial\phi_2)+\phi_1\phi_2(\partial^2 g/\partial\phi_2^2) \qquad (3.1)$$

which is identical to eq 1.23. In order to obtain accurate values of the interaction function, the approach taken in this dissertation was to obtain g from the $\partial^2\Gamma/\partial\phi_2^2$ data using Koningsveld's empirical form of g (eq 1.39).

Substituting eq 1.39 into eq 3.1 provides for the analytical relationship between $\partial^2\Gamma/\partial\phi_2^2$ and g as [69]

$$\partial^2\Gamma/\partial\phi_2^2 = (2g_1-2g_0) + (6g_2-6g_1)\phi_2 - 12g_2\phi_2^2 \qquad (3.2)$$

where g_0, g_1, and g_2 are the coefficients of the empirical interaction function. The $\partial^2\Gamma/\partial\phi_2^2$ values were calculated

from the scattering data according to eq 1.44 and fit to equation 3.2 using a computer algorithm which weights the error in each value of $\partial^2\Gamma/\partial\phi_2^2$ before assigning the best fit of the data. The interaction function was then generated from the g coefficients determined by the fitting algorithm and the definition of g given by eq 1.39.

Computer programs were written by this author to calculate the following quantities: program CHI to calculate $\partial^2\Gamma/\partial\phi_2^2$ from the R(0) values, program POLYFT and GFUN to calculate g_0, g_1, and g_2 from the composition dependence of $\partial^2\Gamma/\partial\phi_2^2$ data, and program GCALC to obtain g from the coefficients g_0, g_1, and g_2. These programs are provided in Appendix II.

PS / POCS Results and Discussion. The phase diagram for the PS(50)/POCS(81) blend system was obtained by Gilmer [7], and is reproduced in Figure 3.1. From the phase diagram in Figure 3.1 it can be seen that the blend exhibits LCST behavior; upon heating the homogeneous material decomposes into two phases. Zacharius [4,5] has used the equation-of-state theory to predict that PS/POCS blends will exhibit both LSCT and UCST behavior for suitably chosen molar masses of each components. Ryan [3] has also observed an hourglass phase diagram for PS/POCS which suggests that the UCST and LCST have merged. For the PS(50)/POCS(81) blend system the molar mass of the

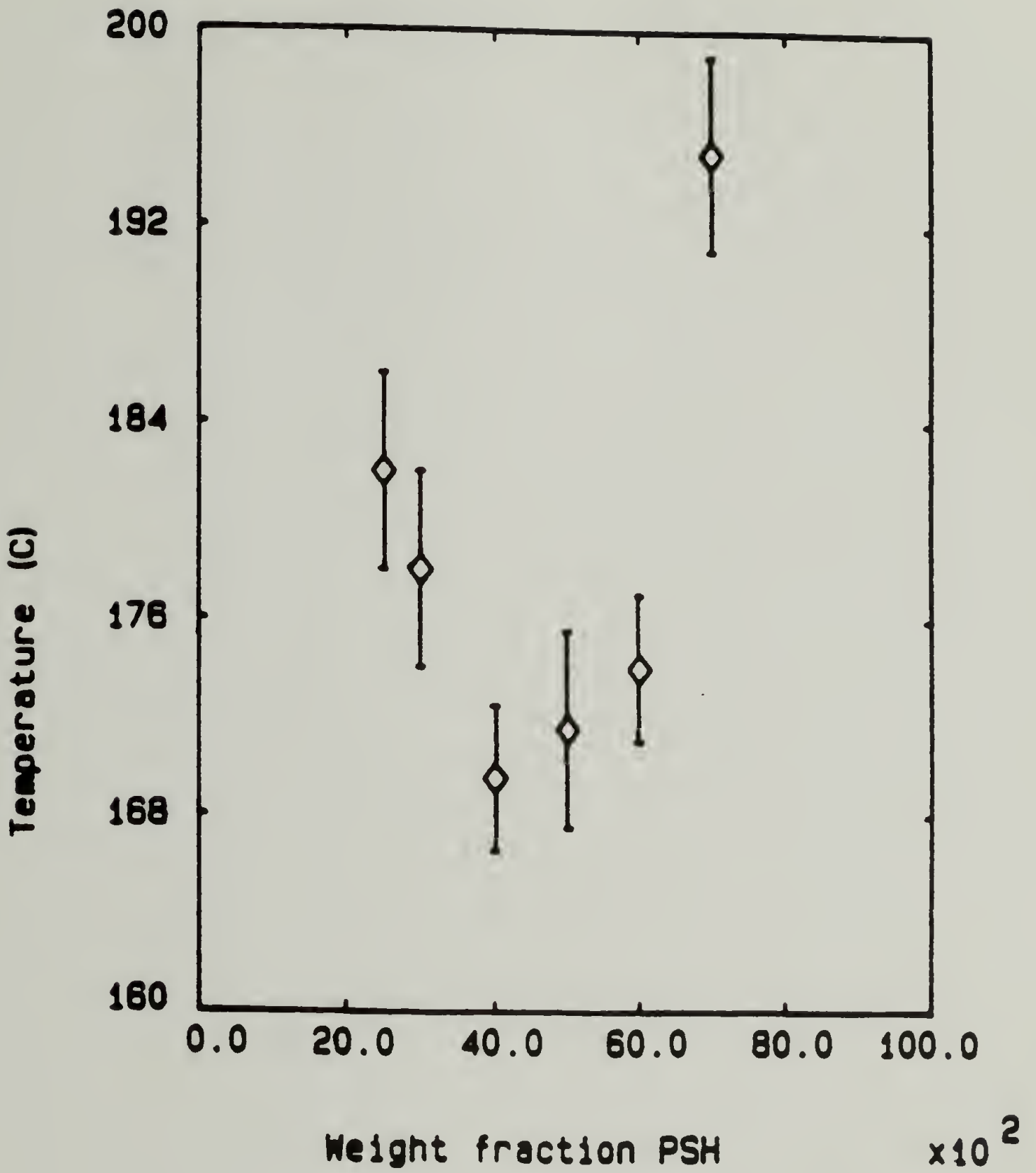

Figure 3.1 Cloud Point Phase Diagram for the Blend of PSD(50)/POCS(81)

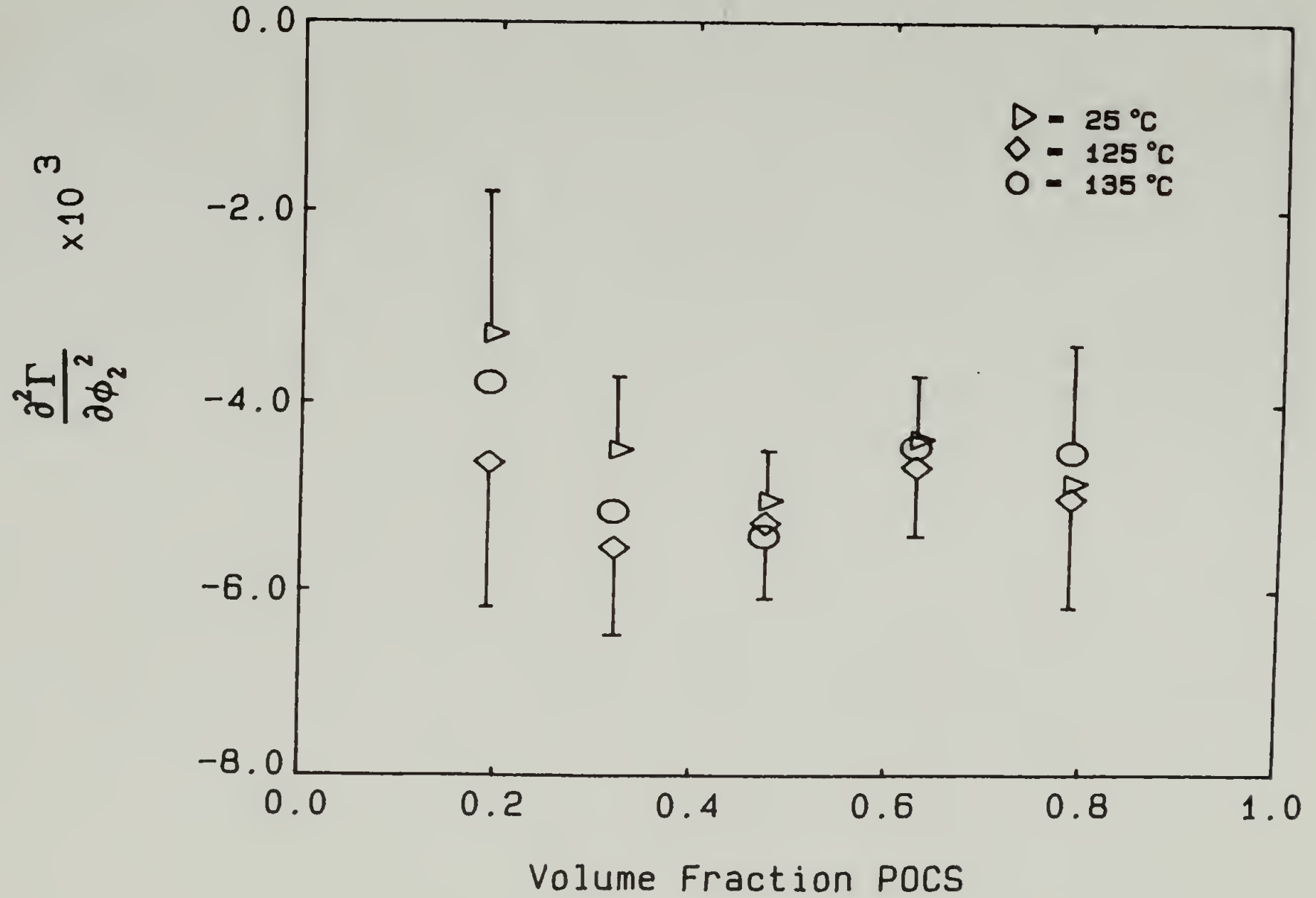

Figure 3.2 Composition Dependence of $\partial^2\Gamma/\partial\phi_2^2$ for PSD(30.5)/POCS(65.4) at All Temperatures

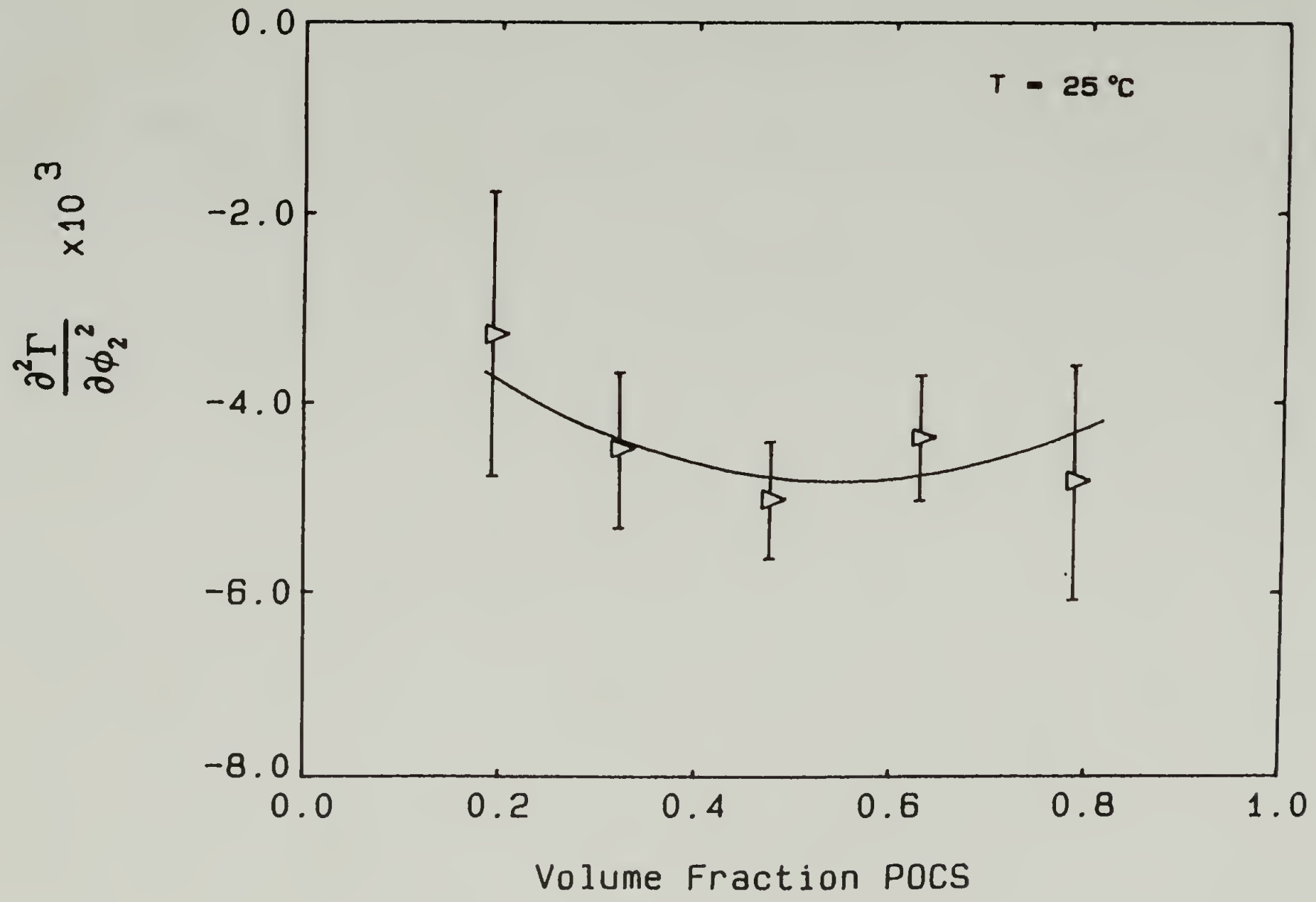

Figure 3.3 Composition Dependence of $\partial^2\Gamma/\partial\phi_2^2$ for PSD(30.5)/POCS(65.4) at 25°C

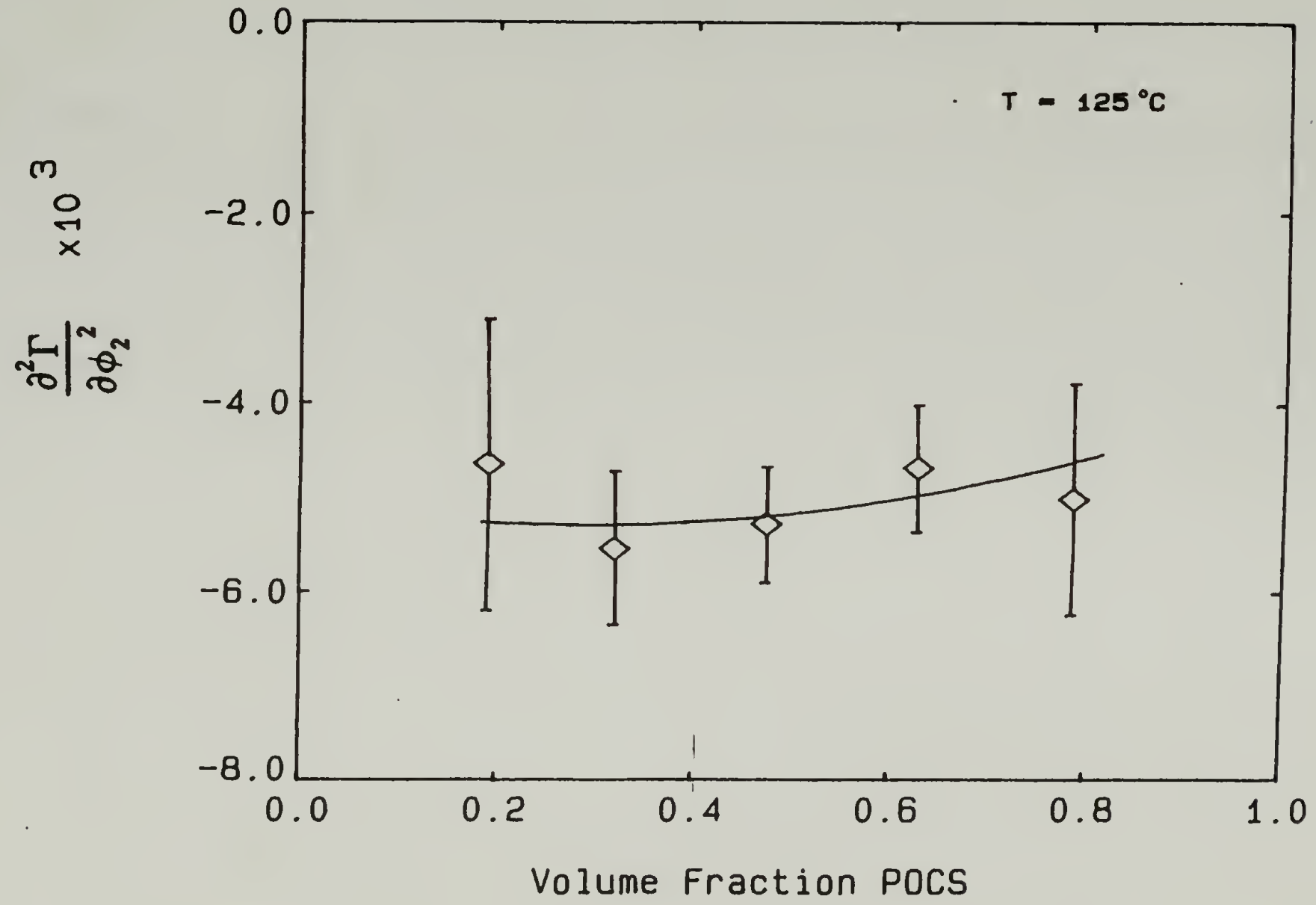

Figure 3.4 Composition Dependence of $\partial^2\Gamma/\partial\phi_2{}^2$ for PSD(30.5)/POCS(65.4) at 125°C

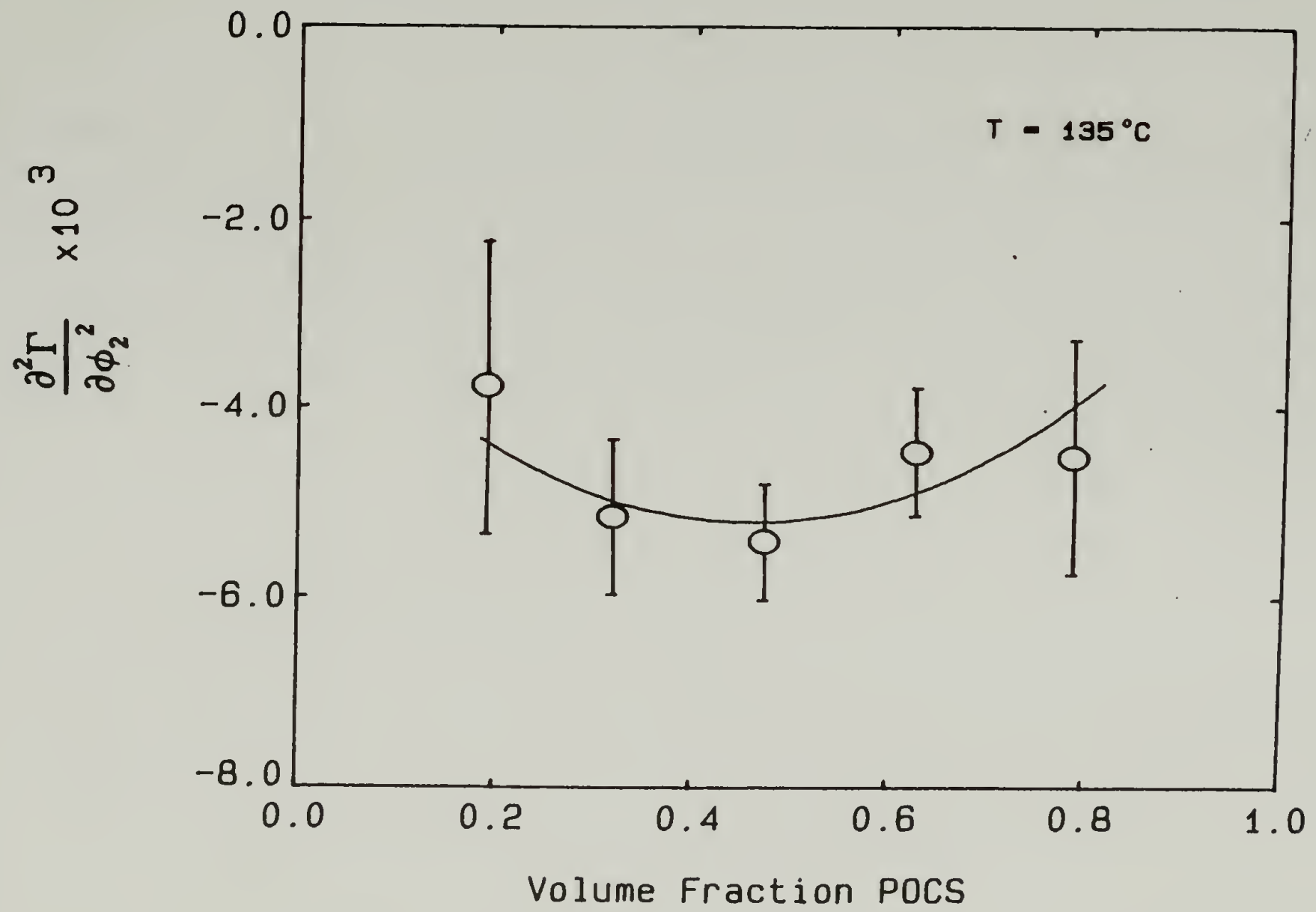

Figure 3.5 Composition Dependence of $\partial^2\Gamma/\partial\phi_2{}^2$ for PSD(30.5)/POCS(65.4) at 135^{o}C

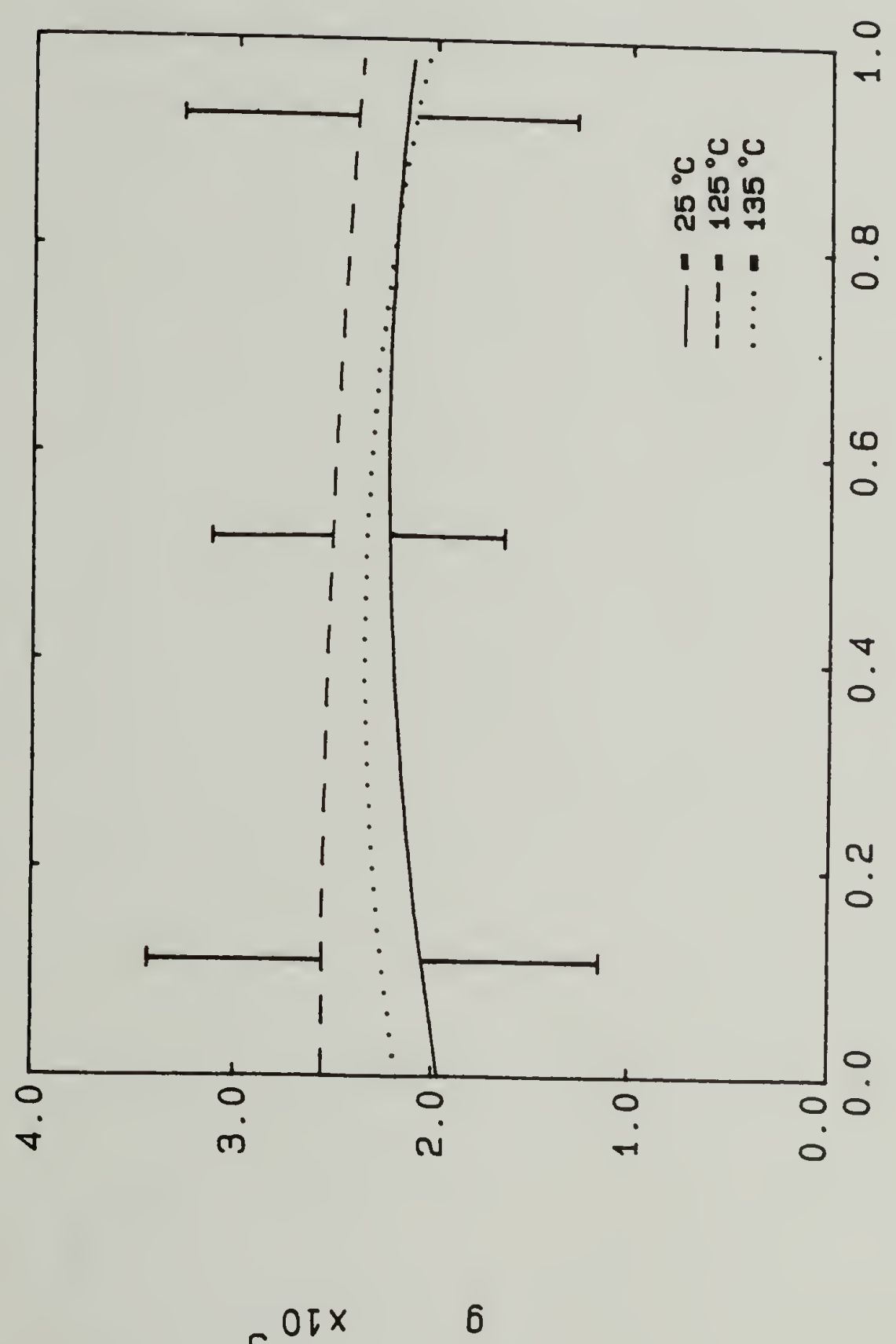

Figure 3.6 Composition Dependence of the Interaction Function for PSD(30.5)/POCS(65.4) at All Experimental Temperatures

Table 3.1

Molecular Parameters of Poly(styrene) and Poly(o-chlorostyrene)

Molecular Mass (g mol^{-1})		
	PSD Monomer	112.20 ± 0.01
	POCS Monomer	138.60 ± 0.02
	PSD Polymer	30,500
	POCS Polymer	65,400
Coherent Scattering Length (10^{12} cm)		
	PSD	10.656 ± 0.015
	POCS	3.662 ± 0.025

Gravemetric Density (g cm^{-3})

Temperature (^{o}C)	PSD	POCS
25	1.132	1.246
125	1.096	1.218
135	1.090	1.213

Table 3.2

Calculated Values of $\partial^2\Gamma/\partial\Phi_2^2$ and the

Interaction Coefficients for PSD(30.5)/POCS(65.4)

Volume Fraction		$\partial^2\Gamma/\partial\phi^2$ (10^3)			Deviation (10^3)
PSD	POCS	25	125	135	
0.80	0.20	-3.28	-4.64	-3.78	1.54
0.68	0.32	-4.51	-5.53	-5.15	0.82
0.52	0.48	-5.04	-5.27	-5.41	0.61
0.37	0.63	-4.38	-4.68	-4.47	0.67
0.21	0.79	-4.85	-5.01	-4.51	1.23

Temperature (^oC)	Interaction Coefficient (10^3)		
	g_0	g_1	g_2
25	1.97	0.90	-0.76
125	2.56	0.04	-0.23
135	2.18	0.81	-0.97

components is sufficiently small such that only LCST behavior is observed. The SANS measurements were performed upon the PSD(10.5)/POCS(65.4) blend system, and from the phase diagram given in Figure 3.1, this blend system should be miscible up to 160°C or higher.

The enthalpy correction term $\partial^2\Gamma/\partial\phi_2^2$ was determined for the PSD(30.5)/POCS(65.4) system from the R(0) values contained in Table 2.4 and the molecular parameters for blend pure components listed in Table 3.1. In Figure 3.2 the calculated values of $\partial^2\Gamma/\partial\phi_2^2$ as a function of blend composition for all three experimental temperatures are plotted.

The composition dependence of $\partial^2\Gamma/\partial\phi_2^2$ at 25°, 125°, and 135°C are plotted in Figures 3.3-3.5. The solid lines in Figures 3.3-3.5 represent the best fit of the data according to eq 3.2 and the resulting coefficients g_0, g_1, and g_2 are listed in Table 3.2. The calculated interaction functions are plotted in Figure 3.6. From Figure 3.6 it can be seen that the interaction function obtained at the three experimental temperatures is both composition and temperature-independent.

Russell and Stein [6] had previously determined the Flory interaction parameter, χ, for a dilute solution of PSD(114) in POCS(220). From a SANS determination of an expanded PSD(114) radius-of-gyration and a χ value less than zero, these authors concluded that the POCS made a

good solvent for PSD. This result contrasts with the interaction function for concentrated PS/POCS blends measured in this study where g > 0. Several possible explanations exist for the difference between Russell's results and the results presented here: 1) due to the large error of Russell's measurements the Rg and χ values reported may be in error; 2) in dilute solution PSD/POCS blends have g < 0 and the interaction function is concentration dependent, but the concentrated solution studies presented here do not measure this effect.

The first possible explanation arises because of the large error reported by Russell [6] for the measurement of the second virial coefficient. Also, the determination of an expanded Rg for the blend system was based upon measurement of the PSD(114) Rg in the blend and calculation of a Rg in the bulk. A more accurate determination of the Rg in the bulk by a SANS measurement would have been more satisfactory. These two concerns cast doubt upon the accuracy of the dilute solution measurement of χ being negative.

The possibility certainly exists that the concentrated SANS measurements of g obtained in this study have missed the concentration dependent region. There is evidence in PVF_2/PMMA amorphous blends that χ is concentration dependent in dilute solutions and concentration independent in concentrated solutions [75]. The PVF_2/PMMA

system is somewhat different from the PS/POCS system in that the PVF_2/PMMA blend exhibited $\chi < 0$ over all compositions while the PS/POCS blend shows no such specific interactions in the concentrated blends. Also, the PVF_2/PMMA results indicated that if g were concentration dependent, measurements of the 80/20 or 20/80 PSD(30.5)/POCS(65.4) blends should have detected such behavior.

The temperature independence of the interaction function seen in Figure 3.6 supports the critical double point hypothesis put forth by Zacharius [4,5] for the PS/POCS blend system. This result will be discussed further in the equation-of-state section of this chapter.

PS / PαMS Results and Discussion. An estimate of the miscibility of poly(styrene) in poly(α-methylstyrene) was obtained by the DSC annealing study reported in this investigation. The results from the DSC annealing study (Table 2.2) show that the PSH(233)/PαMS(30) blend has equilibrium miscibility at 227°C. Previous investigations of the PS/PαMS glass transition also found compatibility for blends where the components have molar masses less than 50,000 [15,76]. The preliminary optical microscopy and cloud point experiments performed in this investigation confirm the DSC annealing results; phase separation is found to occur slowly at 230°C for the

PS(>50)/PαMS(>50) blends. Therefore, it was assumed that the PSD(10.7)/PαMS(30) blends used in the SANS experiments were miscible.

The PSD(10.7)/PαMS(30) $\partial^2\Gamma/\partial\phi_2^2$ values were calculated from the zero-angle Rayleigh ratios contained in Table 2.5 as well as the PS and PαMS molecular parameters given in Table 3.3. The measured $\partial^2\Gamma/\partial\phi_2^2$ values are listed in Table 3.4 and plotted as a function of composition in Figure 3.7. The solid line drawn in Figure 3.7 represents fit of the data to eq 3.2 and the coefficients g_0, g_1, and g_2 are also given in Table 3.4. The calculated interaction function at 25°C is plotted in Figure 3.8.

From the DSC annealing study it is possible to obtain an estimate of the critical value of the interaction function, g_c, which represents the largest value g can achieve before equilibrium miscibility is no longer possible. For the purposes of calculation, the interaction function is assumed to have no composition dependence and g_c is then obtained from eq 1.24 and 1.23 as [77]

$$g_c = \frac{1}{2}\left(y_{w,1}^{-1/2} + y_{w,2}^{-1/2} \right) \qquad (3.4)$$

where $y_{w,i}$ is the weight average degree of polymerization of component i. The miscible blend of PSD(233)/PαMS(30)

Table 3.3

Molecular Parameters of Poly(styrene)
and Poly(α-methylstyrene) Molecular Parameters

Molar Mass (g mol^{-1})	
PSD Monomer	112.20 ± 0.01
PαMS Monomer	118.18 ± 0.01
PSD Polymer	10,700
PαMS Polymer	23,000
Coherent Scattering Length (10^{12} cm)	
PSD	10.656 ± 0.015
PαMS	2.245 ± 0.015

Table 3.4

Calculated Values of $\partial^2\Gamma/\partial\phi_2^2$ and the Interaction Coefficients for PSD/PαMS Blends

PSD(10.7)/PαMS(30)

Volume Fraction PαMS	$\partial^2\Gamma/\partial\phi_2^2$ (10^2)	Deviation (10^3)
.083	-2.23	2.0
.456	-.63	2.0
.615	-.30	2.0
.677	-.32	2.0
.687	-.33	2.0
.784	-.39	2.0
.860	-.47	2.0

Interaction coefficients 10^2

q_0	.634
q_1	-.764
q_2	.437

Polymer Blend	Volume Fraction PαMS	$\partial^2\Gamma/\partial\phi_2^2$ (10^2)	Deviation (10^3)
PS(10.7)/ PαMS(25)	.517	-.28	2.0
PS(10.7)/ PαMS(75)	.517	-.20	2.0
PS(10.7)/ PαMS(139)	.514	-.18	2.0

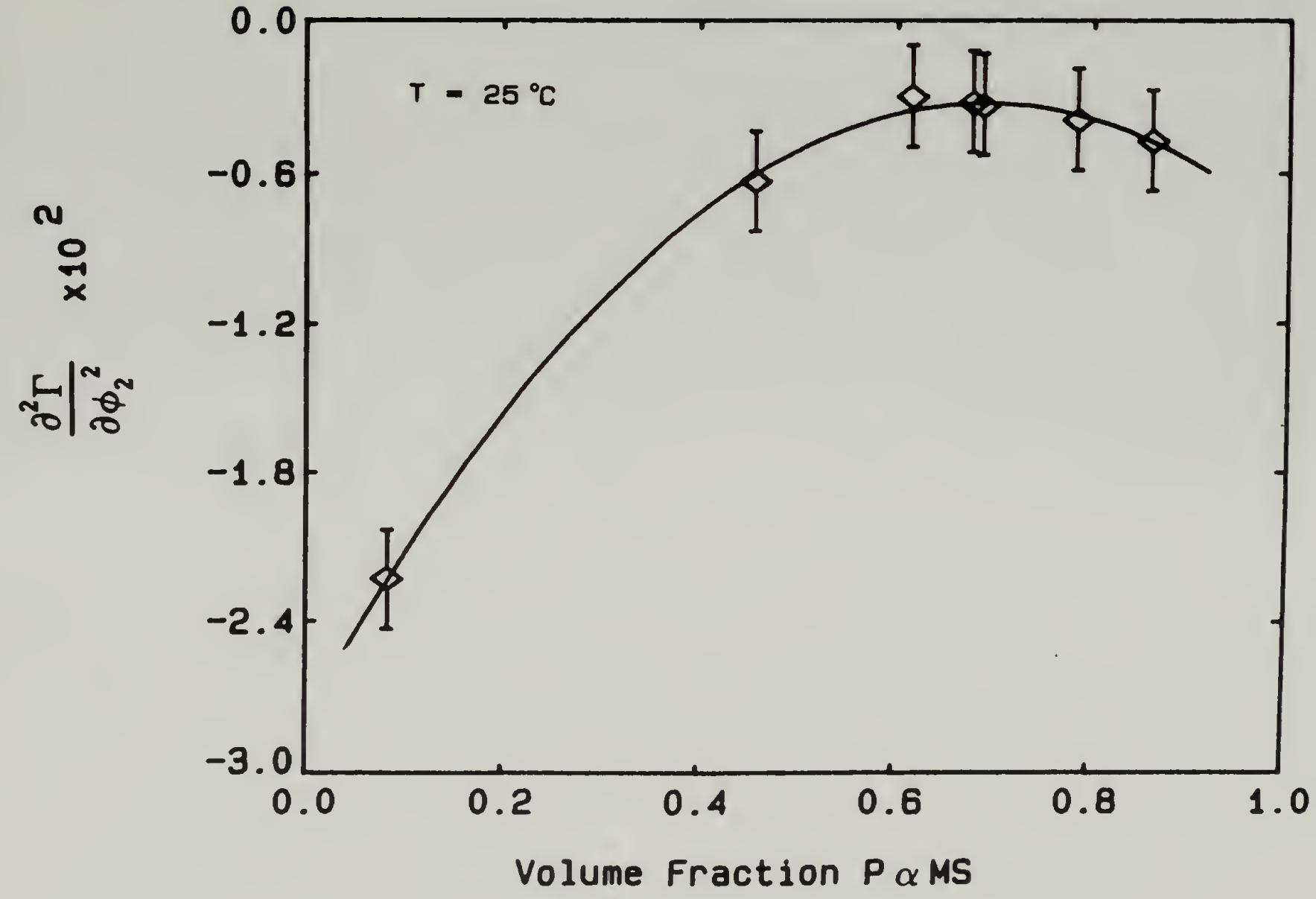

Figure 3.7 Composition Dependence of $\partial^2\Gamma/\partial\phi_2^2$ for PSD(10.7)/PαMS(30) at 25°C

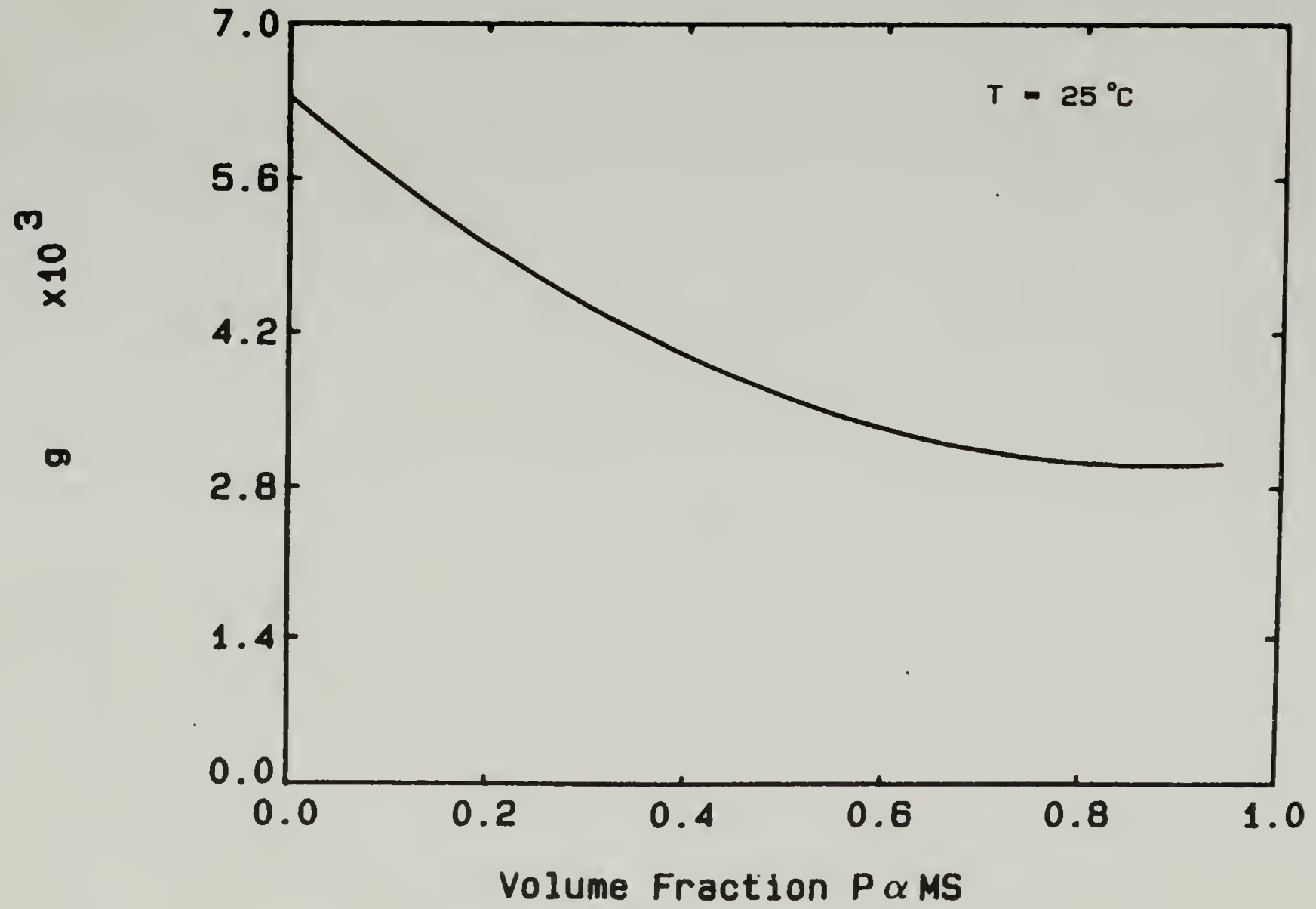

Figure 3.8 Composition Dependence of the Interaction Function for PSD(10.7)/PαMS(30) at 25°C

sets the lower limit of q_c as 1.61×10^{-2}. All values of q reported for the PSD(10.7)/PαMS(30) blends are below this estimate of the critical value.

The concentration dependence of the PSD(10.7)/PαMS(30) interaction function indicates that blends dilute in PαMS have reduced miscibility (a more positive q value) compared with other compositions of the blend. This concentration dependence agrees with Wunderlich's [15] previous DSC examination of all combinations of high, medium and low molar mass mixtures of PS with PαMS. Wunderlich's study concluded that poly(styrene) showed solubility in poly(α-methylstyrene) to a much higher molar mass than ploy(α-methylstyrene) showed in poly(styrene) rich mixtures. The results presented here also show that for equivalent changes in molar mass of either component, the critical value of the interaction function will initially intersect the measured value of q (plotted in Figure 3.8) for blends dilute in poly(α-methylstyrene).

Experimental difficulties arose in measuring the PSD(10.7)/PαMS(30) interaction function at temperatures above the glass transition. The neutron scattering measurements at 25°C represent the concentration fluctuations frozen in at the blend Tg, which depend upon the blend composition. Therefore, there is some uncertainty as to the temperature equivalence of the data

obtained for different blend compositions. Also, the region of highest concentration dependence in Figure 3.7 is defined by a small number of data points.

PS / PVME Results and Discussion. The phase diagram for the PSD(233)/PVME(99) blend was determined from light and neutron scattering cloud point experiments by Yang [13], and this diagram is reproduced in Figure 3.9. The PSD(233)/PVME(99) blend exhibits LCST behavior, and although UCST behavior has been reported for some PSH/PVME blends, no such behavior was observed in these samples.

The enthalpy correction term, $\partial^2\Gamma/\partial\phi_2^2$ was determined from the zero-angle Rayleigh ratios measured by Yang [13] which are contained in Table 2.6. The importance of Yang's SANS data is that measurements were taken over a wide range of sample compositions and experimental temperatures.

Provided with the molecular constants for PSD and PVME given in Table 3.5, $\partial^2\Gamma/\partial\phi_2^2$ values were obtained from the zero-angle Rayleigh ratios listed in Table 2.6 and they are listed in Table 3.6. Figures 3.10 and 3.11 plot the composition dependence of $\partial^2\Gamma/\partial\phi_2^2$ for the various experimental temperatures. For the sake of clarity, the high temperature data (121^{o}-157^{o}C) and low temperature data (25^{o}-121^{o}C) are plotted on separate graphs. A common curve of the 121^{o}C data is provided in each plot to serve as a reference point.

The measured $\partial^2\Gamma/\partial\phi_2^2$ values for the PSD(233)/PVME(99) blends at temperatures of 25°, 71°, 121°, 131°, 136°, 141°, 147°, 152°, and 157°C are plotted in Figures 3.12-3.20. The solid lines in Figures 3.12-3.20 are the fit of the $\partial^2\Gamma/\partial\phi_2^2$ data according to eq 3.2. The fitted coefficients g_o, g_1, and g_2 are listed in Table 3.7 for all experimental temperatures. The calculated interaction functions are plotted in Figure 3.21 for all experimental temperatures. In order to provide more detail, the high temperature PSD(233)/PVME(99) interaction functions are replotted on a larger scale in Figure 3.22.

Inspection of Figures 3.21 and 3.22 shows that the PSD(233)/PVME(99) interaction function is negative as well as composition and temperature-dependent. The PSD(233)/PVME(99) blends become less miscible (g becomes more positive) with either increasing PVME content or increasing temperature. Also, the interaction function becomes slightly positive for high PVME content blends at high temperatures.

As indicated in eq 1.21 it is not possible to directly compare values of g and χ when there exists a composition dependence, although eq 1.21 could be used to calculate χ from g measurements. The composition dependence in measured by Kwei [12] shows the same trends as was observed for g from the SANS measurements. Yang has

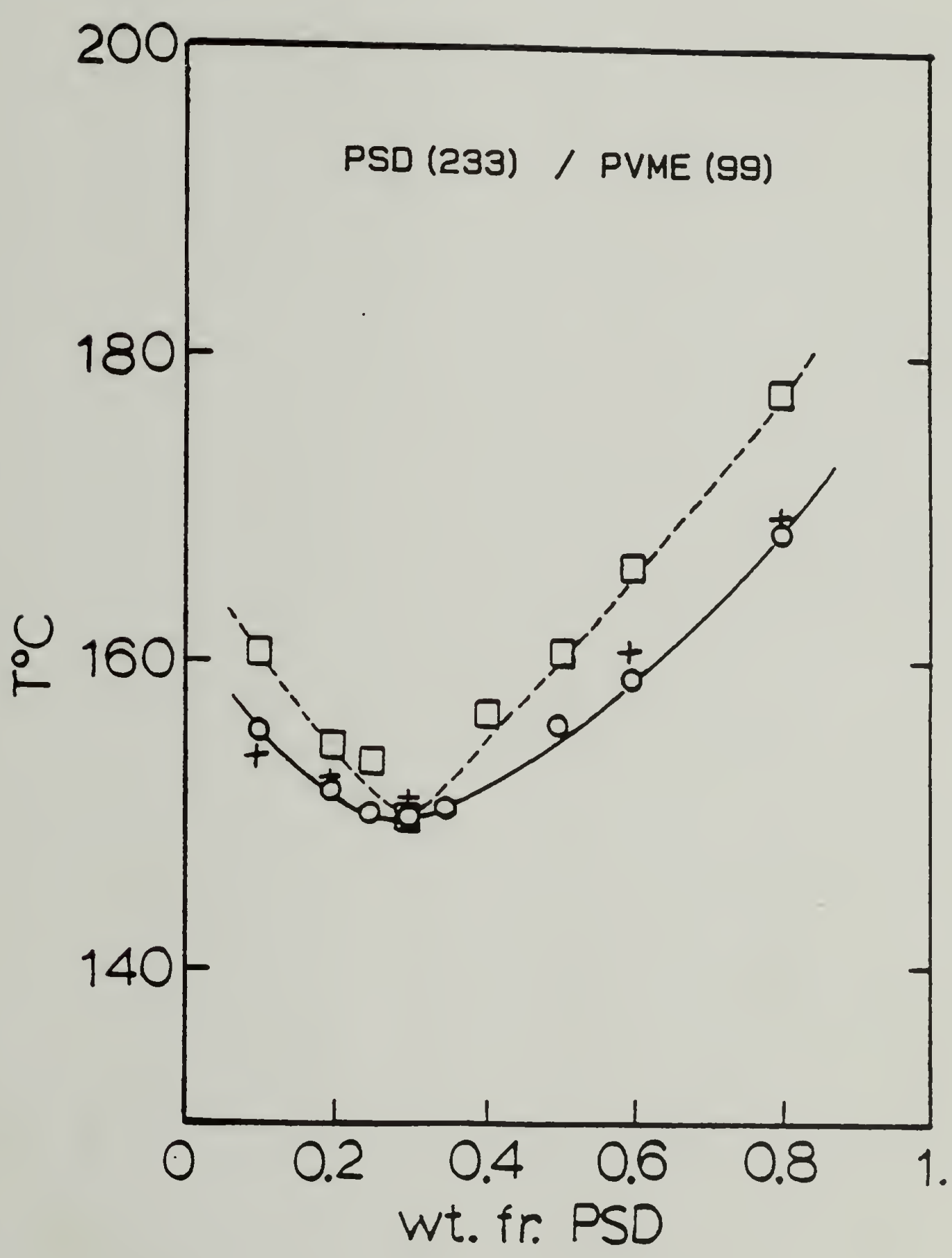

Figure 3.9 Cloud Point Phase Diagram for PSD(233)/PVME(99)

Table 3.5

Molecular Parameters of Poly(styrene)

and Poly(vinylmethylether)

Molar Mass ($g\ mol^{-1}$)	
PSD Monomer	112.20 ± 0.01
PVME Monmer	58.04 ± 0.01
PSD Polymer	255,000
PVME Polymer	99,000
Coherent Scattering Lenght (10^{12} cm)	
PSD	10.656 ± 0.015
PVME	0.330 ± 0.015

Gravimetric Density ($g\ cm^{-3}$)

Temperature ^{o}C	PSD	PVME
25	1.132	1.047
71	1.120	1.018
121	1.099	.987
131	1.093	.980
136	1.090	.977
141	1.087	.974
147	1.083	.970
152	1.081	.967
157	1.078	.964

Table 3.6

Calculated Values of $\partial^2\Gamma/\partial\phi_2^2$ (10^2)

for PSD(233)/PVME(99)

Temperature °C	Volume Fraction PVME in Blend								
	.906	.890	.810	.762	.713	.615	.516	.415	.210
25	7.50			8.11	8.19	8.27			10.00
71	3.65				3.47		5.05		6.07
121						.78	1.47	1.88	2.80
131			.64	.44	.31		.98	1.41	2.27
136	.18		.25	.36	.17	.56	.68		1.87
141	-.03	.16		.11	-.01	.30	.48	.83	1.54
147	-.11	-.11		-.23		.13	.26	.60	
152	-.35		-.23			-.05	0.0	.33	.89
157						-.18	-.11	.09	.70

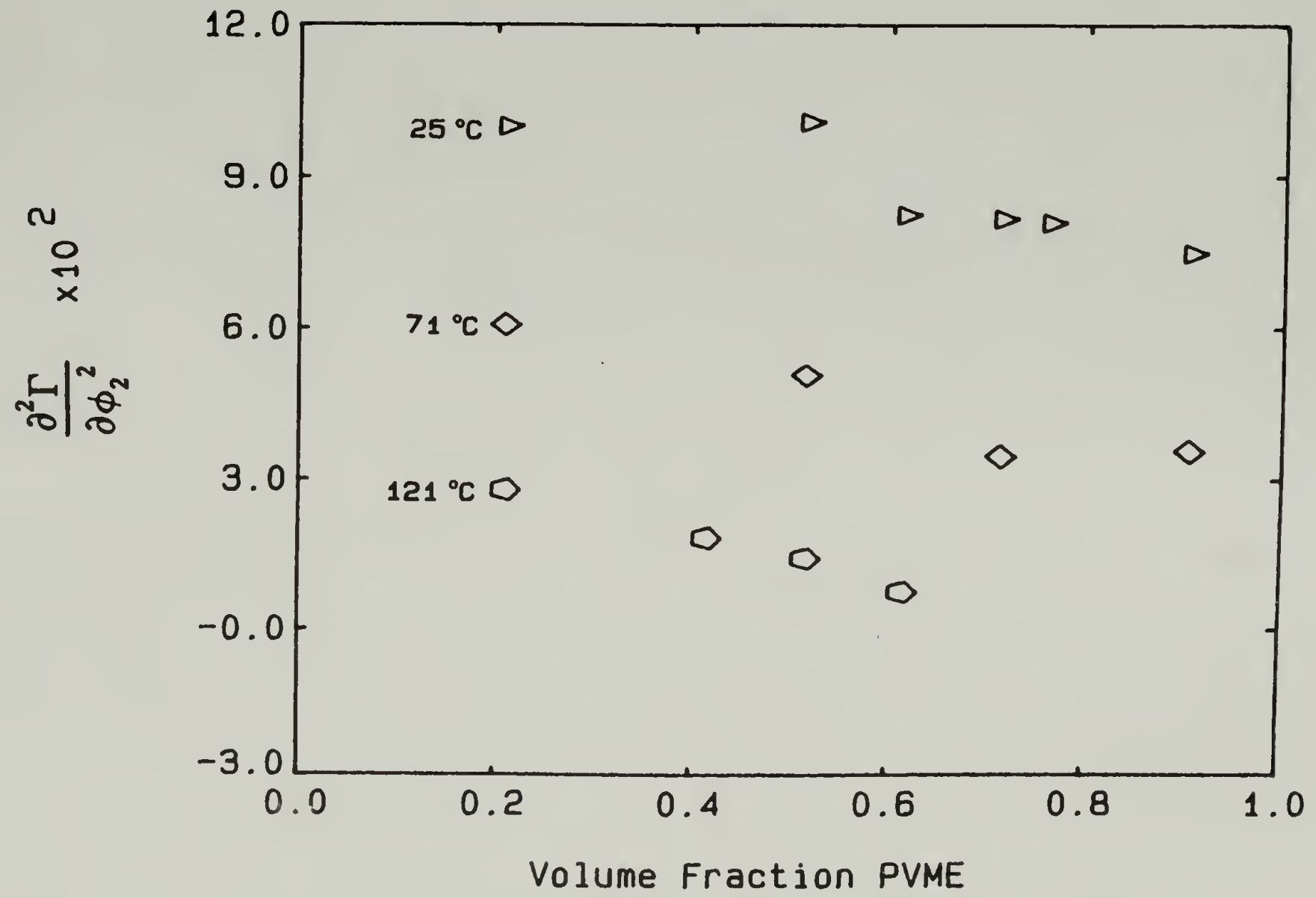

Figure 3.10 Composition Dependence of $\partial^2\Gamma/\partial\phi_2{}^2$ for PSD(233)/PVME(99) at Low Temperatures

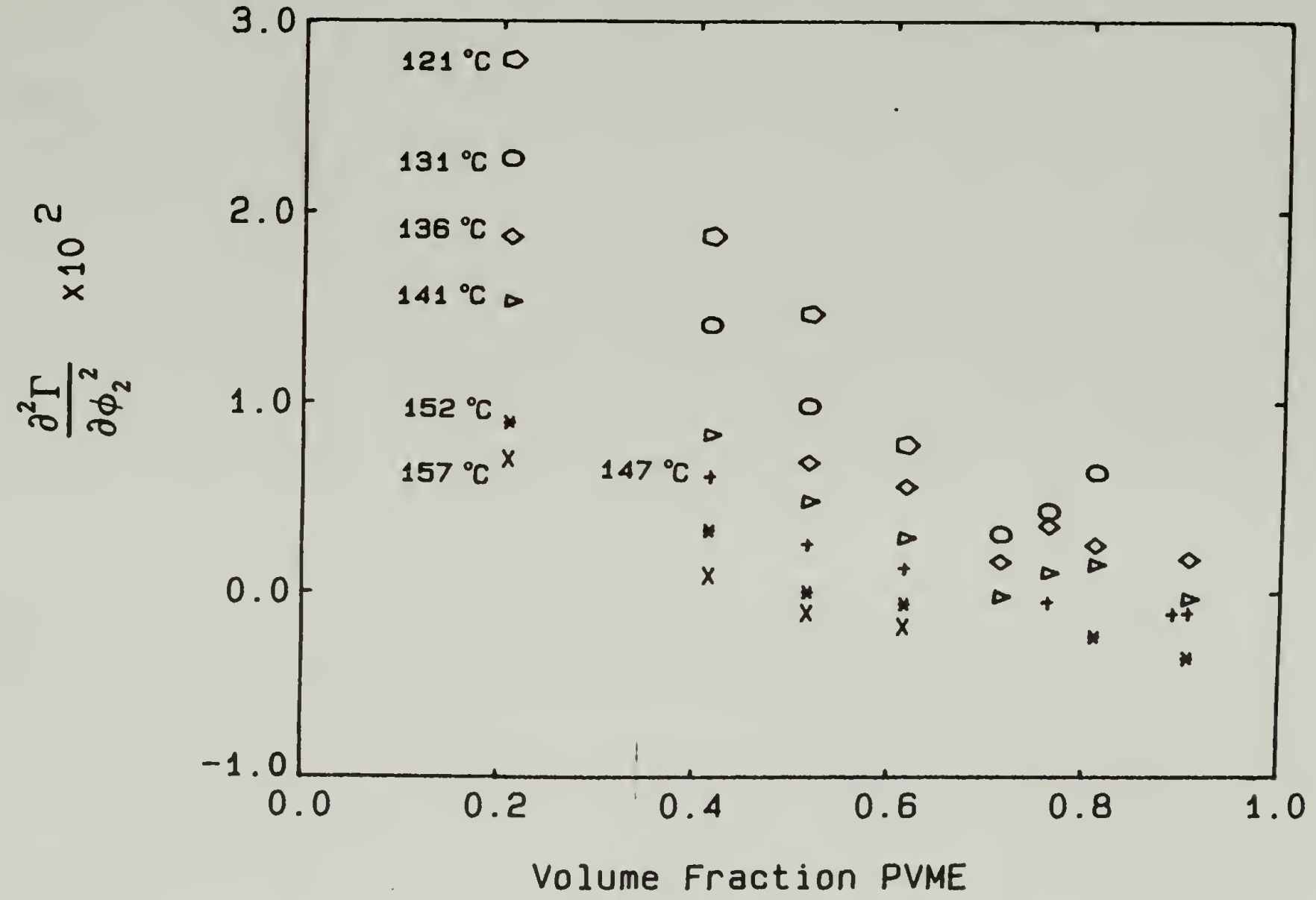

Figure 3.11 Composition Dependence of $\partial^2\Gamma/\partial\phi_2^2$ for PSD(233)/PVME(99) at High Temperatures

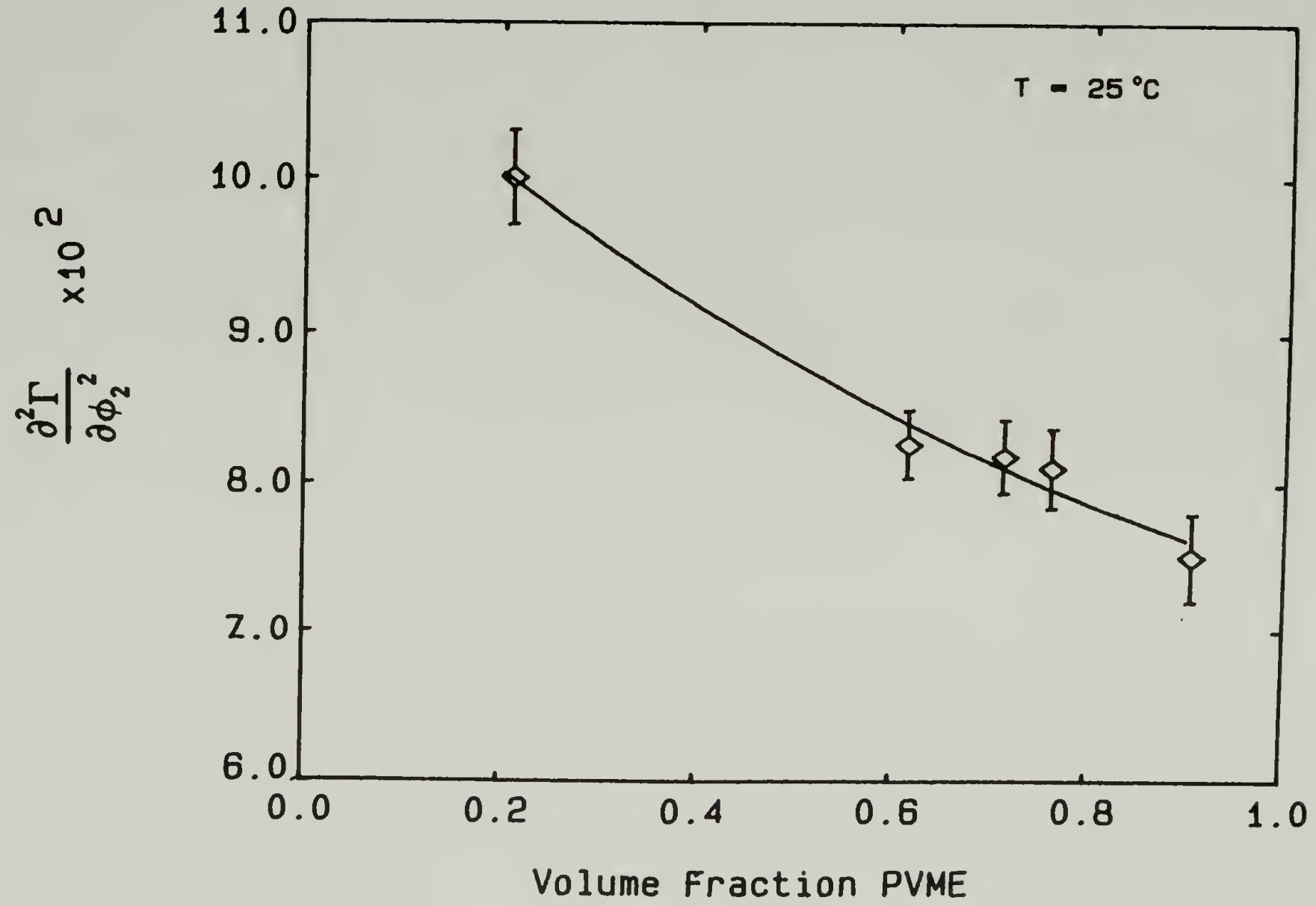

Figure 3.12 Composition Dependence of $\partial^2\Gamma/\partial\phi_2^2$ for PSD(233)/PVME(99) at 25^{o}C

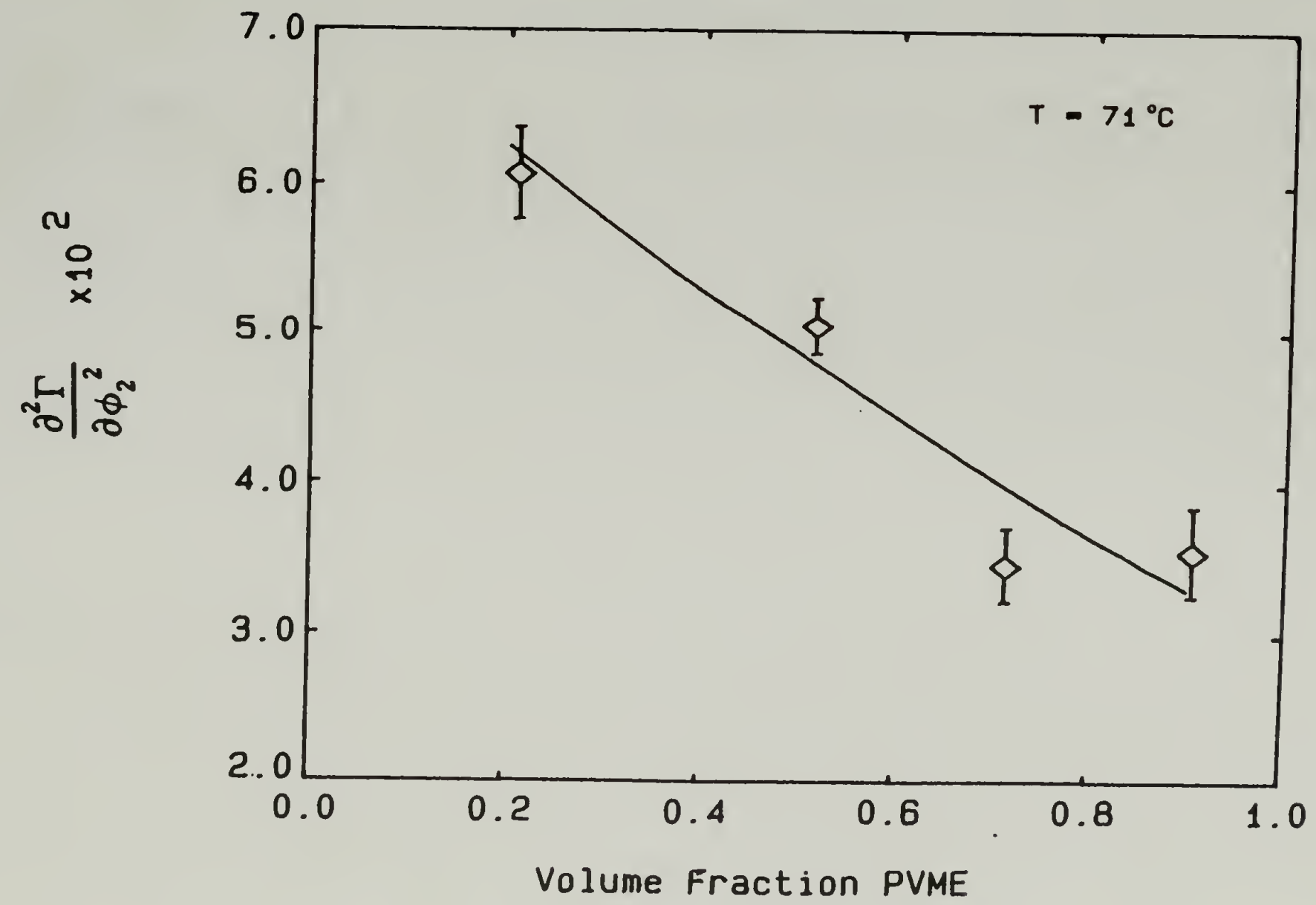

Figure 3.13 Composition Dependence of $\partial^2\Gamma/\partial\phi_2{}^2$ for PSD(233)/PVME(99) at 71^{o}C

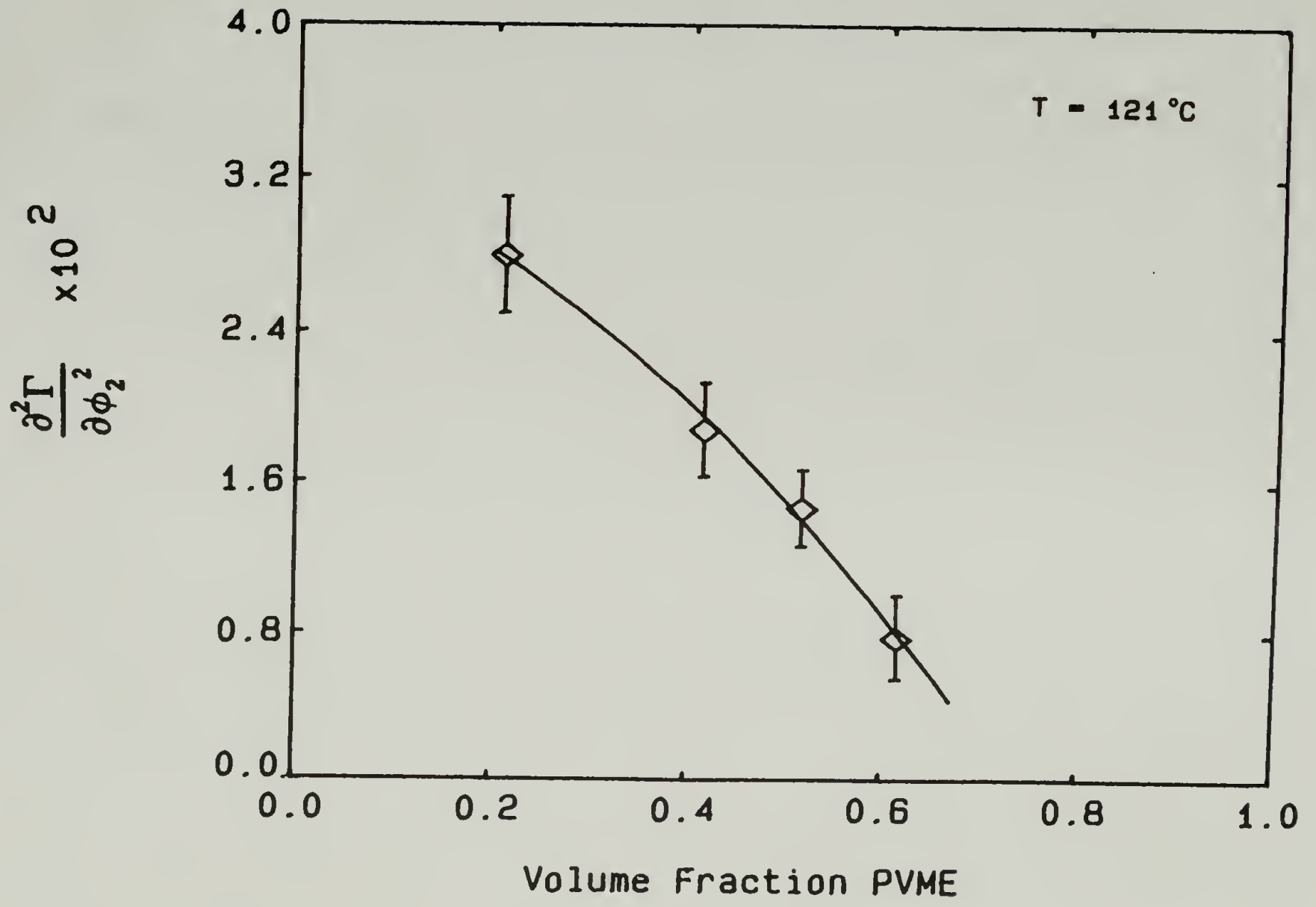

Figure 3.14 Composition Dependence of $\partial^2\Gamma/\partial\phi_2^2$ for PSD(233)/PVME(99) at 121^{o}C

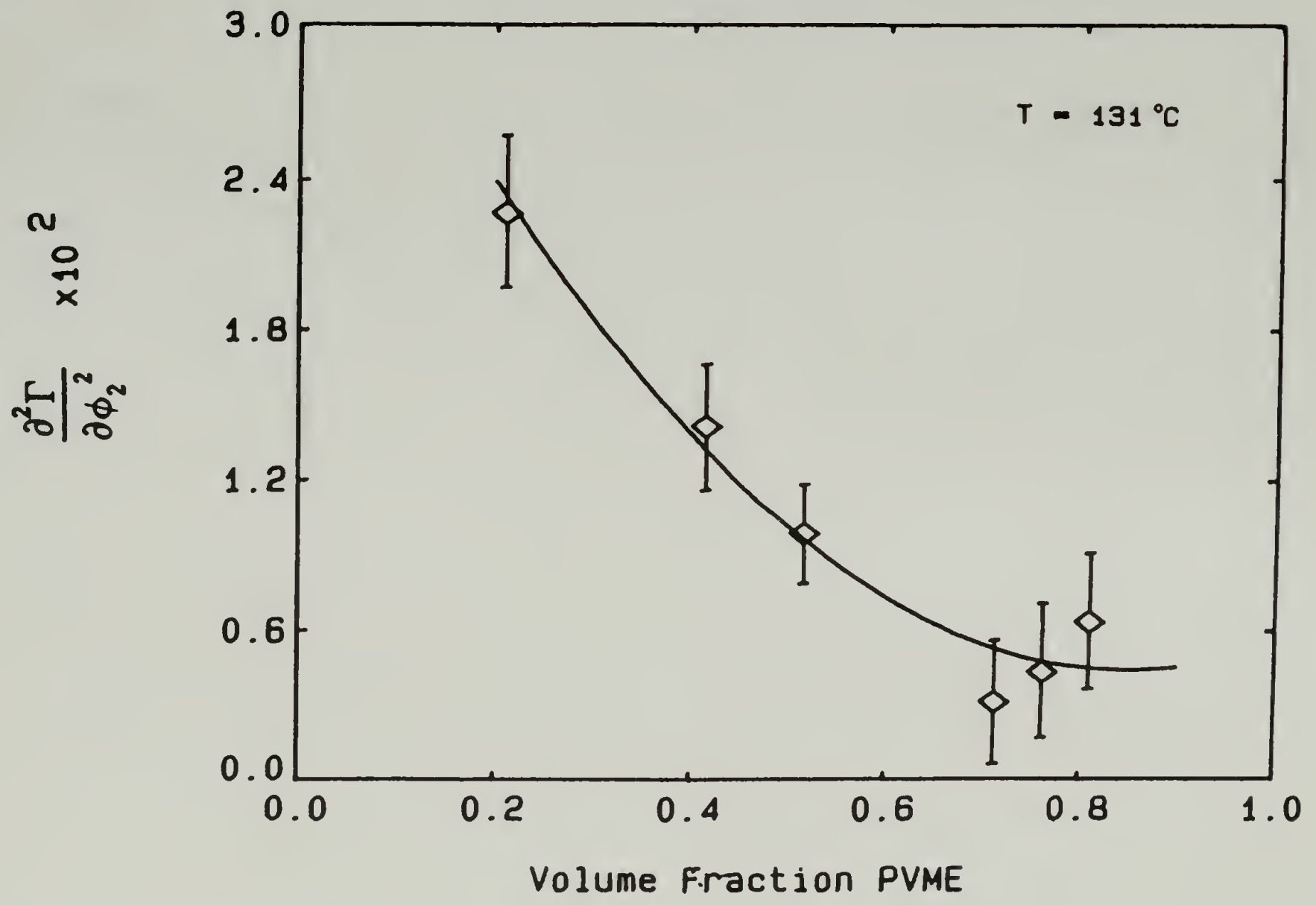

Figure 3.15 Composition Dependence of $\partial^2\Gamma/\partial\phi_2^2$ for PSD(233)/PVME(99) at 131^{o}C

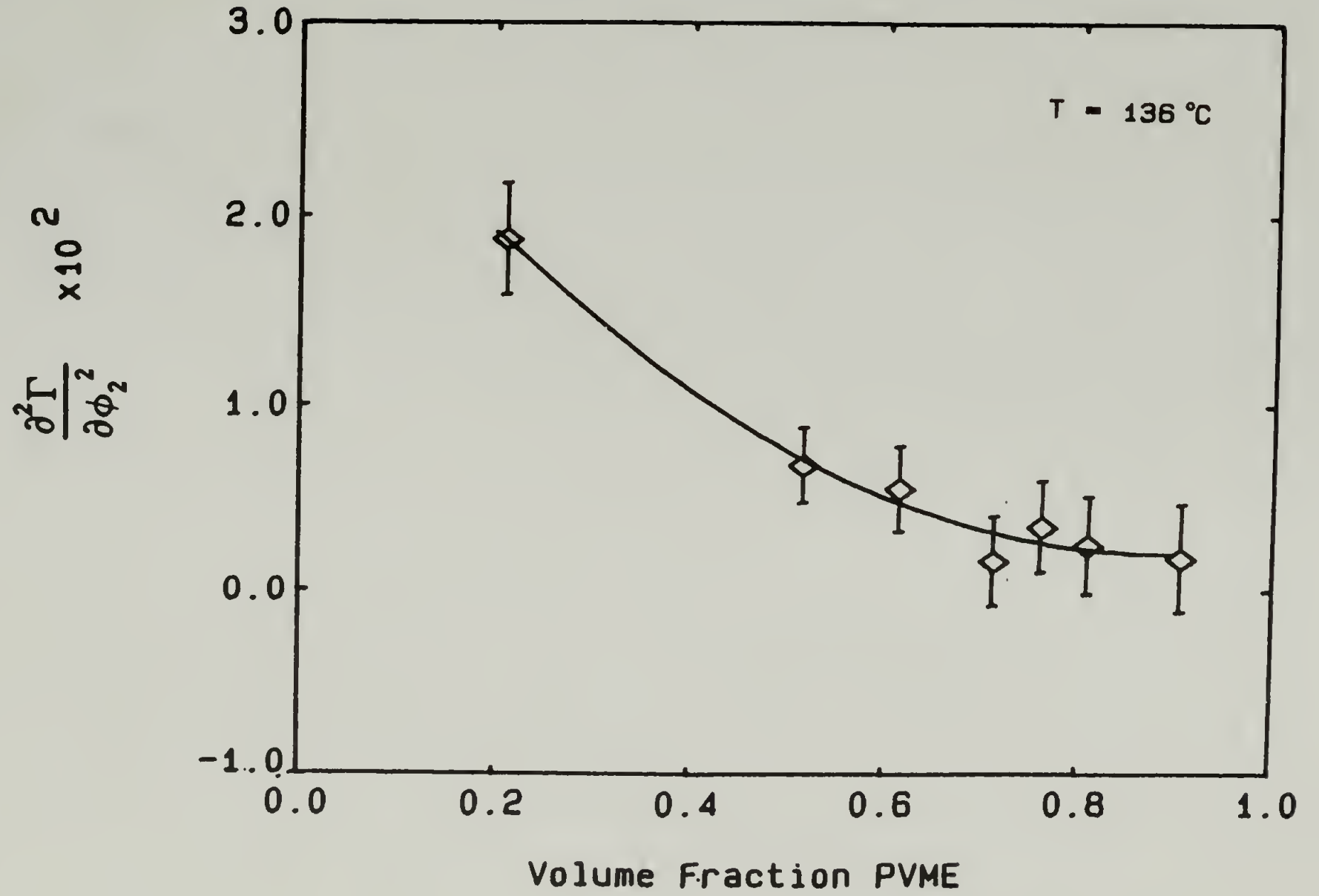

Figure 3.16 Composition Dependence of $\partial^2\Gamma/\partial\phi_2^2$ for PSD(233)/PVME(99) at 136^{o}C

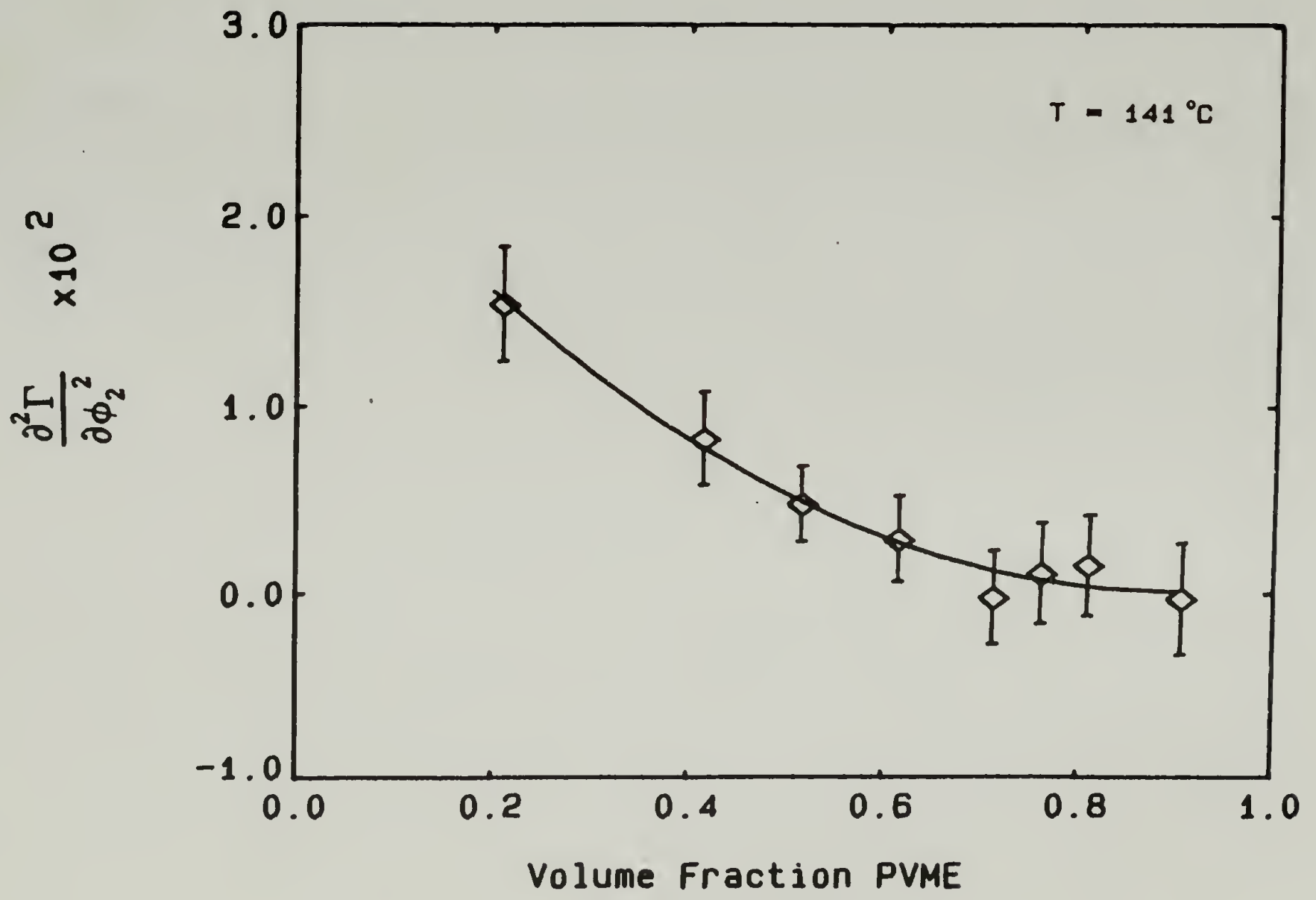

Figure 3.17 Composition Dependence of $\partial^2\Gamma/\partial\phi_2^2$ for PSD(233)/PVME(99) at 141^{o}C

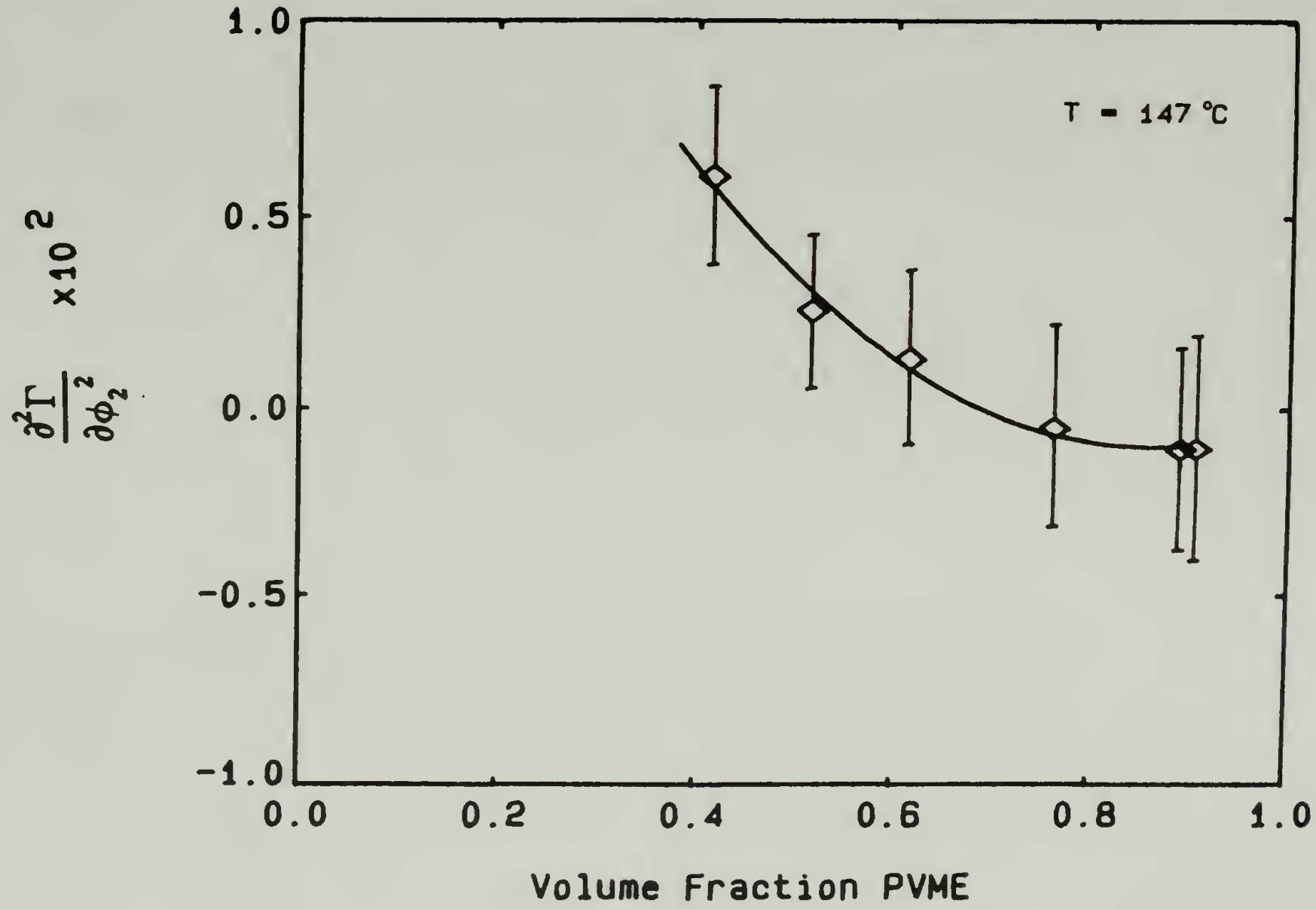

Figure 3.18 Composition Dependence of $\partial^2\Gamma/\partial\phi_2^2$ for PSD(233)/PVME(99) at 147^{o}C

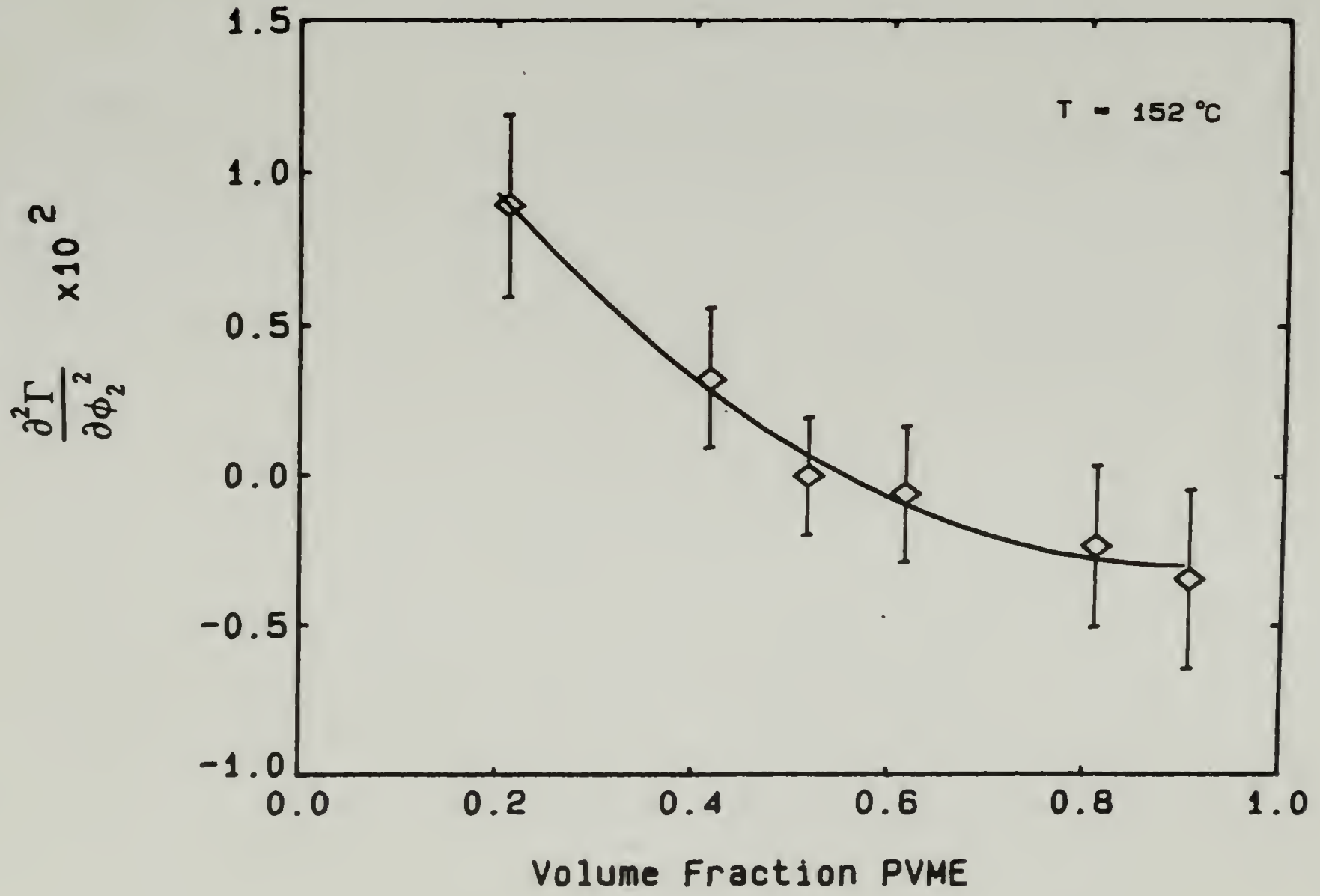

Figure 3.19 Composition Dependence of $\partial^2\Gamma/\partial\phi_2^2$ for PSD(233)/PVME(99) at 152^{o}C

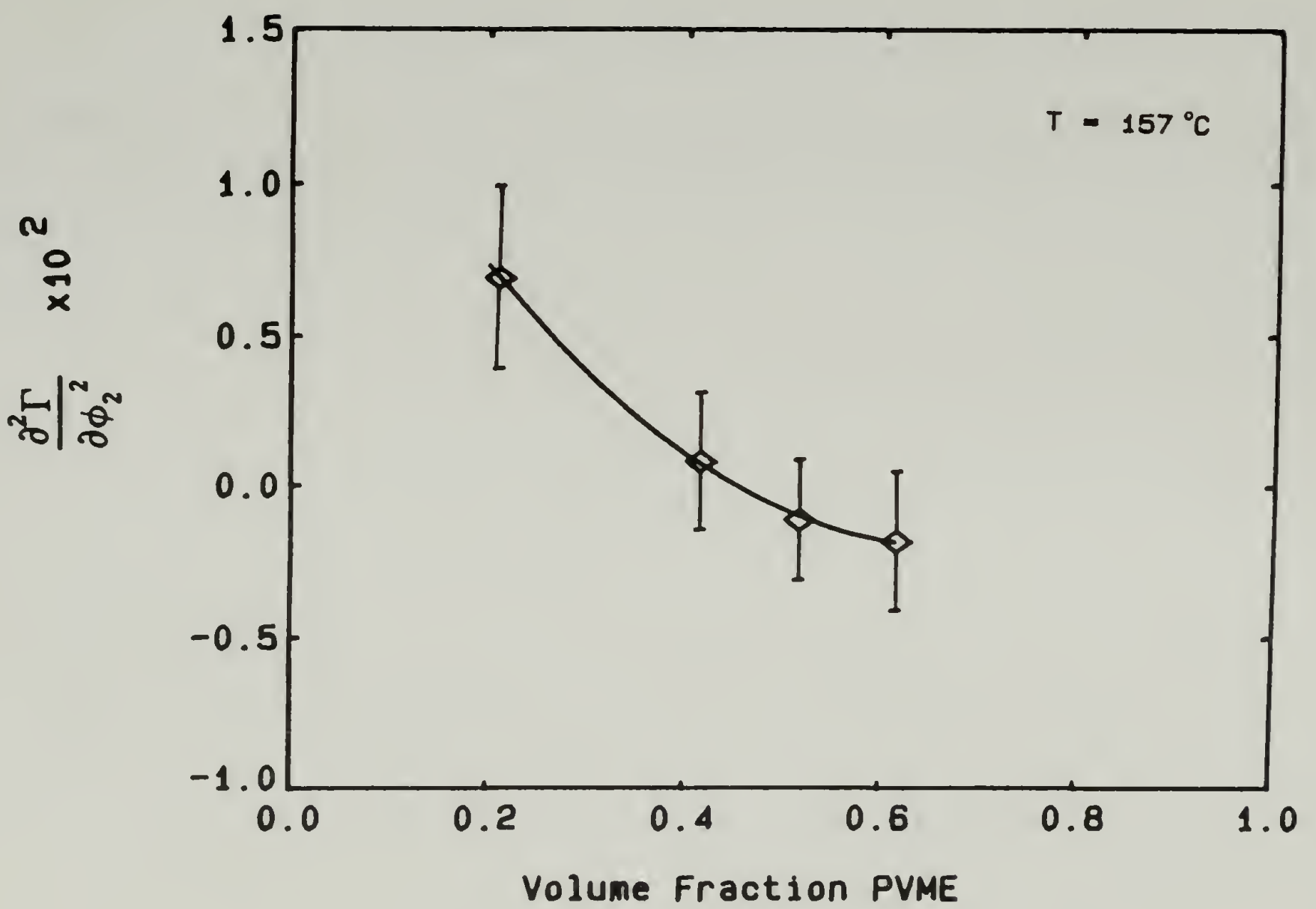

Figure 3.20 Composition Dependence of $\partial^2\Gamma/\partial\phi_2^2$ for PSD(233)/PVME(99) at 157^{o}C

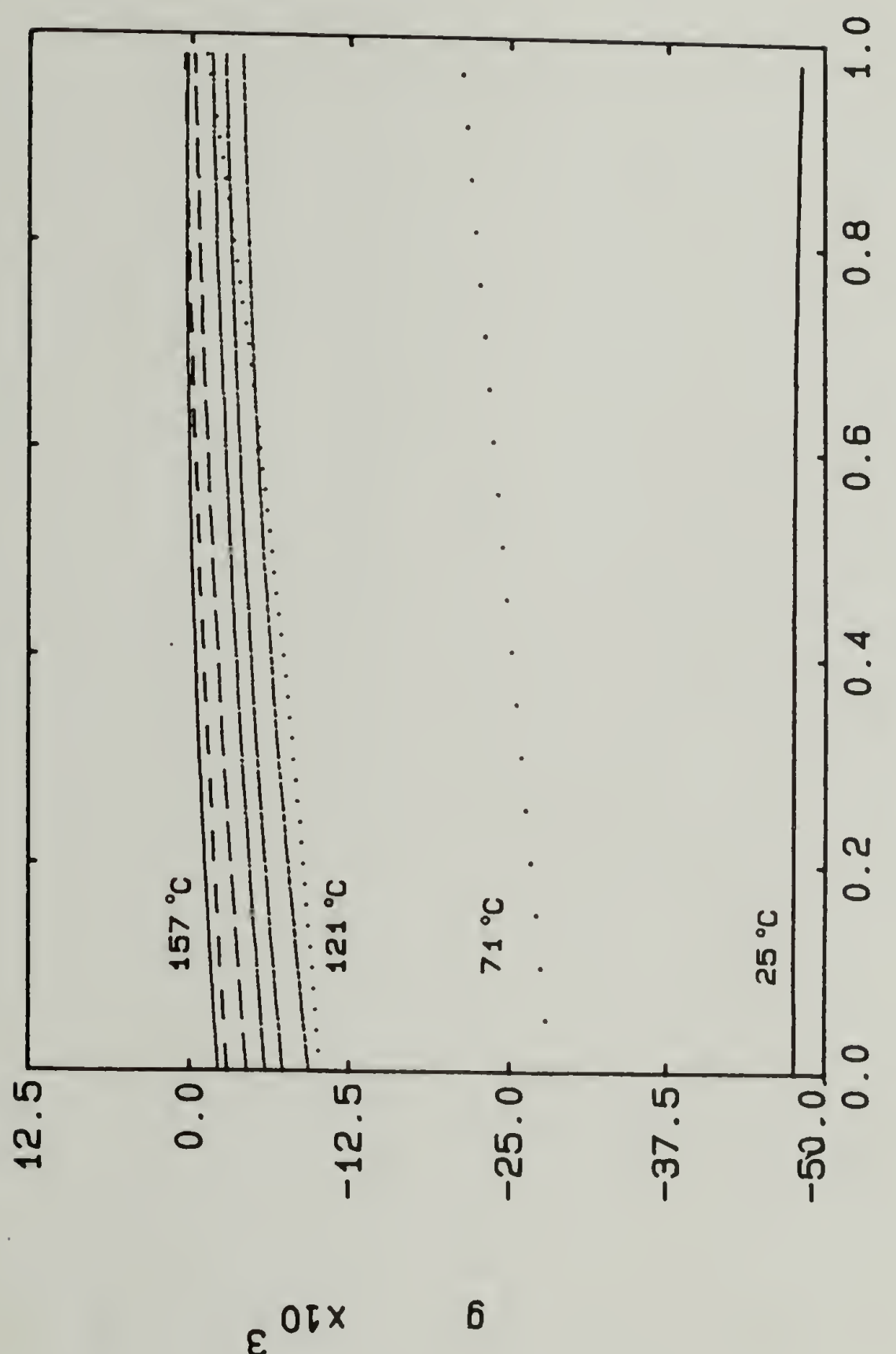

Figure 3.21 Composition Dependence of the Interaction Function for PSD(233)/PVME(99) at All Experimental Temperatures

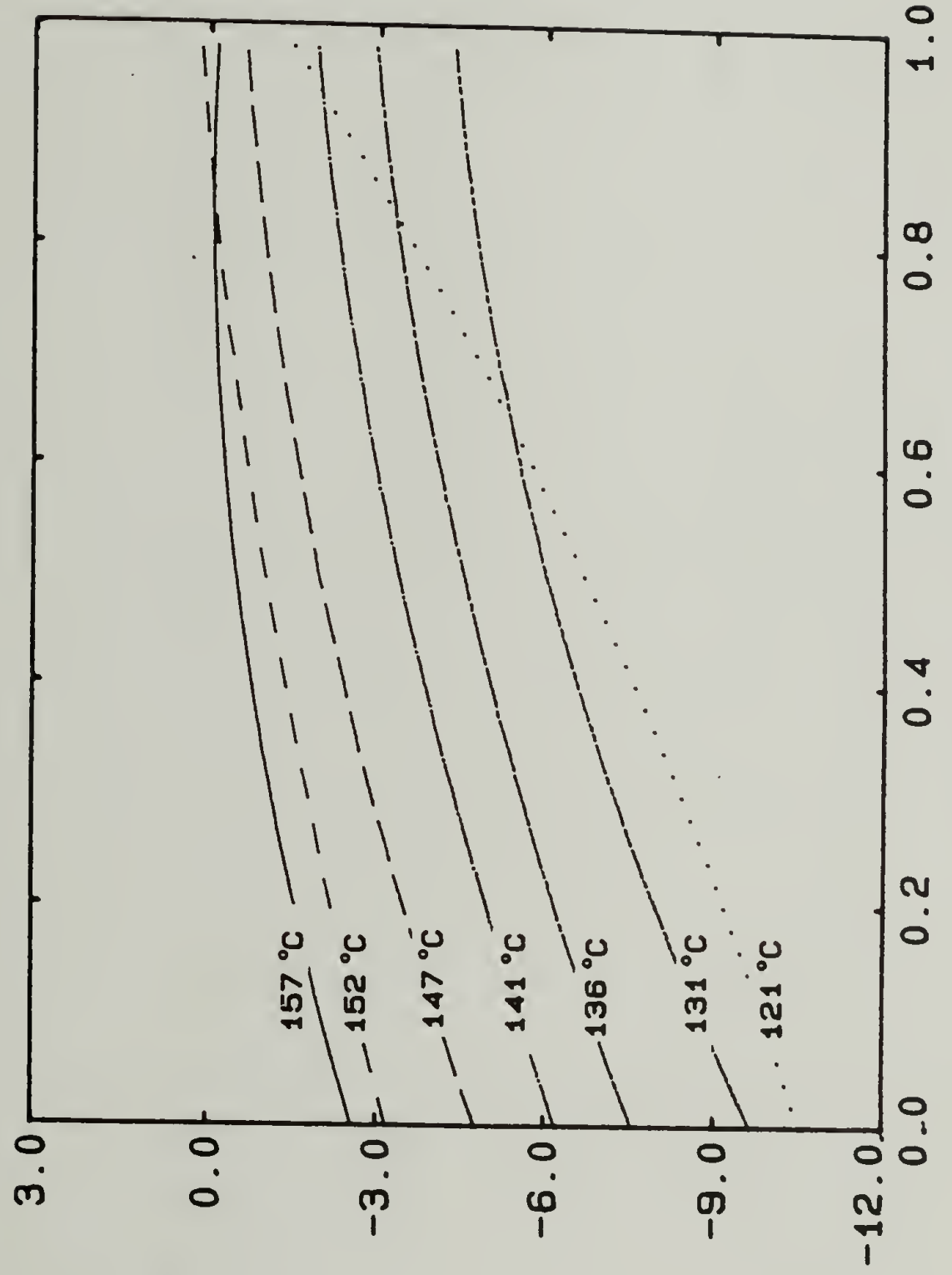

Figure 3.22 Composition Dependence of the Interaction Function for PSD(233)/PVME(99) at High Temperatures

Table 3.7

Interaction Coefficients for

PSD(233)/PVME(99) Blends

Temperature ^{o}C	(10^2) q_0	q_1	q_2
25	-4.76	.74	-.14
71	-2.84	.82	-.10
121	-1.05	.60	.33
131	-.97	.93	-.39
136	-.76	.76	-.30
141	-.62	.71	-.27
146	-.47	.70	-.29
152	-.32	.54	-.21
157	-.26	.59	-.35

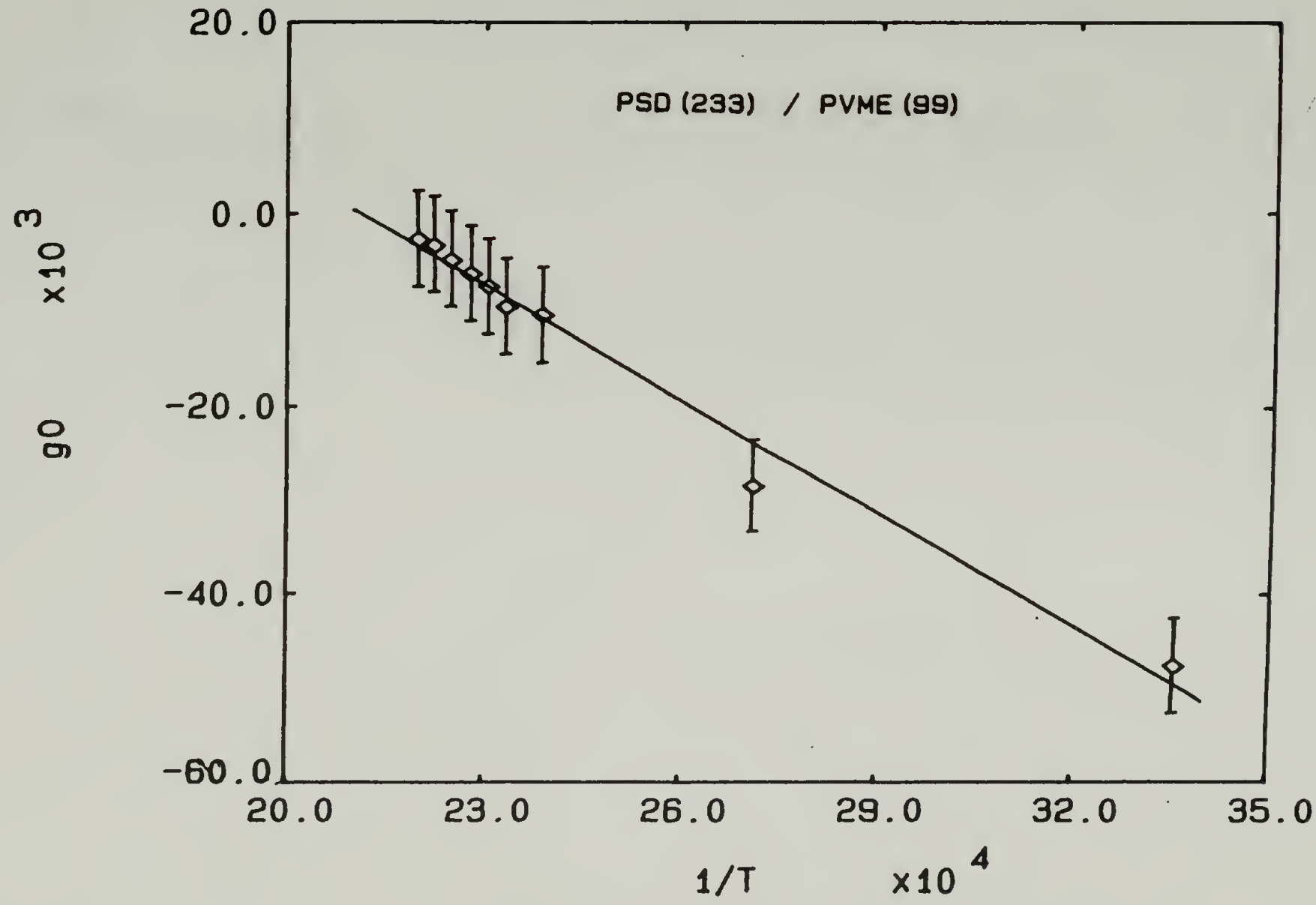

Figure 3.23 Temperature Dependence of the Composition-Independent Interaction Function for PSD(233)/PVME(99)

compared the magnitude of his determination of the PSD/PVME χ to that of other SANS χ measurements, and good agreement between values was found [13].

The PSD(233)/PVME(99) interaction function is obviously temperature-dependent as seen in Figures 3.21 and 3.22. In order to evaluate the temperature dependence of q for the PSD(233)/PVME(99) blend, the values of the composition-independent interaction coefficient q_0 (Table 3.7) are plotted in Figure 3.23. Assuming the temperature and composition dependence of q can be separated (see eq 1.40) a linear inverse temperature dependence is found for PSD(233)/PVME(99) blends in Figure 3.23. An increasing interaction function with temperature is expected for a system with LCST behavior [12], and a linear 1/T dependence can be explained in light of Patterson's equation-of-state analysis of the phase behavior for blends exhibiting specific interactions [47]. In Patterson's calculations it was shown that the loss of the specific interactional driving force for miscibility, and not the onset of free volume effects, causes phase separation upon heating the polymer blends [47]. Therefore, the 1/T dependence of the interaction function observed in the PSD(233)/PVME(99) blends is simply due to the reduction in intermolecular interactions upon heating.

In Kwei's [12] vapor sorption measurements the interaction parameter was found to have both an increasing and a decreasing temperature dependence depending upon blend composition. This behavior was not found in our PSD(233)/PVME(99) study since the $\partial^2\Gamma/\partial\phi^2$ data plotted in Figures 3.10 and 3.11 show no significantly different temperature dependence at the various blend compositions. Kwei concluded that the increasing value of χ due to decreasing temperature occurred because of the proximity of a UCST phase boundary. Since no UCST phase boundary was observed for the PSD(233)/PVME(99) blends, the separation of composition and temperature effects upon the interaction function for this system appears to be valid.

Summary. The empirical form of g (eq 1.39) used to describe the blend interactions does a good job of fitting the experimentally measured $\partial^2\Gamma/\partial\phi^2$ data. The advantage of the empirical approach is to generalize the treatment of data from various blend systems and to properly permit evaluation of a concentration-dependent interaction function. The disadvantage to this approach is the lack of a model by which the molecular origin of the interaction function might be evaluated.

It is usually thought that ΔH_{int} has to be negative for miscibility to occur, because the combinatorial entropy is very small for high polymer mixtures and the free volume terms are always positive. The results of

this investigation show that low molar mass component blends, such as the PSD(10.7)/PαMS(30) and PSD(30.5)/POCS(65.4) blends, have an entropy driving force large enough such that equilibrium miscibility can occur even when the total interaction function is positive.

A composition-dependent interaction function is often found in polymer mixtures with low molar mass solvents and other polymers. In concentrated mixtures a simple composition dependence, such as found in this study of the PSD(233)/PVME(99) system, can be explained by considering the size disparity between the components. The various molecular models of mixing have provisions for accommodating a composition dependent surface area of interaction between the components.

Occasionally, dilute polymer mixtures exhibit unusual phase behavior, such as double peaked spinodals, and an unusual composition dependence to the interaction function. Koningsveld [57,78,79] has applied Huggins [41] new theory of blend thermodynamics to account for polymer-solvent double peaked spinodals. In Huggins approach the addition of a inflexible polymer chain to a flexible polymer matrix creates an additional 'orientational' entropy contribution to the free energy of mixing which opposes miscibility. The influence of this orientational entropy in more concentrated blends has not been investigated, although this entropy effect is predicted to

be a dilute solution effect. Qualitatively, some sort of entropy effect or effect due to the coil nature of the polymeric solute might have a contribution to the free energy of mixing such as to cause the observed composition dependence of the PSD(10.7)/PαMS(30) interaction function. In general, Koningsveld has noted that dilute solution thermodynamics are dominated by the coil nature of the polymeric solute [57,78,79].

Also complicating the understanding of poly(styrene) dilute solution miscibility is the recent report of superchain structures in amorphous, oriented poly(styrene)[80]. Windle [80] concluded from X-ray diffraction studies that poly(styrene) intra- and interchain phenyl rings pack into superstructure stacks. The chains assume this low entropy conformation in order to maximize ring intermolecular interactions and to reduce free volume. This superchain morphology, if it exists in unoriented poly(styrene), could also influence the composition dependence of the interaction function.

One reason that the PSD(10.7)/PαMS(30) system might be sensitive to the small enthalpic and non-combinatorial entropic effects is the overall delicate balance of free energy effects leading to miscibility. On the other hand, a system like PSD(233)/PVME(99) where intermolecular

interactions are so strong, the miscibility behavior of the blend is dominated by this contribution to the free energy of mixing.

Equation-of-State Calculations

Method of calculation. The interaction function can be calculated from the equation-of-state theory through eq 1.38. Pure component values of the thermal expansion coefficient (α), the thermal pressure coefficient (γ), and the specific volume (ν_{sp}) are required for this calculation. The P-V-T data for the pure components was not measured in this study, but rather they were obtained from the literature.

The characteristic temperature, pressure and specific volume of the i^{th} component, T_i^*, p_i^*, and $\nu_{sp,i}^*$, are obtained from the pure component P-V-T data and the definitions provided in eqs 1.31-1.33 where T in these equations is the experimental temperature. By definition, the hard core molecular volume, ν^*, for both components are equal in the mixture. Arbitrarily setting $\nu^* = \nu_1^*$ the hard core molar volume is then calculated from [81]

$$\nu^* = (Mw_1/N_A)\nu_{sp,1} / r_1 \qquad (3.5)$$

where r_1 and Mw_1 are the degree of polymerization and polymer molecular weight of component 1, respectively. N_A

is Avagadro's number. The degree of polymerization of component 2, r_2, is then calculated from r_1 by [81]

$$r_2 = r_1(Mw_2 \nu_{sp,2}) \; / \; (Mw_1 \nu_{sp,1}) \qquad (3.6)$$

The number of external degrees of freedom per submolecule of the i^{th} component is determined from [81]

$$c_i = (Mw_i / N_A) \nu_{sp,i}^{*} \; / \; (T_i^{*} r_i k) \qquad (3.7)$$

where k is Boltzman's constant, equal to 1.380×10^{-23} J K. The number of external degrees of freedom per submolecule in the mixture is defined in eq 1.34. The variable c_{12} in eq 1.34 is the non-linear term introduced as an adjustable, system dependent parameter and ψ_i is the segment fraction of component i defined as

$$\psi_i = r_i x_i \; / \; r \qquad (3.8)$$

where x_i is the mole fraction of component i in the mixture and r has been defined in eq 1.34.

The surface fraction of component 2, Θ_2, is also required for the calculation of q from eq 1.38. Θ_2 can be written as [31]

$$\Theta_2 = \psi_2 s_2 \; / \; s \qquad (3.9)$$

where all terms have been defined previously.

Substitution of the expression for s given in eq 1.34 into the equation above yields Θ_2 as

$$\Theta_2 = \psi_2 / (s_{12}\psi_1 + \psi_2) \qquad (3.10)$$

where s_{12} represents the ratio of the pure components surface area per segment s_1/s_2.

The last value required for the calculation of eq 1.38 is $\tilde{v}$, the reduced volume of the mixture. $\tilde{v}$ is related to the reduced temperature by [81]

$$\tilde{T} = \tilde{v}^{4/3}T / (\tilde{v}^{1/3}-1) \qquad (3.11)$$

where $\tilde{T} = T/T^*$ and T^* is defined in eq 1.35. At each composition T^* must be calculated and then eq 3.11 can be solved for $\tilde{v}$.

The second line of eq 1.38 contains the expression

$$[(2\pi m_2 kT)^{1/2}/h](\gamma v^*)^{1/3} \qquad (3.12)$$

which can be evaluated with the following definitions: m_2 is the mass per segment of component 2 with units of kg per segment, h is Plank's constant equal to 6.626×10^{-23} J s, and γ is the geometric factor defined in eq 1.28 and not the thermal pressure coefficient γ.

Computer program STATE was written by this author to calculate g from eq 1.38 as a function of composition. Program STATE is listed in Appendix II.

Polymer - Polymer Blend Calculations. The most extensive equation-of-state calculations for any of the three amorphous blends of interest in this investigation has been done on the PS/POCS system. This investigation will also focus on the PS/POCS system as far as the equation-of-state calculations are concerned. Preliminary attempts were made to evaluate the composition dependence of the PSD(233)/PVME(99) interaction function but the two literature values for the PS and PVME pure component equation-of-state parameters [49,82] differ greatly and neither set provides reasonable agreement with the measured function. No attempt was made to apply the equation-of-state theory to the PSD(10.7)/PαMS(30) system because of the total absence of P-V-T data for the poly(α-methylstyrene) component.

The equation-of-state calculation of q as a function of composition for the PSD(30.5)/POCS(65.4) blends was made using the equation-of-state parameters listed in Table 3.8. The surface segment ratio, s_1/s_2, was estimated by Zacharius [5] to be equal to unity using both Flory's [51,83] and Bondi's [84] calculation methods. The selection of $s_1/s_2 = 1$ implies that there is no difference in size between the components. In such a case, the equation-of-state theory will predict a composition-independent interaction function. The chemical similarity between the components of this blend also dictates the

choice of $c_{12} = 0$. Often the parameter c_{12} is used to 'adjust' the equation-of-state predictions to match experimental data, but for this blend there is no justification for deviation from the zero value selected [4].

The exchange energy parameter X_{12} is expected to be positive for a mixture with no polar or specific interactions [D10]. Zacharius' [4,5] previous equation-of-state calculations have estimated values of $X_{12} = .046$ or .091 J cm^{-3} and Q_{12} was assumed to be zero. This value of X_{12} is very low for a system with dispersion force interactions (5 to 10 J cm^{-3} is typical [47]). In order to used Zacharius' X_{12} values they must be considered as 'effective' interactions that are the sum of the real X_{12} and Q_{12} values. Therefore, it is more appropriate to say that the PS/POCS system exhibits no net specific interactions and that the effective interaction is given by Zacharius' values.

The equation-of-state calculated interaction functions for Zacharius' values of X_{12} are plotted as a function of composition in curves A and B in Figure 3.24, respectively. Our SANS determined interaction function at 125^{o}C is plotted on Figure 3.24 as curve C. The experimental data seems to fit well with the predicted data when $X_{12} = .046$. The only reservation in praising the agreement between theory and experiment is that the

Table 3.8

Equation-of-State Parameters for
Poly(styrene) and Poly(orthochlorosytrene)
(398 K)

	ν_{sp} (cm^3/g)	$\alpha \times 10^4$ (K)	γ (J/cm^3K)	p^* (J/cm^3)	T^* (K)	ν_{sp}^* (cm^3/g)
PSD	.912[1]	6.05[2]	.879[3]	509.6	7906	.765
POCS[1]	.821	6.41	.824	486.0	7635	.674

1. obtained from reference 5
2. obtained from reference 85
3. obtained from reference 86

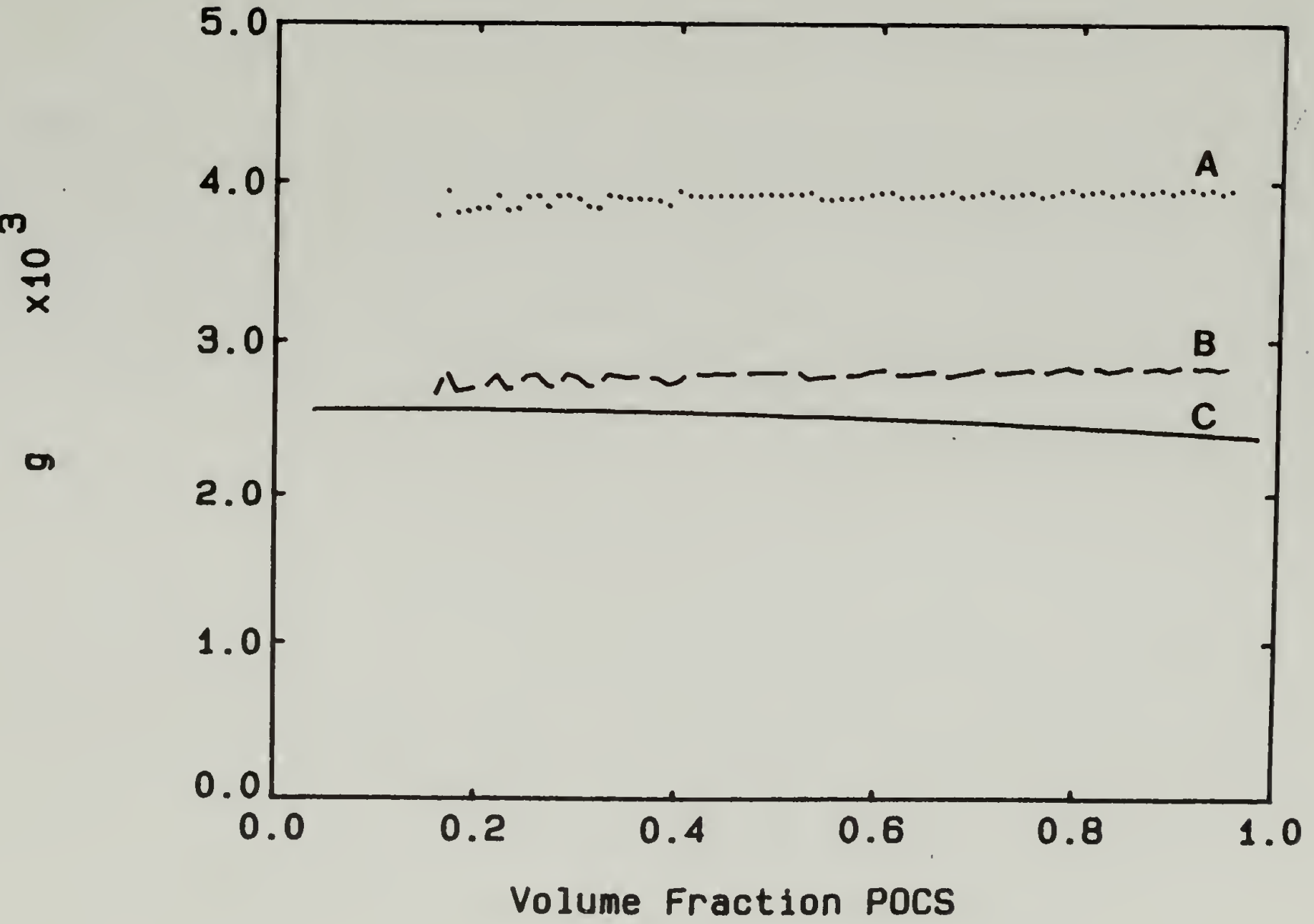

Figure 3.24 Equation-of-State Predicted Interaction Function for PSD(30.5)/POCS(65.4) Blends

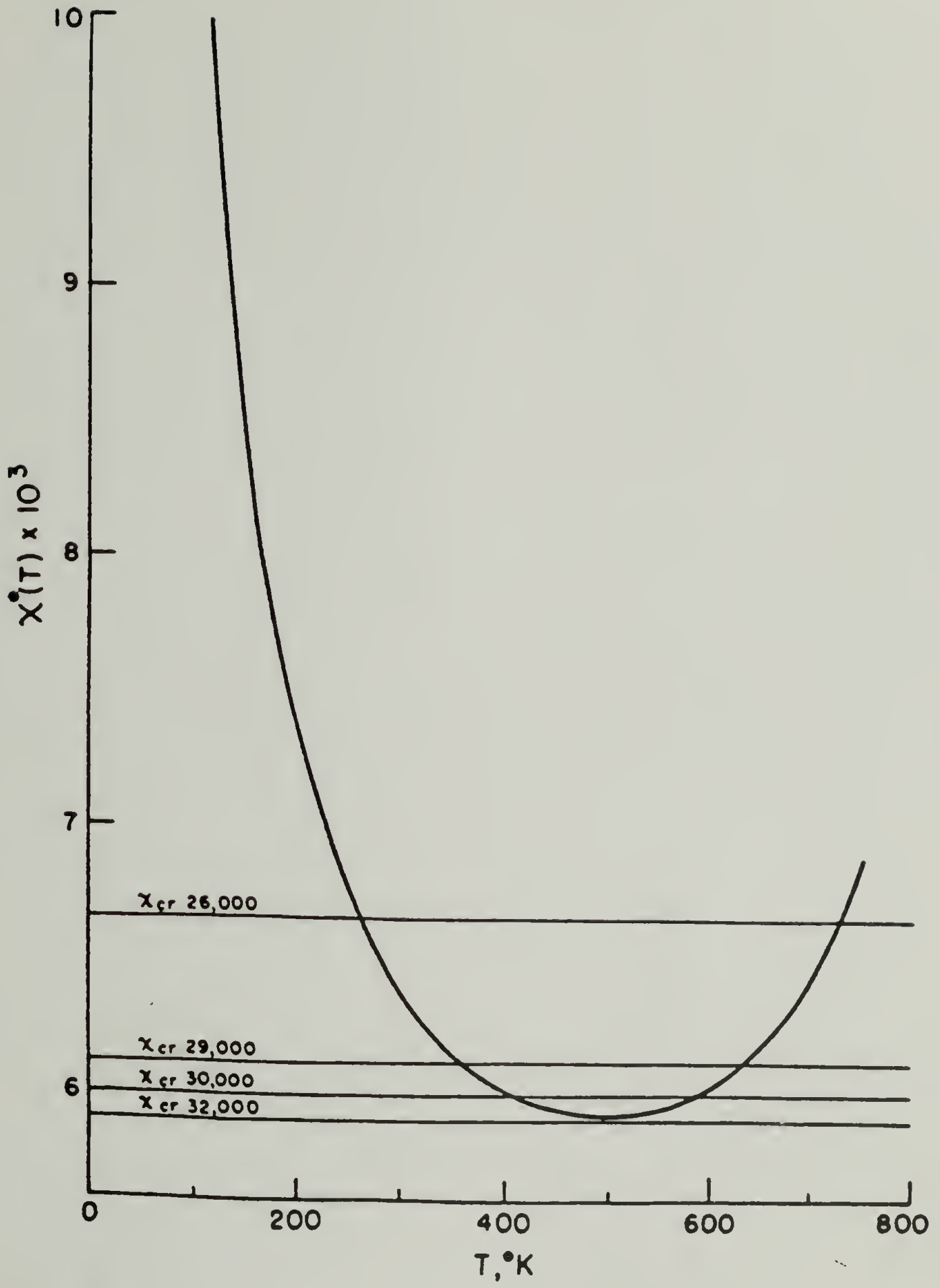

Figure 3.25 Equation-of-State Calculated Temperature Dependence of the Interaction Function

values for all POCS equation-of-state parameters are estimates determined from the poly(styrene) values and the X_{12} values are not measured quantities.

The equation-of-state predicted temperature dependence of the interaction function was determined by Zacharius [4,5] for the PSH/POCS blend and is reproduced in Figure 3.25 for the case of X_{12} = .046. The horizontal lines in Figure 3.25 represent the critical value of g for poly(styrene) having the indicated molar mass mixed with POCS(100). Where $g < g_c$ the blends are miscible, at the intersections of g with g_c the UCST (low temperature intersection) and LCST (high temperature intersection) will occur. The UCST and LCST can be seen to merge in Figure 3.25 when the molar mass of poly(styrene) becomes 32,000 (g_c becomes tangential to the g(T) curve). The critical value of g for the PSD(30.5)/POCS(65.4) system is very similar to those shown in Figure 3.25.

The point where the UCST and LCST merge is called the critical double point (CDP). The flatness of the g(T) curve in the vicinity of the CDP is responsible for a large change in critical temperature with a small changes in molar mass. For a system not to far from the CDP, a small change in critical temperature, T_c to T_{c1}, due to a

small change in the degree of polymerization, r to r_1 can be expressed as [5]

$$T_{c1} - T_c = \left(\frac{2}{(\partial g/\partial T)}\right) \frac{r - r_1}{r r_1} \qquad (3.13)$$

where $(\partial g/\partial T)$ is the temperature derivative of the interaction function near the critical temperature. The sensitivity of $T_{c1} - T_c$ to $r - r_1$ is determined by $(\partial g/\partial T)$. If the change in g with respect to temperature is very small, as found by SANS for the PSD/POCS blends in this investigation, then a small change in the molar mass of either component will result in a large change in the critical temperature. A large molar mass dependence of the phase diagrams is predicted for the PS/POCS system, and this was found experimentally by Ryan [3].

Summary. In the equation-of-state formalism the free energy of mixing is considered to have contributions from the combinatorial entropy, the enthalpy arising from dissimilar chain contacts, and the enthalpy and entropy arising from the free volume differences between the components. This is expressed as

$$\Delta G_{mix} = \Delta H_{mix} - T\Delta S_{comb} + \Delta H_{fv} - T\Delta S_{fv} \qquad (3.14)$$

where the first two terms are also considered in the Flory-Huggins theory. The free volume contributions to ΔG_{mix} are always positive and the combinatorial entropy term is small for polymer-polymer mixtures, and sometimes

negligible. Therefore, the enthalpy of interaction usually dominates the sign of the free energy function and the miscibility of the system.

For the low molar mass blends of PSD(30.5)/POCS(65.4) the previous work of Zacharius [4,5] showed that miscibility occurred even when $\Delta H_{mix} > 0$. Also, the SANS investigation reported here shows that the overall interaction function (all the terms in eq 3.4 except $T\Delta S_{comb}$) is positive, yet smaller than $T\Delta S_{comb}$ since miscibility was observed. Obviously, the miscibility of PS/POCS blends is the result of a delicate balance of the various contributions to the free energy of mixing. The combinatorial entropy can also be seen to be the dominant contribution to ΔG_{mix} because its molar mass and temperature dependence is reflected in the measured molar mass dependence of the phase diagram. The equation-of-state theory was used by Zacharius [4,5] to propose the critical double point hypothesis which explains the observed phase behavior of the PS/POCS blends.

The Flory equation-of-state theory has only recently been quantitatively compared to experimental results from polymer-polymer blends, with the studies presented here representing one such comparison. The equation-of-state theory has theoretical imperfections such as

non-vanishing residual entropy even when the excess volume of mixing vanishes [53]. Despite such concerns, the equation-of-state theory has been successfully used to qualitatively understand the influence of the segment surface ratio and the exchange energy function upon the miscibility of polymer mixtures [53].

C H A P T E R I V

CONCLUSIONS

Small-angle neutron scattering measurements have been performed to determine the polymer-polymer interaction function in three quasi-binary, miscible, amorphous blend systems. The neutron scattering data was analyzed using a refinement of the concentrated blend scattering theory developed earlier in this laboratory [7,19]. The scattering measurements were performed in a manner to obtain the composition and temperature dependence of the interaction functions.

The PSD(30.5)/POCS(65.4) interaction function was found to be independent of composition and temperature as well as positive for all compositions measured. The observed behavior of the interaction function agrees with the previous equation-of-state predictions for PS/POCS system near a critical double point [4,5].

The PSD(10.7)/PαMS(30) study represents the first measurement of the interaction function for this miscible blend system. The interaction function was found to be positive and to have an unusual composition dependence. The composition dependence found represents the results of

a preliminary study, but if confirmed, may be a consequence of non-combinatorial entropy or the bulk morphology of amorphous poly(styrene).

The results of both the PSD(30.5)/POCS(65.4) and PSD(10.7)/PαMS(30) studies indicate that miscibility can occur for blends where the interaction function is positive (or $\Delta H_{mix} > 0$) if the molar mass of the components is sufficiently low. These investigations also show that in cases where the interaction between components is found to be small, positive or negative, the combinatorial entropy contribution to the free energy cannot be ignored, and in fact may be the dominating force determining miscibility.

The PSD(233)/PVME(99) interaction function was found to be negative valued with a composition and temperature dependence. The composition dependence observed was found to agree with previous studies and can qualitatively be explained by consideration of the size disparity of the component interacting surfaces. The temperature dependence of the interaction function showed an inverse temperature dependence, as expected for an interaction function dominated by the attractive intermolecular interactions between the components.

The equation-of-state calculations performed in this study represent an attempt to quantitatively compare measured interaction functions to the theoretical

predictions. Using an exchange energy value of 0.046 J cm^{-3} and a segment surface ratio of 1.0, the equation-of-state theory was able to predict the magnitude and composition dependence of the measured interaction functions.

Proposed Future Studies

It is strongly suggested that all future amorphous blend studies include measurement of the interaction function as a function of blend composition and temperature. The small-angle neutron scattering determination of the interaction function measurements provide a reasonably accurate probe of the thermodynamics of the miscible system. Also, it is recommended that the concentrated blend measurements be combined with experiments in dilute solution to accurately determine the composition dependence of the interaction function.

In particular, the PS/PαMS blend studies should be continued to better quantify the composition dependence and measure the temperature dependence of the interaction function. The radius-of-gyration of each component should be measured for all compositions of the blend from dilute to concentrated. If an orientational entropy contribution to the free energy is affecting the miscibility of this system, the PαMS component should have a reduced R_g in

dilute blends than in the concentrated blends. Also, the PS component should show expansion of the unperturbed dimension in dilute blends with PαMS.

The effect of blending upon the poly(styrene) superchain could be examined by wide-angle x-ray diffraction. Windle [80] reports that the superchain scattering peak is outside the angular range of the amorphous halo of other non-crystalline polymers. Also, the effect of substituent, such as ortho, para, meta, and alpha chlorination or methylation, upon the bulk morphology of the modified poly(styrene) should be examined. This study would help relate blend miscibility behavior to the chemical nature of the solute.

The equation-of-state theory should be quantitatively compared to the results for both the interaction function and phase behavior of other amorphous, miscible blends. Until recently, the equation-of-state theory has only been used to qualitatively describe phase behavior. In order to compare experiment with theory, reliable values of the pure component equation-of-state parameters will have to be measured.

Finally, a light and neutron scattering investigation of nucleation and growth polymer-polymer phase decomposition should be initiated. Spinodal phase decomposition behavior has been extensively examined for polymer blends [12,13,87-89] while the nucleation and

growth mechanism has only been qualitatively observed [12]. Nucleation and growth phase separation opens an avenue to two phase polymer morphology that has yet to be investigated while the theoretical background for the study already exists in previous studies of inorganic glass and polymer-solvent phase separation [90-97]. Any blend system investigated for nucleation and growth decomposition should have narrow distribution molar masses of both components to avoid complications of fractionation. The blend of poly(styrene) with poly(α-methylstyrene) satisfies the molar mass criteria but it suffers from small light scattering contrast and a high temperature glass transition. If poly(vinylmethylether) could be obtained in narrow molar mass distribution by fractionation, then the PS/PVME blend system would be ideal for this study. The PS/PVME system has the benefits of good light scattering contrast, well defined phase behavior, high molar mass compatibility, and a well understood spinodal decomposition behavior.

REFERENCES

1. O. Olabisi, L.M. Robeson, and M.T. Shaw, Polymer-Polymer Miscibility, Academic Press, New York, 1979, Chapter 5

2. S. Krause in, Polymer Blends, D.R. Paul, and S. Newman eds., Academic Press, New York, 1978, Chapter 2.

3. C.L. Ryan, Ph.D Dissertation, University of Massachusetts, Amherst, 1979

4. S.L. Zacharius, Ph.D. Dissertation, University of Massachusetts, Amherst, 1982

5. S.L. Zacharius, G. ten Brinke, W.J. MacKnight and F.E. Karasz, Macromolecules, 16, 381 (1983)

6. T.P. Russell and R.S. Stein, J. Polym. Sci., Polym Phys. Ed., 20, 1593 (1982)

7. J.W. Gilmer, Ph.D. Dissertation, University of Massachusetts, Amherst, 1983

8. M. Bank, J. Leffingwell, and C. Theis, Macromolecules, 4, 43 (1971)

9. M. Bank, J. Leffingwell, and C. Theis, J. Polym. Sci., Part A-2:, 10, 1097 (1972)

10. F.J. Lu, E. Benedetti, and S.L. Hsu, Macromolecules, 16, 1525 (1983)

11. D. Garcia, J. Polym. Sci., Polym. Phys. Ed., 22, 107 (1984)

12. T.K. Kwei, T. Nishi, and R.F. Roberts, Macromolecules, 7, 667 (1974)

13. H.E. Yang, Ph.D. Dissertation, University of Massachusetts, Amherst, 1985

14. M. Baer, J. Polym. Sci., Part A:, 2, 417 (1964)

15. S. Lau, J. Pathak and B. Wunderlich, Macromolecules, 15, 1278 (1982)

16. D.J. Dunn and S. Krause, J. Polym. Sci, Polym. Lett. Ed., 12, 591 (1974)

17. D. Rahlwes and U. Biskup, Angew. Makromol. Chem., 78, 49 (1981)

18. D.G.H. Ballard and M.G. Rayner, Polymer, 17, 640 (1976)

19. G. Hadziioannou, J.W. Gilmer and R.S. Stein, Polym. Bull., 9, 563 (1984)

20. K.H. Meyer and R. Luhdeman, Helv. Chim. Acta, 18, 307 (1935)

21. Ch.G. Bossonnas, Helv. Chim. Acta, 20, 768 (1937)

22. K.H. Meyer, Z. Phys. Chem, Abt. B:, 44, 383 (1939)

23. P.J. Flory, J. Chem. Phys., 9, 660 (1942)

24. P.J. Flory, J. Chem. Phys., 10, 51 (1942)

25. M.L. Huggins, J. Chem. Phys, 9, 440 (1941)

26. M.L. Huggins, Ann. N.Y. Acad. Sci., 43, 1 (1942)

27. F.H. Fowler and G.S. Rushbrooke, Trans. Faraday Soc., 33, 1272 (1937)

28. W.C. Orr, Trans. Faraday Soc., 40, 320 (1944)

29. E.A. Guggenheim, Proc. R. Soc. London, A:, 183, 203 (1944)

30. A.J. Staverman, Recl. Trav. Chim. Pays-Bas, 69, 163 (1950)

31. P.J. Flory, Disc. Faraday Soc., 49, 7 (1970)

32. R.L. Scott, J. Chem. Phys., 17, 279 (1949)

33. H. Tompa, Trans. Faraday. Soc., 45, 1142 (1949)

34. E.A. Guggenheim, Proc. R. Soc. London, A:, 183, 212 (1944)

35. G. Scatchard, Chem. Rev., 8, 321 (1931)

36. J.J. van Laar, Z. Phys. Chem, Abt. A:, 137, 421 (1928)

37. J.H. Hildebrand, J. Am. Chem. Soc., 57, 866 (1935)

38. R. Koningsveld, L.A. Kleintjens and H.M. Schoffeleers, Pure Appl. Chem., 39, 7 (1974)

39. P.J. Flory, J. Am. Chem. Soc., 87, 1833 (1965)

40. R.H. Lacombe and I.C. Sanchez, J. Phys. Chem., 80, 2568 (1976)

41. M.L. Huggins, J. Phys. Chem., 74, 371 (1970); 75, 1255 (1971); 80, 1317 (1976)

42. R. Koningsveld, Ph.D. Dissertation, University of Leiden, Amsterdam, Holland, 1967

43. E.A. Guggenheim, Trans. Faraday. Soc., 44, 1007 (1948)

44. S.H. Maron, J. Polym. Sci., 38, 329 (1959); S.H. Maron and N. Nakajima, J. Polym. Sci., 54, 587 (1964)

45. P.J. Flory, J. Chem. Phys., 12, 425 (1944)

46. R. Koningsveld, H.A.G. Chermin and M. Gordon, Proc. R. Soc. London, A:, 319, 331 (1970)

47. D. Patterson and Andree Robard, Macromolecules, 11, 690 (1978)

48. I. Prigogine, The Molecular Theory of Solutions, North Holland Publishing Co., Amsterdam, 1957

49. L.P. McMaster, Macromolecules, 6, 760 (1973)

50. P.H. Lin, Sc.D. Thesis, Washington University, St. Louis, Mo., 1970

51. B.E. Eichenger and P.J. Flory, Trans. Faraday Soc., 64, 2053, 2061, 2066 (1968)

52. E.A. Guggenheim, Proc. R. Soc. London, A:, 135, 181 (1932)

53. O. Olabisi, L.M. Robeson and M.T. Shaw, Polymer-Polymer Miscibility, Academic Press, New York, 1979, p89

54. G. ten Brinke, A. Eshuis, E. Roerdink and G. Challa, Macromolecules, 14, 867 (1980)

55. H. Tompa, Polymer Solutions, Butterworth, London, 1956

56. R. Koningsveld, Adv. Colloid. Interf. Sci., 2, 151 (1968)

57. R. Koningsveld and L.A. Kleintjens, J. Polym. Sci., Polym. Symp., 61, 221 (1977)

58. M. Smoluchowski, Ann. Phys. (Leipzig), 25, 205 (1908)

59. A. Einstein, Ann. Phys. (Leipzig), 33, 1275 (1910)

60. L.H. Sperling, Polym. Eng. Sci., 24, 1 (1984)

61. J.S. Higgins and R.S. Stein, J. Appl. Cryst., 11, 346 (1978)

62. R.S. Stein and C.C. Han, Phys. Today, 38, 74 (1985)

63. G. Kostorz and S.W. Lovesey in, Treatise on Material Science and Technology, 15, G. Kostorz ed., Academic Press, New York, 1979

64. P. Debye and A. Bueche, J. Chem. Phys., 18, 1423 (1950)

65. Th.G. Scholte, J. Polym. Sci., Polym. Symp., 39, 281 (1972)

66. Th.G. Scholte, J. Polym. Sci., Part A-2:, 9, 1553 (1971)

67. Th.G. Scholte, Eur. Polym. J., 6, 1063 (1970)

68. O. Glatter and O. Kratky, Small-Angle X-ray Scattering, Academic Press, New York, 1982, Chapter 12

69. C.T. Murray, J.W. Gilmer and R.S. Stein, Macromolecules, 18, 996 (1985)

70. W.C. Kohler and R.W. Hendricks, J. Appl. Phys., 50, 1951 (1979)

71. W.J. MacKnight, F.E. Karasz and R. Freid, in Polymer Blends, D.R. Paul and S. Newman eds., Academic Press, New York, 1978

72. D.H. Richards and D.A. Slater, Polymer, 8, 127 (1967)

73. R. Ullman, J. Polym. Sci., Polym. Lett. Ed., 21, 521 (1983)

74. H. Yang, R.S. Stein and C. Han, to be published

75. J.H. Wendorf, J. Polym. Sci, Polym. Lett. Ed., 18, 439 (1980)

76. S. Sueki, J.M.G. Cowie and I.J. McEwen, Polymer, 24, 60 (1983)

77. P.J. Flory, Principles of Polymer Chemistry, Cornell University Press, Ithica, 1953

78. R. Koningsveld, Bull. Soc. Chim. Beog., 44, 5, (1979)

79. R. Koningsveld, Contribution to the NATO Advanced Study Institute on Polymer Blends and Mixtures, London, July 1984, to be published

80. G.R. Mitchell and A.H. Windle, Polymer, 25, 906 (1985)

81. I. Sanchez, in Polymer Blends, D.R. Paul and S. Newman eds., Academic Press, New York, 1978, Chapter 3

82. T. Shiomo, K. Kohno, K. Yoneda, T. Tomita, M. Miya and K. Imai, Macromolecules, 18, 414 (1985)

83. P.J. Flory and H. Hocker, Trans. Faraday Soc., 67, 2270 (1971)

84. A.J. Bondi, J. Chem. Phys., 68, 441 (1964)

85. W. Patnode and W.J. Scheiber, J. Am. Chem. Soc., 61, 3449 (1939)

86. H. Hocker and P.J. Flory, Trans Faraday Soc., 67, 2270 (1971)

87. K. Binder, J. Chem. Phys., 79, 6387 (1983)

88. K. Binder, C. Billotet, and P. Mirold, Z. Physik B, 30, 183 (1978)

89. H.L. Snyder, P. Meakin, and S. Reich, Macromolecules, 16, 757 (1983)

90. J.J. Hammel and S.M. Ohlberg, J. Appl. Phys., 36, 1442 (1965)

91. J.J. Hammel, J. Mickey, and H.R. Golob, J. Coll. Interf. Sci., 27, 329 (1968)

92. N.S. Andreev, J. Non-Cryst. Solids, 30, 99 (1978)

93. M. Goldstein, J. Am. Ceram. Soc., 48, 126 (1965)

94. G.F. Neilson, Dis. Faraday Soc., 50, 145 (1974); J. Appl. Phys., 43, 3728 (1972)

95 J.J. Hammel, J. Chem. Phys., 46, 2234 (1967)

96. S. Krishnamurthy and W.I. Goldberg, Phys. Rev. A, 22, 2147 (1980)

97. S. Krisnamurthy and R. Bansil, Phys. Rev. Lett., 50, 2010 (1983)

98. P.R. Bevington, Data Reduction and Error Analysis for the Physical Sciences, McGraw-Hill, New York, 1969

Appendix I

Error Analysis

The second derivative of the enthalpy correction term, $\partial^2\Gamma/\partial\phi_2^2$, is calculated from an equation requiring several independent, experimentally determined values. Each value has an associated error in measurement and the error in calculating $\partial^2\Gamma/\partial\phi_2^2$ is the result of propagation of these random errors. If a parameter is defined

$$F = f(x,y,z)$$

then the error in F, $\varepsilon(F)$ is equal to

$$\varepsilon(F) = \Big[(\partial F/\partial x)^2(\varepsilon(x))^2 + (\partial F/\partial y)^2(\varepsilon(y))^2 + \ldots$$
$$\ldots + 2(\partial F/\partial x)(\partial F/\partial y)\varepsilon(x)\varepsilon(y)\Big]^{1/2}$$

and if the deviations of F with respect to x and y are uncorrelated, then the cross product terms vanish [98].

The $\partial^2\Gamma/\partial\phi_2^2$ data was calculated using eq 1.44. The errors associated with the independent variables are listed in Tables 2.4, 2.5, 3.1, and 3.4. The largest sources of error in the calculation are the uncertainties in the molecular values for the non-poly(styrene) components of the blends. The deviations of $\partial^2\Gamma/\partial\phi_2^2$ are listed in Tables 3.2 and 3.4.

Appendix II

Computer programs utilized in the Data Analysis.

CHI - Program to calculate $\partial^2\Gamma/\partial\phi_2{}^2$ from neutron scattering data, according to eq 1.44

POLYFT - Polynomial fitting program, derived from examples given in reference 98.

DEBYE - Debye function fitting program, derived from examples given in reference 98 and the similar program written at ORNL.

GFUN - This program determines coefficients g_o, g_1 and g_2 from POLYFIT coefficients.

GCALC - GCALC calculates interaction function g from g_o, g_1, and g_2 according to equation 1.39.

STATE - calculates g from equation 1.38.

TSTATE - calculates g as a function of temperature according to Patterson, reference 47.

Program source code can be found on the SANS floppy disk.

```
      PROGRAM CHI
      DOUBLE PRECISION AVN,VA,VB,AA,AB,ATER1,SATER1
C-----------------------------------------------------------------------
C     Program designed to calculate chi for a Polystyrene,
C     Poly  X blend from SANS data. This is
C     the analysis of Gilmer, Hadz and Stein ; found in
C     Gilmer's thesis for two component blend.
C-----------------------------------------------------------------------
C
      TYPE 5
5     FORMAT(' Enter solute values (A) for polymer molecular weight'
     + ,/,' monomer molar vol and scattering length (CM-1)',/,
     + ' and monomer molecular weight')
C
      ACCEPT *, PMA,VA,AA,AMA
C
C
      TYPE 6
6     FORMAT(' Enter solvent (B) values for polymer molecular weight'
     + ,/,' monomer molar vol and scattering length (CM-1)',/,
     + ' and monomer molecular weight')
C
      ACCEPT *, PMB,VB,AB,AMB
C
C
C---  calculate values of molar volume va,vb and degrees of
C     polymerization iza,izb
C
      AVN = 6.023E+23
      VA = VA/AVN
      VB = VB/AVN
      SVB = SVB/AVN
      SVA = SVA/AVN
      IZA = PMA/AMA
      IZB = PMB/AMB
      AZA = FLOAT(IZA)
      AZB = FLOAT(IZB)
      ZA2 = AZA*AZA
      ZB2 = AZB*AZB
C
C
C--   enter in the volume fraction PS and the scattering length
C--   a zero volume fraction signifies end session
C
      DO 100, I=1,30
      TYPE 20
20    FORMAT(' Enter volume fraction solute (A) , Rc(0) ')
      ACCEPT *,VFA, RC
      IF (VFA.EQ.0) GO TO 101
      VFB = 1-VFA
```

```
      ATER1 = (AA-AB*(VA/VB))
      SATER1 = (ATER1/(RC*VA))*ATER1
      BTER1 = 1/(IZA*VFA)
      CTER1 = 1 / (IZB*(VB/VA)*VFB)
C
D     TYPE 45, ATER1,SATER1,BTER1,CTER1
45    FORMAT(' ',4(E12.5,2X))
C
      CHIMA = (SATER1 - BTER1 - CTER1)
C
C---- assume polystyrene is the lattice v0 = va
C     CHIMA - chi per monomer A unit, Bsolvent
C     CHIB - chi for B solvent
C     repeating calculation reversing roles of solvent
C     and solute shoul yield chima's related by the ratio
C     of the molar volumes
C
C
      TYPE 49, VFA,VFB,RC
49    FORMAT(' Volume fraction A =',F5.2,' Volume fraction B = ',F5.2,
     + '  Rc(o) = ',F7.3)
      TYPE 50, CHIMA
50    FORMAT(' Enthalpy correction term per monomer A unit, B solvent '
     + ,E12.5)
100   CONTINUE
101   TYPE *,' Thank you for your patience'
      STOP
      END
```

```
      PROGRAM POLFIT
      DOUBLE PRECISION SUMX,SUMY,XTERM,YTERM,ARRAY
      DIMENSION INPFL(12),X(500),Y(500),ARRAY(20,20),A(20),
     +  SIGMAY(100),SUMX(40),SUMY(40),FMT(30)
C -------------------------------------------------------------
C       THIS PROGRAM FITS EXPERIMENTAL DATA TO THE EQUATION:
C          Y=A(1) + A(2)*X + A(3)*X**2...+A(N)*X**(N-1)
C       ACCORDING TO THE TECHNIQUES OUTLINED IN P.R. BEVINGTON'S
C       BOOK "DATA REDUCTION AND ERROR ANALYSIS FOR THE
C       PHYSICAL SCIENCES".
C -------------------------------------------------------------
      TYPE*,' ENTER 1 IF YOU WANT INSTRUCTIONS,'
      TYPE*,' 2 IF YOU DO NOT NEED THEM:'
      ACCEPT*,INST
      IF(INST.EQ.2) GO TO 10
      TYPE*,' ENTER THE FILE NAME OF THE DATA TO BE FIT:'
10    ACCEPT 20, INPFL
20    FORMAT(12A2)
      OPEN(UNIT=1,NAME=INPFL,TYPE='OLD')
      IF(INST.EQ.2) GO TO 30
      TYPE*,' ENTER THE NUMBER OF LINES TO SKIP IN THE DATA FILE',
     +  ' (INTEGER):'
30    ACCEPT*,ISKIP
      IF(ISKIP.EQ.0) GO TO 70
50    FORMAT(A1)
      DO 60 I=1,ISKIP
60    READ(1,50) B
70    IF(INST.EQ.2)GO TO 80
      TYPE*,' ENTER THE NUMBER OF DATA POINTS (INTEGER):'
80    ACCEPT*,NPTS
      IF(INST.EQ.2) GO TO 85
      TYPE*,' ENTER THE FORMAT TO USE TO READ THE X,Y DATA'
      TYPE*,' FROM THE INPUT DATA FILE.  ENTER 0 FOR FREE FORMAT.'
85    ACCEPT 86,FMT
      IF(FMT(1).EQ.'0')GO TO 102
      IF(FMT(1).NE.'1')GO TO 87
86    FORMAT(30A2)
87    DO 100 I=1,NPTS
      READ(1,FMT) X(I),Y(I),SIGMAY(I)
100   CONTINUE
      GO TO 104
102   DO 103 I=1,NPTS
      READ(1,*) X(I),Y(I),SIGMAY(I)
103   CONTINUE
104   CLOSE(UNIT=1)
C
      TYPE *,' Enter the initial and final points to fit : '
      ACCEPT *, NBEG,NEND
      TYPE*,' THE FIRST 2 DATA POINTS ARE:'
      TYPE*,X(NBEG),Y(NBEG),X(NBEG+1),Y(NBEG+1)
```

```
      IF(INST.EQ.2)GO TO 105
      TYPE*,' ENTER THE NUMBER OF COEFFICIENTS (INTEGER):'
105   ACCEPT*,NUMCOF
      IF(INST.EQ.2)GO TO 106
      TYPE 113
113   FORMAT(' ENTER THE WEIGHTING MODE (-1 FOR 1/Y OR 0 ',
     +  'FOR NO WEIGHTING,',/,'  +1 FOR INSTRUMENTAL):')
106   ACCEPT*,MODE
C -------------------------------------------------------------------
C     BEGIN FITTING PROCEDURES
C -------------------------------------------------------------------
      NMAX=2*NUMCOF - 1
      DO 110 I=1,NMAX
110   SUMX(I)=0.
      DO 120 I=1,NUMCOF
120   SUMY(I)=0.
      DO 200 I=NBEG,NEND
      XI=X(I)
      YI=Y(I)
      IF(MODE) 122,127,128
122   IF(YI) 125,127,123
123   WEIGHT=1./YI
      GO TO 129
125   WEIGHT=1./(-YI)
      GO TO 129
127   WEIGHT=1.
      GO TO 129
128   WEIGHT=1./SIGMAY(I)**2
129   XTERM=WEIGHT
      DO 130 N=1,NMAX
      SUMX(N)=SUMX(N) + XTERM
130   XTERM=XTERM*XI
      YTERM=WEIGHT*YI
      DO 140 N=1,NUMCOF
      SUMY(N)=SUMY(N) + YTERM
140   YTERM=YTERM*XI
200   CONTINUE
C -------------------------------------------------------------------
C     CONSTRUCT MATRICES AND CALCULATE COEFFICIENTS
C -------------------------------------------------------------------
      DO 210 J=1,NUMCOF
      DO 210 K=1,NUMCOF
      N=J + K - 1
210   ARRAY(J,K)=SUMX(N)
      DELTA=DETERM(ARRAY,NUMCOF)
      IF(DELTA) 240,220,240
220   DO 230 J=1,NUMCOF
230   A(J)=0.
      GO TO 300
240   DO 270 L=1,NUMCOF
      DO 260 J=1,NUMCOF
```

```
      DO 250 K=1,NUMCOF
      N=J + K -1
250   ARRAY(J,K)=SUMX(N)
260   ARRAY(J,L)=SUMY(J)
270   A(L)=DETERM(ARRAY,NUMCOF)/DELTA
300   TYPE 310,(A(I),I=1,NUMCOF)
310   FORMAT(' COEFFICIENTS ARE:',20(/,2X,E14.7)/)
      IF(INST.EQ.2) GO TO 320
      TYPE*,' DO YOU WANT TO GENERATE A SET OF X,Y POINTS'
      TYPE*,' ACCORDING TO THE COEFFICIENTS, Y OR N:'
320   ACCEPT 50,IGEN
      IF(IGEN.NE.'Y')GO TO 400
      CALL GEN(A,INST,NUMCOF)
400   STOP
      END
C
C
C
C
      FUNCTION DETERM(ARRAY,NORDER)
C -----------------------------------------------------------
C     THIS FUNCTION CALCULATES THE DETERMINATE OF A MATRIX
C     OF ORDER 'NORDER'.
C -----------------------------------------------------------
      DOUBLE PRECISION ARRAY,SAVE
      DIMENSION ARRAY(20,20)
10    DETERM=1.
11    DO 50 K=1,NORDER
C -----------------------------------------------------------
C     INTERCHANGE COLUMNS IF DIAGONAL ELEMENT IS ZERO
C -----------------------------------------------------------
      IF(ARRAY(K,K)) 41,21,41
21    DO 23 J=K,NORDER
      IF(ARRAY(K,J)) 31,23,31
23    CONTINUE
      DETERM=0.
      GO TO 60
31    DO 34 I=K,NORDER
      SAVE=ARRAY(I,J)
      ARRAY(I,J)=ARRAY(I,K)
34    ARRAY(I,K)=SAVE
      DETERM=-DETERM
C -----------------------------------------------------------
C     SUBTRACT ROW K FROM LOWER ROWS TO GET DIAGONAL MATRIX
C -----------------------------------------------------------
41    DETERM=DETERM*ARRAY(K,K)
      IF(K - NORDER) 43,50,50
43    K1=K + 1
      DO 46 I=K1,NORDER
      DO 46 J=K1,NORDER
46    ARRAY(I,J)=ARRAY(I,J) - ARRAY(I,K)*ARRAY(K,J)/ARRAY(K,K)
```

```
50      CONTINUE
60      RETURN
        END
C
C
C
C
        SUBROUTINE GEN(A,INST,NUMCOF)
        DIMENSION IOUTFL(12),A(20)
C ---------------------------------------------------------------
C       THIS SUBROUTINE GENERATES Y VALUES FOR A RANGE OF X VALUES
C       ACCORDING TO THE EQUATION:
C          Y=A(1) + A(2)*X + A(3)*X**2...A(N)*X**(N-1).
C ---------------------------------------------------------------
        IF(INST.EQ.2) GO TO 5
        TYPE*,' ENTER THE INITIAL AND FINAL X VALUES:'
5       ACCEPT*,XINIT,XFIN
        IF(INST.EQ.2) GO TO 7
        TYPE*,' ENTER THE OUTPUT FILE NAME:'
7       ACCEPT 10,IOUTFL
10      FORMAT(12A2)
        OPEN(UNIT=2,NAME=IOUTFL)
        IF(INST.EQ.2) GO TO 15
        TYPE*,' ENTER THE NUMBER OF X,Y PAIRS TO BE GENERATED',
     +  ' (INTEGER):'
15      ACCEPT*,NUMPAR
        AINT=(XFIN-XINIT)/(NUMPAR-1)
        X=XINIT
        DO 1 I=1,NUMPAR
        Y=A(1)
        DO 3 J=2,NUMCOF
        Y=Y + A(J)*X**(J-1)
3       CONTINUE
        WRITE(2,20) X,Y
20      FORMAT(5X,E14.7,5X,E14.7)
        X=X + AINT
1       CONTINUE
        WRITE(2,30)
30      FORMAT(/,' THE COEFFICIENTS ARE:')
        WRITE(2,40) (A(I),I=1,NUMCOF)
40      FORMAT(10(/,5X,E14.7))
        CLOSE(UNIT=2)
        STOP
        END
```

```
      PROGRAM FIT
C-------------------------------------------------------------
C     Program to optimize adjustable parameters lamda 1 and
C     lamda 2 from the Koningsveld, Stockmayer, Kennedy and
C     Kleintjens approach to fitting thermodynamic data from
C     polymer blends to semi-empirical interaction function
C
C     Subroutines used:
C           Curfit- performs major portion of mathematics of fit
C           Matinv- matrix inversion for parameter optimization
C           Fderiv- calculates derivative of function w.r. to parameters
C           Functn- calculates the function
C           Fchisq- calculates deviation from fit
C-------------------------------------------------------------
C
      VIRTUAL AVX(100),AVY(100),ASIGMY(100)
      VIRTUAL ITITLE(80)
      DIMENSION AVA(10),ASIGMA(10),AYFIT(50)
      DIMENSION XPLT(100),YPLT(100)
      BYTE INFIL(27),OUTFL(27),INPUT(27),POUTFL(27),IBUF
      COMMON/VLUE/NPTS,FLAMDA,CHISQ,MODE,NTERMS
C
C     READ IN DATA TO BE FIT
      TYPE *, ' Welcome to the Debye fit program '
C
1     TYPE 2
2     FORMAT(' Enter input device, TI: for terminal input : ')
      ACCEPT 3,LEN,(INPUT(K),K=1,LEN)
3     FORMAT(Q,80A1)
      INPUT(LEN+1)=0
      OPEN (UNIT=2,NAME=INPUT,TYPE='OLD',ERR=1)
C
4     TYPE 5
5     FORMAT(' Enter input data file name : ')
      READ(2,3) LEN,(INFIL(K),K=1,LEN)
      INFIL(LEN+1)=0
      OPEN(UNIT=4,NAME=INFIL,TYPE='OLD')
C
      TYPE *,' Enter the number of lines to skip'
      READ(2,*) NSKIP
      IF(NSKIP.EQ.0)GO TO 17
      DO 16 I=1,NSKIP
      READ(4,15) ALINE
15    FORMAT( A2)
16    CONTINUE
C
17    TYPE *,'Number of points = '
      READ(2,*) NPTS
C
      DO 400 K=1,NPTS
```

```
      READ(4,*) AVX(K),AVY(K),ASIGMY(K)
      TYPE*,AVX(K),AVY(K),ASIGMY(K)
400   CONTINUE
C
      CLOSE(UNIT=4)
C
C     Initialize search parameter FLAMDA
C     and set the number of parameters in fit
C
      NTERMS = 3
      FLAMDA=1.E-03
C
C     Calculate the initial guesses for the fit
C
      KMID = (NPTS-30)/2
      IF(KMID.LE.60) KMID=NPTS/2
      XMID = AVX(KMID)
      AVA(1) = AVY(1)
      AVA(2) = 1.0/XMID**2
      AVA(3) = 0.0
      TYPE *,' Initial guesses', AVA(1),AVA(2),AVA(3)
C
      TYPE*,' Enter a title describing data :'
      READ(2,3) LENTIT,(ITITLE(I),I=1,LENTIT)
C
C
C     END OF PARAMETER SELECTION,NOW FOR THE GOOD STUFF
C
C
C
            TYPE 90
90          FORMAT(' Enter weighting mode for curve fitting:',/,
     +      ' -1 = statistical weighting,0 = no weighting,',/,
     +      ' +1 = instumental weighting : ')
            READ(2,*)MODE
C
      CALL CURFIT(AVX,AVY,ASIGMY,ASIGMA,AYFIT,AVA,NPTS,MODE
     +  ,NTERMS,FLAMDA,CHISQ)
      FIRST=CHISQ
      TYPE *,' BACK FROM CALL 1, FIRST= ',FIRST
      DO 192 I=1,20
      CALL CURFIT(AVX,AVY,ASIGMY,ASIGMA,AYFIT,AVA,NPTS,MODE
     +  ,NTERMS,FLAMDA,CHISQ)
      TYPE *,' FIRST,CHISQ : ',FIRST,CHISQ
      IF(ABS(FIRST-CHISQ).LE..000001) GO TO 19
      FIRST=CHISQ
192   CONTINUE
C
C--------- Write to the parameter file
C
19    TYPE 20
```

```
20      FORMAT(' Enter parameter output file name : ')
        READ(2,3) LEN,(OUTFL(K),K=1,LEN)
        OUTFL(LEN+1)=0
        OPEN(UNIT=3,NAME=OUTFL,TYPE='NEW',ERR=19)
C
        WRITE(3,290) (ITITLE(N),N=1,LENTIT)
395      FORMAT('FITTED PARAMETERS',7X,'ERROR(SIGMA)')
        WRITE(3,395)
290     FORMAT(' ',80A1)
        WRITE(3,303) AVA(1), ASIGMA(1)
        WRITE(3,304) AVA(2), ASIGMA(2)
        WRITE(3,305) AVA(3),ASIGMA(3)
303     FORMAT(' I(0) = ',E12.5,3X,E12.5)
304     FORMAT(' RG**2 = ',E12.5,3X,E12.5)
305     FORMAT(' INC = ',E12.5,3X,E12.5)
25      CONTINUE
        CLOSE(UNIT=3)
C
C
C---------- Write the fitted data to a file
21      TYPE 22
22      FORMAT(' Enter fitted data output file name')
        READ(2,3) LEN,(POUTFL(K),K=1,LEN)
        POUTFL(LEN+1)=0
        OPEN(UNIT=4,NAME=POUTFL,TYPE='NEW',ERR=21)
C
C
        TYPE *,' Enter xmin and xmax for the output file'
        READ (2,*) XMIN,XMAX
        TYPE *,' 100 data points to the file, free format'
        XP = XMIN
        DX = (XMAX-XMIN)/100.
C
        WRITE(4,290) (ITITLE(N),N=1,LENTIT)
        WRITE(4,350)
350     FORMAT(5X,'X',7X,'YFITTED')
C
C--------- Calculate fitted points
C
        DO 80 I=1,100
        XPLT(I) = XP
        YPLT(I) = FUNCTN(XPLT(I),AVA,NTERMS)
        XP = XP+DX
80      CONTINUE
c
c------ second data point is screwy, change
c
        YPLT(2)=(YPLT(1)+YPLT(3))/2.
c
c----- write out data to the output file
c
```

```
      DO 82 I=1,100
      WRITE(4,360) XPLT(I),YPLT(I)
360   FORMAT(1X,E12.5,2X,E12.5)
82    CONTINUE
      CLOSE(UNIT=4)
C
C-------- ASK IF ANOTHER CURVE IS TO BE FITTED
C
      TYPE 78
78    FORMAT(' Do you want another curve fitted ? (y or n)')
      READ(2,79) ANS
79    FORMAT(A2)
      IF(ANS.EQ.'Y') GO TO 4
      CLOSE(UNIT=2)
      TYPE *,' Curve fitting completed!'
      STOP
      END
      SUBROUTINE CURFIT(X,Y,SIGMAY,SIGMAA,YFIT,A,NPTS,MODE,
     +  NTERMS,FLAMDA,CHISQR)
c-----------------------------------------------
c     Purpose
c      Make a least squares fit to a non-linear
c     function with a linearization of the fitting
c     function.
c
c     Usage
c      Call Curfit(vsigmy,va,vsigma)
c     with common blocks
c      common/array/x(300),y(300),yfit(300)/
c      common/vlue/npts,flamda,chisq,mode,nterms/
c      virtual vby(300),va(20),vsigmy(300),vsigma(20)
c
c     Description of parameters
c       x      -array of corrected x data
c       y      -array of corrected y data
c     sigma    -array of standard deviations for y array
c     npts     -number of pairs of data pts (<=300)
c     nterms   -number of parameters to be fit (<=20)
c     mode     -determines method of weighting
c               +1 (instrumental) weight(i)=1./sigmay(i)**2
c                0 (no weighting) weight(i)=1.
c               -1 (statistical)  weight(i)=1./y(i)
c       a      -array of parameters
c     flamda   -proportion of gradient searsh included
c     yfit     -array of calculated values of y
c     chisq    -reduced chi square for fit
c     vby      -virtual array of background y values
c     sigmay   -virtual array of y standard deviations
c     frac     -gaussian fraction
c     ifix     -fixed parameter array
c
```

```
c       Subroutines required:
c         FUNCTN(XI,A,NTERMS)
c               Evaluates the fitting function for the Ith term
c         FCHISQ(Y,SIGMY,NFREE,YFIT)
c               Evaluates the reduced chi squared for fit to data
c         FDERIV(XI,A,DERIV,NTERMS)
c               Evaluates the analytical derivatives for the fitting
c               function for the Ith term w.r. to each parameter
c         MATINV(ARRAY,DET)
c               Inverts a symmetric 2-D matrix of degree nterm and
c               calculates its determinant
c
c       Comments:
c         Set flamda=0.001 at outset of the search
c         from P.R.BEVINGTON,'Data Reduction and Error Analysis'
c         using Marquardt method,modified for multiple peaks by
c         Cameron T. Murray
c-----------------------------------------------------------------------
c
        DOUBLE PRECISION ARRAY
        VIRTUAL X(100),Y(100),SIGMAY(100)
        VIRTUAL WEIGHT(50),ALPHA(20,20)
        DIMENSION ARRAY(20,20),SIGMAA(20),YFIT(100)
        DIMENSION BETA(20),DERIV(20),B(20),A(20)
        COMMON/ABLK/PL2
        COMMON/CONS/G0,G1,G2,G1S,G2S
c
11      NFREE=NPTS-NTERMS
        IF(NFREE) 13,13,20
13      CHISQR=0.
        GO TO 110
c
c       Evaluate weights
c
20      DO 30 I=1,NPTS
          IF(MODE) 22,27,29
22          IF(Y(I)) 25,27,23
23              WEIGHT(I)=1./Y(I)                !Statistical weighting
                GO TO 30
25              WEIGHT(I)=1./(-Y(I))             !Statictical weighting
                GO TO 30
27              WEIGHT(I)=1.                     !No weighting
                GO TO 30
29              WEIGHT(I)=1./SIGMAY(I)**2        !Instrumental
30      CONTINUE
c
c       Evaluate alpha and beta matricies
c
31      DO 34 J=1,NTERMS
           BETA(J)=0.
                DO 34 K=1,J
```

```
34              ALPHA(J,K)=0.
C
C-------------- THIS LOOP GOES TWO FUNCTN TWICE FOR EACH XI VALUE
C-------------- TO DETERMINE ELEMENTS OF BETA ARRAY
C
41      DO 50 I=1,NPTS
          XI=X(I)
          CALL FDERIV(XI,A,DERIV,NTERMS)
          DO 46 J=1,NTERMS
          BETA(J)=BETA(J)+WEIGHT(I)*(Y(I)-FUNCTN(XI,A,NTERMS))*
     +  DERIV(J)
          DO 46 K=1,J
46        ALPHA(J,K)=ALPHA(J,K)+WEIGHT(I)*DERIV(J)*DERIV(K)
50      CONTINUE
c
51      DO 53 J=1,NTERMS
        DO 53 K=1,J
53      ALPHA(K,J)=ALPHA(J,K)
c
c       Evaluate chi square at starting point
c
61      DO 62 I=1,NPTS
        XI=X(I)
62      YFIT(I)=FUNCTN(XI,A,NTERMS)
63      CHISQ1=FCHISQ(Y,SIGMAY,NFREE,YFIT,NPTS,MODE)
c
c       Invert modified curvature matrix to find new parameters
c
        TYPE *,' CHISQ1= ',CHISQ1
        ICAM=0
71      DO 74 J=1,NTERMS
          DO 73 K=1,NTERMS
73        ARRAY(J,K)=ALPHA(J,K)/SQRT(ALPHA(J,J)*ALPHA(K,K))
74      ARRAY(J,J)=1.+FLAMDA
80      CALL MATINV(ARRAY,DET,NTERMS)
c
c---    Calculation of new parameters (B),B=A if parameter fixed
c
81      DO 84 J=1,NTERMS
          B(J)=A(J)
          DO 84 K=1,NTERMS
        B(J)=B(J)+BETA(K)*ARRAY(J,K)/SQRT(ALPHA(J,J)*ALPHA(K,K))
84      CONTINUE
c
c       If chi square increased,increase flamda and try again
c
91      DO 92 I=1,NPTS
        XI=X(I)
92      YFIT(I)=FUNCTN(XI,B,NTERMS)
93      CHISQR=FCHISQ(Y,SIGMAY,NFREE,YFIT,NPTS,MODE)
        TYPE *,' MATINV CHISQR= ',CHISQR
```

```
      IF (CHISQ1-CHISQR) 95,101,101
95    FLAMDA=10.*FLAMDA
      ICAM=ICAM+1
      TYPE *,' MATINV ITERATION NUMBER : ',ICAM
            GO TO 71
C
C     Evaluate parameters and uncertainties
C
101   DO 103 J=1,NTERMS
      A(J)=B(J)
103   SIGMAA(J)=SQRT(ARRAY(J,J)/ALPHA(J,J))
      FLAMDA=FLAMDA/10.
110   RETURN
      END

      FUNCTION FCHISQ(VY,VSIGMY,NFREE,VYFIT,NPTS,MODE)
C-----------------------------------------------------------------
      DOUBLE PRECISION CHISQ,WEIGHT
      VIRTUAL VY(50),VSIGMY(50)
      DIMENSION VYFIT(50)
C
      CHISQ=0.
12    IF(NFREE) 13,13,20
13    FCHISQ=0.
      GO TO 40
C
C     ACCUMULATE CHI SQUARE
C
20    DO 30 I=1,NPTS
21     IF(MODE) 22,27,29
22     IF(VY(I)) 25,27,23
23         WEIGHT=1./VY(I)
           GO TO 30
25         WEIGHT=1./(-VY(I))
           GO TO 30
27         WEIGHT=1.
           GO TO 30
29         WEIGHT=1./(VSIGMY(I)**2)
30    CHISQ=CHISQ+WEIGHT*(VY(I)-VYFIT(I))**2
C
C     DIVIDE BY THE NUMBER OF DEGREES OF FREEDOM
C
31    FREE=NFREE
31    FCHISQ=CHISQ/FREE
40    RETURN
      END
      SUBROUTINE MATINV(VARRAY,DET,NTERMS)
C-----------------------------------------------------------------
      DOUBLE PRECISION VARRAY,AMAX,SAVE
      DIMENSION VARRAY(20,20),IK(20),JK(20)
10    DET=1.
```

```
11      DO 100 K=1,NTERMS
C
C       FIND LARGEST ELEMENT VARRAY(I,J) IN REST OF THE MATRIX
C
        AMAX=0.
21       DO 30 I=K,NTERMS
         DO 30 J=K,NTERMS
23             IF(DABS(AMAX)-DABS(VARRAY(I,J))) 24,24,30
24             AMAX=VARRAY(I,J)
               IK(K)=I
               JK(K)=J
30       CONTINUE
C
C        INTERCHANGE ROWS AND COLUMNS TO PUT AMAX IN VARRAY(K,K)
C
31       IF(AMAX) 41,32,41
32       DET=0.
         GO TO 140
41       I=IK(K)
         IF(I-K) 21,51,43
43       DO 50 J=1,NTERMS
                SAVE=VARRAY(K,J)
                VARRAY(K,J)=VARRAY(I,J)
50       VARRAY(I,J)=-SAVE
51       J=JK(K)
         IF(J-K) 21,61,53
53       DO 60 I=1,NTERMS
                SAVE=VARRAY(I,K)
                VARRAY(I,K)=VARRAY(I,J)
60       VARRAY(I,J)=-SAVE
C
C        ACCUMULATE ELEMENTS FOR THE INVERSE MATRIX
C
61       DO 70 I=1,NTERMS
                IF(I-K) 63,70,63
63              VARRAY(I,K)=-VARRAY(I,K)/AMAX
70       CONTINUE
71       DO 80 I=1,NTERMS
         DO 80 J=1,NTERMS
                IF(I-K) 74,80,74
74              IF(J-K) 75,80,75
75              VARRAY(I,J)=VARRAY(I,J)+VARRAY(I,K)*VARRAY(K,J)
80       CONTINUE
81       DO 90 J=1,NTERMS
                IF(J-K) 83,90,83
83              VARRAY(K,J)=VARRAY(K,J)/AMAX
90       CONTINUE
         VARRAY(K,K)=1./AMAX
100      CONTINUE
C100     DET=DET*AMAX CAUSED OVERFLOW AND IS NOT NEEDED
C
```

```
C       RESTORE ORDERING OF MATRIX
C
101     DO 130 L=1,NTERMS
              K=NTERMS-L+1
              J=IK(K)
              IF(J-K) 111,111,105
105           DO 110 I=1,NTERMS
                        SAVE=VARRAY(I,K)
                    VARRAY(I,K)=-VARRAY(I,J)
110                 VARRAY(I,J)=SAVE
111                 I=JK(K)
                    IF(I-K) 130,130,113
113                 DO 120 J=1,NTERMS
                    SAVE=VARRAY(K,J)
                    VARRAY(K,J)=-VARRAY(I,J)
120                 VARRAY(I,J)=SAVE
130     CONTINUE
140     RETURN
        END
```

```
      SUBROUTINE FDERIV(XI,FVA,DERIV,NTERMS)
C
C-----------------------------------------------------------------
C     Subroutine of FIT program, in this case the DEBYE version
C     calculates derivatives of data w.r. to the parameters
C     used in the fitting. Three parameters for DEBYE function
C
C     fva(1) = I(0)
C     fva(2) = Rg**2
C     fva(3) = Incoherent level
C-----------------------------------------------------------------
C
      DIMENSION FVA(10), DERIV(10)
C
      F = 2
C
      Q = XI*XI
      A = FVA(1)
      R = FVA(2)
      F2 = F*F
C
      U = Q*R*(F2/(3.0*F-2.0))
      U2 = U*U
      V = U-F*(1.0-EXP(-U/F))+F*(F-1.0)*(1.0-EXP(-U/F))**2/2.0
      C = FVA(3)
      Y = 2.0*A*V/(U2)+C
C
      DERIV(1) = 2.0*V/U2
      DERIV(2) = -2.0*Q*A*(1.0+F*(F-3.0)/U+2.0*(2.0*F-F2)*EXP(-U/F)/U
     +  +(2.0*F-F2)*EXP(-U/F)/F+F*(F-1.0)*EXP(-2.0*U/F)/U +
     +  (F-1.0)*EXP(-2.0*U/F))
      DERIV(2) = DERIV(2)/U2
      DERIV(3) = 1.0
C
C
      RETURN
      END
```

```
      FUNCTION FUNCTN(XI,VA,NTERMS)
C
C-----------------------------------------------------------
C     Calculates the function at a given x value, function is
C     for a functionality = 2 Debye coil (gaussian)
C     belongs with program DEBYE.FTN, a version of FIT
C-----------------------------------------------------------
c
      DIMENSION VA(10)
C -------------------------------------------------------------
C     VA(1) = I(0) , zero angle scattering intensity
C     VA(2) = Rg**2, assuming a dilute solution coil ?
C     VA(3) = INC, incoherent level
C-------------------------------------------------------------
      F = 2
C
      Q = XI*XI
      A = VA(1)
      R = VA(2)
      C = VA(3)
      U = Q*R*(F*F/(3.0*F-2.))
      U2 = U*U
C
      IF(U.EQ.0.0) GO TO 10
C
      UEXP = EXP(-U/F)
      V = U-F*(1.0-UEXP)+F*(F-1.0)*(1.0-UEXP)**2/2.0
D     TYPE *,A,V,U2,C,UEXP
      FUNCTN = 2.0*A*V/(U2)+C
      GO TO 20
C
10    FUNCTN = A+C
20    RETURN
C
      END
```

```
      PROGRAM GFUN
C
C-- Calculate the g parameters from the polynomial fit----
C
      TYPE *,' Input fit coefficients a1, a2, a3'
      ACCEPT *, A1, A2, A3
C
      G2 = A3/-12
      G1 = (A2-(6*G2))/-6
      G0 = (A1-(2*G1))/-2
C
      TYPE *, ' G0 =     , G1=        , G2='
      TYPE 5, G0,G1,G2
5     FORMAT (1X,E10.3,E10.3,E10.3)
      STOP
      END
```

```
      PROGRAM GENCUR
      DIMENSION IOUTFL(27),A(20)
C -------------------------------------------------------------
C     THIS SUBROUTINE GENERATES Y VALUES FOR A RANGE OF X VALUES
C     ACCORDING TO THE EQUATION:
C        Y=A(1) + A(2)*X + A(3)*X**2,..A(N)*X**(N-1).
C -------------------------------------------------------------
4     TYPE*,' Enter the initial and final x values:'
5     ACCEPT*,XINIT,XFIN
C
C
6     TYPE*,' Enter the output file name:'
7     ACCEPT 10,LEN,(IOUTFL(J),J=1,LEN)
      IOUTFL(LEN+1) = 0
10    FORMAT(Q,80A1)
      OPEN(UNIT=2,NAME=IOUTFL,TYPE='NEW',ERR=6)
C
C
      TYPE*,' Enter the number of x,y pairs to be generated',
     +  ' (INTEGER):'
15    ACCEPT*,NUMPAR
      TYPE *, 'Enter the number of coefficients : '
      ACCEPT*, NUMCOF
C
      DO 50 I=1,NUMCOF
      TYPE *,' Enter coefficient ',I
      ACCEPT *, A(I)
50    CONTINUE
C
      AINT=(XFIN-XINIT)/(NUMPAR-1)
      X=XINIT
      DO 1 I=1,NUMPAR
      Y=A(1)
      DO 3 J=2,NUMCOF
      Y=Y + A(J)*X**(J-1)
3     CONTINUE
      WRITE(2,20) X,Y
20    FORMAT(5X,E14.7,5X,E14.7)
      X=X + AINT
1     CONTINUE
      CLOSE(UNIT=2)
      TYPE 30
30    FORMAT(/,' The coefficients were :')
      TYPE 40, (A(I),I=1,NUMCOF)
40    FORMAT(10(/,5X,E14.7))
      TYPE *,'Do you wish to generate new curves (Y,N) ? '
      ACCEPT 45, ANS
45    FORMAT(A2)
      IF(ANS.EQ.'Y') GO TO 4
      STOP
```

```
      PROGRAM STATE
C
C-------------------------------------------------
C     Calculation of the interaction function g
C     from the equation of state approach
C     Zacharius et al, Macromolecules, 16, 381 (1983)
C-------------------------------------------------
c
      BYTE OUTFL(27)
C
C---- OPEN OUTPUT FILE
C
C
      TYPE*,' Enter alpha and gamma (J/(CM**3K) for PSD (unknown=0)'
      ACCEPT*, ALPH1 ,GAM1
      TYPE*,' Enter alpha and gamma (J/(CM**3K) COMP. 2 (unkn. =0)'
      ACCEPT*, ALPH2 ,GAM2
      TYPE*,' Enter polymer molecular weight (G/MOL) of 1 and 2'
      ACCEPT*, PW1,PW2
      TYPE*,' Enter monomer molecular weight (G/MOL) of 1 and 2'
      ACCEPT*, AMW1, AMW2
      TYPE*,' Enter specific volume of components 1 and 2'
      ACCEPT*, VSP1,VSP2
      TYPE*,' Enter the value of c12, and the ratio s1/s2'
      ACCEPT*, C12, S12
C
      DO 1500 IAN=1,10
      TYPE*,' Enter X12(J/CM**3), Q12 and the temperature T (K) '
      ACCEPT*, X12, Q12, T
      IF(T.EQ.0) GO TO 1501
C
      AK = 1.380E-23
      AV = 6.022E+23
C
1     TYPE*,' Enter output file name (interaction function): '
      ACCEPT 2, LEN, (OUTFL(I),I=1,LEN)
2     FORMAT( Q,80A1)
      OUTFL(LEN+1) = 0
      OPEN (UNIT=3,NAME=OUTFL,TYPE='NEW')
C
C-----  Characteristic volumes----
C
      IF(ALPH1.NE.0) GO TO 20
      TYPE *,' Enter characteristic specific volumes 1 and 2'
      ACCEPT*,VSPS1,VSPS2
      GO TO 21
20    VSPS1 = VSP1*((1+T*ALPH1)/(1+4*T*ALPH1/3.))**3.
      VSPS2 = VSP2*((1+T*ALPH2)/(1+4*T*ALPH2/3.))**3.
C
C----   Reduced volumes----------
```

```
C
21      IF(ALPH1.NE.0) GO TO 22
        TYPE*,' Enter reduced volumes 1 and 2'
        ACCEPT*,VRD1,VRD2
        GO TO 23
22      VRD1 = VSP1/VSPS1
        VRD2 = VSP2/VSPS2
23      VRD13 = VRD1**(1./3.)
        VRD23 = VRD2**(1./3.)
C
C---    Charateristic temperatures and pressures
C
        IF(ALPH1.NE.0)GO TO 24
        TYPE*,' Enter characteristic pressure for 1,2'
        ACCEPT*,P1S,P2S
        TYPE*,' Enter the characteristic temperatures 1 and 2 '
        ACCEPT*,T1S,T2S
        GO TO 25
24      P1S = VRD1*VRD1*T*GAM1
        P2S = VRD2*VRD2*T*GAM2
        T1S = VRD1*VRD13*T/(VRD13-1)
        T2S = VRD2*VRD23*T/(VRD23-1)
C
C---    Molecular weight per segment, polymer and monomer
C
25      PW1S = PW1/AV
        PW2S = PW2/AV
C
C---    Degrees of polymerization
C
        R2 = PW2/AMW2
        R1 = R2*(PW1*VSPS1)/(PW2*VSPS2)
C
C---    Characteristic hard core volume, degrees of freedom
C---    per segment
C
        VHCM = PW1S*VSPS1/R1
        C1 = (PW1S*P1S*VSPS1)/(T1S*R1*AK)
        C2 = (PW2S*P2S*VSPS2)/(T2S*R2*AK)
        AMW1S = (AMW1/1000.)/AV
        AMW2S = (AMW2/1000.)/AV
C
        TYPE*, ' Characteristic specific volume'
        TYPE*, VSPS1, VSPS2
        TYPE*, ' Reduced volumes'
        TYPE*, VRD1,VRD2
        TYPE*, ' Characteristic temperatures'
        TYPE*, T1S, T2S
        TYPE*, ' Characteristic pressures'
        TYPE*, P1S, P2S
        TYPE*, ' Molecular weight / segment; polymer, monomer'
```

```
      TYPE*, PW1S, PW2S
      TYPE*, AMW1S, AMW2S
      TYPE*,' Enter Hterm,'
      ACCEPT*, HTERM
      TYPE*, ' Degree of polymerization comp 1,2 base upon r1'
      TYPE*, R1,R2
      TYPE*, ' hard core volume and freedom/segments 1 and 2'
      TYPE*, VHCM,C1,C2
C
      THIRD = 0.0
      FOURTH = 0.0
      DO 100 J=1,99
      FRAC1 = J/100.
      FRAC2 = 1-FRAC1
      R = (FRAC1*R1 + FRAC2*R2)
      X1 = R1*FRAC1/R
      X2 = 1-X1
      X22 = X2*X2
C
D     IF(J.GT.3) GO TO 35
D     TYPE*,' X1= ',X1,' X2= ',X2
35    THET2 = X2/(S12*X1+X2)
      PMS = P1S*X1 + P2S*X2 - X1*X12*THET2
C
      TMS = PMS / ((X1*P1S/T1S) + (X2*P2S/T2S))
      TMRD = T/TMS
D     IF(J.GT.3) GO TO 45
D     TYPE*,' TMS= ',TMS,' TMRD = ', TMRD
45    V = 1.
      VINC = .1
      DO 200 L=1,4
      CALL SIGN(VINC,IDIGIT,V,TMRD)
      V = V + VINC*IDIGIT
      VINC = VINC/10.
200   CONTINUE
      VRDM = V
C
C
      ATERM = 3*C1/X22
      VRDM3 = VRDM**(1./3.)
      BTERM = ALOG((VRD13-1)/(VRDM3-1))
      FIRST = ATERM*BTERM
D     IF(J.GT.3) GO TO 50
D     TYPE*,' ATERM= ',ATERM,' BTERM= ',BTERM,' FIRST= ',FIRST
D     TYPE*,' VRDM = ',VRDM,' VHCM= ',VHCM
D     TYPE*,' VRDM3= ',VRDM3,' VRD13= ',VRD13
D     TYPE*,' R= ',R,' THET2= ',THET2,' TMRD= ',TMRD
C
50    CTERM = VHCM/(AK*T*X22)
      DTERM = P1S*(1/VRD1 - 1/VRDM)
      ETERM = (THET2*THET2)*(X12/VRDM-T*VRD1*Q12)
```

```
      SECOND = CTERM*(DTERM + ETERM)
D     IF(J.GT.3)GO TO 70
D     TYPE*,' CTERM= ',CTERM,' DTERM= ',DTERM,' ETERM= ',ETERM
D     TYPE*,' SECOND = ',SECOND
C
70    FTERM = SQRT(AMW1/AMW2)
      GTERM = ALOG(FTERM)
      THIRD = 3*GTERM*(C1-C2+2*X1*C12)
D     IF(J.GT.3)GO TO 80
D     TYPE*,' FTERM= ',FTERM,' GTERM= ',GTERM
D     TYPE*,' THIRD = ',THIRD
C
C--------- Factor 1.3 is the geometric factor
C     ---McMaster says=1.3
C
      IF(C12.EQ.0)GO TO 75
80    QTERM =(1.3*VHCM)**(1./3.)
      PTERM = (HTERM*QTERM*(VRDM3-1))
      FOURTH = 3*C12*ALOG(PTERM)
D     IF(J.GT.3) GO TO 75
D     TYPE*,' QTERM = ',QTERM,' PTERM= ',PTERM
D     TYPE*,' FOURTH = ',FOURTH
C
75    G = FIRST + SECOND + THIRD + FOURTH
C
D     IF(J.GT.3)GO TO 85
D     TYPE*,' G = ',G
85    WRITE (3,300) FRAC2,G,TMRD,VRDM,THET2
300   FORMAT(E12.5,5X,E12.5,1X,E12.5,1X,E12.5,1X,E12.5)
C
C
100   CONTINUE
      CLOSE(UNIT=3)
1500  CONTINUE
1501  STOP
      END
C
      SUBROUTINE SIGN(VINC,IDIGIT,V,TMRD)
C
C-----------------------------------------
C Calculate the sign change of the TMIX function
C-----------------------------------------
c
      IDIGIT = 0
C
      A = V
      DO 100 I=1,10
      A = A +VINC
      P2 = A**(4./3.)*TMRD - A**(1./3.) +1
      IF(P2.LT.0) GO TO 200
      IDIGIT = IDIGIT +1
```

```
100     CONTINUE
200     CONTINUE
C
C
        RETURN
        END
```

```
      PROGRAM TSTATE
      BYTE IOUT(27)
C
C
1     TYPE*,' enter output file name'
      ACCEPT 10, LEN,(IOUT(J),J=1,LEN)
      IOUT(LEN+1) = 0
10    FORMAT(Q,80A1)
      OPEN(UNIT=3,NAME=IOUT,TYPE='NEW',ERR=1)
C
      TYPE*,' Enter T1*, P1*, X12'
      ACCEPT*, T1S,P1S,X12
      TYPE*,' Enter TAU, and alpha'
      ACCEPT*, DTERM, ALPHA
C
      R = 8.314
      CONST = P1S/(R*T1S)
C     DTERM = 1 - (T1S/T2S)
      TYPE*, ' DTERM= ',DTERM
C
      V13 = 1.0
      DV = .25/100.
      DO 100 I=1,100
C
C
      ATERM = V13/(V13-1.)
      BTERM = X12/P1S
      GINT = (ATERM*BTERM)*CONST
C
      CTERM = V13 / (2.*(4./3.-V13))
      GFREE = (CTERM*DTERM*DTERM)*CONST
C
      GTOT = (GINT + GFREE)
D     TYPE*, TEMP,GTOT,GINT,GFREE,V13
      WRITE (3,300) V13,GTOT,GINT,GFREE
300   FORMAT(E12.5,3X,E12.5,3X,E12.5,3X,E12.5)
      V13 = V13 + DV
100   CONTINUE
      CLOSE(UNIT=3)
      STOP
      END
```

Appendix III

Index of small-angle neutron scattering data

Sample: PSD(30.5) / POCS(65.4) 25°C 4/83 experiment CAMDAT2 disk

ORNL Run Number	Composition of Blend
C6317	100 PSD
C6318	100 POCS
C6320	50/50
C6321	35/65
C6322	65/35
C6323	80/20
C6324	20/80

PSD(30.5) / POCS(65.4) 125°C 4/83 experiment CAMDAT2 disk

C6327	100 PSD
C6328	100 POCS
C6329	80/20
C6331	50/50
C6332	65/35
C6333	35/65
C6334	20/80

PSD (30.5) / POCS(65.4) 135°C 4/83 experiment CAMDAT2 disk

C6335	20/80
C6336	100 PSD
C6337	100 POCS
C6338	80/20
C6339	65/35
C6340	50/50
C6341	35/65

Sample: PSD(30.5) / POCS(65.4) 25°C 6/83 experiment CAMDAT1 disk

ORNL Run Number	Composition of Blend
7072	100 POCS
7073	65/35
7074	50/50
7075	35/65
7076	20/80
7077	100 PSD
7078	80/20

PSD(30.5) / POCS(65.4) 125°C 6/83 experiment CAMDAT1 disk

7080	20/80
7081	80/20
7083	65/35
7084	100 POCS
7085	50/50
7086	35/65
7087	100 PSD

PSD(30.5) / POCS(65.4) 135°C 6/83 experiment CAMDAT1 disk

7088	35/65

PSD(10.7) / PαMS(30) 25°C 6/83 experiment CAMDAT5 disk

964	100 PαMS
965	50/50
966	55/45
967	30/70
968	15/85
969	92/08
970	31/69
971	22/78
972	33/67
1974	38/62

1962	PSD(10.7) / PαMS(25)	50/50
963	PSD(10.7) / PαMS(139)	50/50
965	PSD(10.7) / PαMS (75)	50/50